UNIVERSITÀ DI PADOVA FACOLTÀ DI INGEGNERIA

Dipartimento di Ingegneria dell'Informazione

Scuola di Dottorato di Ricerca in Ingegneria dell'Informazione
Indirizzo: Bioingegneria

CICLO XXII

A MUSCLE-FORCE MODEL WITH PHYSIOLOGICAL BASES

Direttore della Scuola: Ch.mo Prof. Matteo Bertocco

Supervisore: Ch.mo Prof. Claudio Cobelli

Dottoranda: Paola Contessa

Gennaio 2010

ACKNOWLEDGENTS

I would like to thank the faculty and staff of the Neuromuscular Research Center, Boston University, where I developed my thesis.

First and foremost, I would like to thank Prof. Carlo J. De Luca for giving me the opportunity of working at the NMRC, for his invaluable guidance in these projects, for his help and support in many occasions. Above all, I'm grateful for the confidence he put in me, for the knowledge he shared and the many things I could learn in his lab.

I would like to thank Prof. Claudio Cobelli for his assistance throughout my PhD program, both in Italy and in the United States, and for allowing me to pursue my thesis projects at the NMRC.

I would also like to thank Prof. Serge Roy, Don Gilmore, and Alexander Adam for their many suggestions; Laura Prusaitis for the help in the administrative aspects of my work; and all the students of the NMRC who contributed in several ways to my thesis: Farah Zaheer, Mike Kuznetsov, Joshua Kline, Jeff Soto, Emily Hostage, and Hiba Younis.

ABSTRACT

Il controllo della forza muscolare si basa principalmente su due fenomeni: il reclutamento di unità motorie e la regolazione della loro frequenza di scarica. Molti aspetti riguardanti i meccanismi coinvolti nel controllo delle unità motorie e nella generazione di forza muscolare restano ancora da investigare.

Parte del lavoro di questa tesi ha riguardato lo studio del comportamento della frequenza di scarica delle unità motorie e dei parametri alla base dell'incremento delle fluttuazioni dell'output di forza durante l'esecuzione di contrazioni muscolari sostenute fino all'affaticamento. Inoltre, è stato analizzato il comportamento della frequenza di scarica delle unità motorie durante lo svolgimento di contrazioni muscolari a livelli di forza crescente fino alla massima forza di contrazione volontaria (a diverse velocità di incremento della forza); ed è stata messa a punto una equazione in grado di modellare il comportamento della frequenza di scarica in funzione dell'eccitazione ricevuta dal pool di unità motorie. I risultati di questa prima analisi sono serviti per creare un modello di produzione della forza muscolare basato su dati fisiologici verificabili. Il modello include il concetto di "common drive", ovvero di un input oscillatorio comune ricevuto da tutte le unità motorie del pool; la dipendenza temporale dei "twitch" di forza delle unità motorie; ed un "feedback loop" per simulare la generazione di forza in contrazioni in "target-force tracking mode".

Si è dimostrato come il modello sviluppato sia in grado di simulare il pattern di forza e il comportamento delle unità motorie sperimentalmente osservati durante l'esecuzione di contrazioni prolungate e sostenute fino all'affaticamento. In particolare, si è potuto osservare come l'eccitazione ricevuta dal pool di unità motorie si modifichi in seguito ad un aumento o ad una diminuzione della capacità di produrre forza delle fibre muscolari e come la variazione dell'eccitazione comporti di conseguenza una diminuzione o un aumento della frequenza di scarica delle unità motorie e del numero di unità motorie attive. La simulazione di contrazioni muscolari prolungate ha anche evidenziato come la crescente variabilità della forza muscolare sia da attribuire al reclutamento di unità motorie caratterizzate da "twitch" di ampiezza maggiore e da un

maggiore grado di cross-correlazione tra la frequenza di scarica delle unità motorie attive, mentre la variabilità della frequenza di scarica non sembra influire sull'output di forza.

ABSTRACT

Muscle force is regulated by varying two main motor unit properties: the recruitment and the firing rates of motor units. Discrepancies still exist on the mechanisms involved in motor unit control and muscle force generation.

This study investigated the behavior of motor unit firing rate during sustained fatiguing contractions and the motor unit parameters that are most likely to influence force fluctuation increase. We also studied the firing rate of motor units during linearly increasing force contractions up to maximum, or near maximum voluntary contraction force, at different rates of force increase, and developed an equation that models the firing rate behavior as a function of increasing excitation to the motor unit pool. Results were used to create a model of muscle force production that is based on verifiable physiological concepts and data. The model also includes the concept of common drive, i.e. of an oscillatory common input received by all motor units in the motor unit pool, the time-dependent changes of motor unit twitches, and a feedback loop to simulate force generation in a target-force tracking mode.

Simulations showed that the model is able to mimic the force and firing rate patterns which have been experimentally observed during repeated contractions sustained to exhaustion: the excitation to the motoneuron pool must be adjusted in response to an increased or decreased force generation capacity of the muscle fibers, and the firing rates of all motor units respond consequently with a decreased or increased firing rate. The simulation of prolonged contractions showed that the increase in force variability may be attributed to the gradual recruitment of higher-recruitment threshold larger-amplitude force twitch motor units. The level of cross-correlation between firing rates appeared to influence force variability, whereas the variability in the firing rates had no clear effect on force variability.

Table of Contents

List of Tables

List of Figures

CHAPTER 1

BACKGROUND AND OBJECTIVES

Introduction

When a muscle contracts, the central nervous system regulates muscle force production by varying two main motor unit parameters: the recruitment of new motor units and the modulation of firing rates of active motor units.

The firing rate of motor units has been reported to decrease during sustained contractions while the force output of the muscle remains constant, or during maximal voluntary contractions (De Luca and Forrest, 1973; De Luca et al., 1982b; Person and Kudina, 1972; Bigland-Ritchie et al., 1983a,b). Two explanations have been proposed.The input to the motoneuron pool is reduced as the motor unit contractile speeds slow (Bigland-Ritchie et al., 1983a,b; Marsden et al., 1983) and this mechanism helps preventing contracting failure during prolonged sustained contractions. This phenomenon is known as “muscle wisdom” and was attributed to reflex inhibition caused mainly by muscle metabolites accumulation which excites Group III and IV afferent nerve endings (Bigland-Ritchie et al. 1986; Woods et al., 1987; Garland 1991). This hypothesis was formulated for maximal voluntary contractions in which muscle force could not be maintained at a constant level. Alternatively, De Luca and Forrest (1973), De Luca et al. (1982b, 1996) and Adam and De Luca (2005) suggested that the central drive adapts to maintain the target force as the force twitches of the motor units change in amplitude, and consequently the excitation to the motoneuron pool alters the firing rates of the motor units to maintain the force output at the desired level. This concept describes the voluntary control of muscle force output as being regulated by a feedback loop.

Contracting muscles do not produce a smooth or steady force. The cause of the force fluctuation has been a topic of some interest during the past 60 years (Halliday and Redfearn, 1956; among others). Force fluctuation is also known to increase both during and after sustained contractions as the muscle is fatigued (Gottlieb and Lippold, 1983; Furness et al., 1977; among others). The literature contains contrasting reports on the behavior, influence and assumed

causality of various motor unit parameters on the increasing force fluctuation during fatigue. For instance, firing rates of motor units were observed to decrease during a fatiguing task by De Luca and Forrest (1973) and Garland et al. (1994); whereas Adam and De Luca (2005) found that this initial decrease was followed by an increase as the muscle progressed towards exhaustion. Firing rate variability increased after a fatiguing exercise in the work of Garland et al. (1994) and Enoka et al. (1989), but remained unchanged in the work of Macefield et al. (2000). In a simulation study, Yao et al. (2000) found that synchronization had a substantial effect on the amplitude of force fluctuations. Both synchronization and low-frequency coherence of motor unit firings were found to increase after eccentric exercise by Dartnall et al. (2008). In contrast, Semmler and Nordstrom (1998) reported no relation between either synchronization or common modulation of firings and force fluctuations when comparing skill-trained and strength-trained subjects.

Since the work of Henneman (1957), it has been well known that motor units are activated in order of increasing size and excitability, and that the range of forces where motor units are recruited differs for different muscles (De Luca et al., 1982a; 1996). Animal studies employing steady injected currents that directly stimulate the motoneurons showed that the frequency versus current relation may be represented by a straight line for all currents up to those causing inactivation (Granit et al., 1963; Kernell, 1965a). In constrast, Gydikov and Kosarov (1974) and Monster and Chan (1977) observed that low threshold motor units tended to saturate as muscle force was increased. Varying reports can also be found for the firing rate at recruitment and the maximal firing rate. It has been reported that earlier recruited motor units display lower minimum firing rates (Kernell, 1965c; De Luca and Erim,1994; Erim et al., 1996; Moritz et al., 2005); or that all motor units start firing with approximately the same firing rate regardless of their recruitment threshold (Freund et al., 1975; Tanji and Kato, 1973; among others). Maximal firing rates have been observed to either converge to the same value near maximal force levels (De Luca and Erim, 1994; Erim et al., 1996), or to reach lower values for later recruited motor units (Tanji and Kato, 1973; De Luca et al., 1982). Moritz et al. (2005) reported that high-threshold motor units might be able to fire faster than low-threshold motor units.

The behavior of motor unit firing rate and force during sustained contractions and the relation of some motor unit parameters on muscle force were analyzed. Results were used to develop a model of muscle force production with physiological bases. The majority of the existing models (Fuglevand et al. 1993; Herbert and Gandevia, 1999; Yao et al. 2000) do not incorporate the concept of common drive (De Luca et al., 1982a; De Luca and Erim, 1994), i.e. of an oscillatory common input received by all motor units in the motor unit pool. Existing models also do not consider the time-dependent changes in the motor unit twitch parameters and are usually used in a pure feed forward mode, without the possibility of simulating the motor unit force in a target-force tracking algorithm mode. The development of a force model which is based on verifiable physiological concepts of motor unit control properties and behavior and that can be used to simulate constant force contractions would be instrumental in explaining the experimentally observed firing rate and force patterns. It may also have the potential to gain insights on the contractile properties of muscles if the firing rate behavior is known, and on the recruitment and firing rate strategies employed by the central and peripheral nervous system to control muscle force.

Main objectives

This project was designed to analyze in detail motor unit behavior and control properties during the performance of sustained isometric contractions and during linearly varying force contractions. Results were used to develop a model of muscle force with physiological bases which is able to explain how the central nervous system and the peripheral nervous system control motor units to produce force.

The specific objectives of the individual chapters are:

Chapter 2: provide some basic knowledge on the electromyographic (EMG) signal and the techniques employed to record and analyze it. A decomposition technique is described, which enables to detect a large number of the motor unit action potential trains that comprise the EMG signal with a high accuracy.

Chapter 3: study the modifications that occur in the neural control of motor units during the performance of intermittent isometric contractions performed to exhaustion with the vastus lateralis (VL) muscle. We investigated the motor unit parameters that are most likely to influence force fluctuation increase during a fatiguing contraction. Data used for this analysis were previously acquired in other projects (see Adam and De Luca, 2003, 2005).

Chapter 4: study the firing rate behavior of motor units during linearly increasing force contractions up to maximum, or near maximum voluntary contraction force (MVC), at different rates of force increase. Experiments performed on five healthy subjects with the VL and the first dorsal interosseous (FDI) muscle are presented, and the results of the analysis were used to develop an equation that model the firing rate behavior as a function of increasing excitation to the motor unit pool.

Chapter 5: develop a model for describing the generation of isometric muscle force that is based on verifiable physiological concepts and data, that includes the concept of common drive, the time-dependent changes of motor unit twitches, and a feedback loop to simulate force generation in a target-force tracking mode.

CHAPTER 2

DECOMPOSITION AND ANALYSIS OF ELECTROMYOGRAPHIC SIGNALS

The electromyographic (EMG) signal is the signal associated with the contraction of a muscle. Over the past 80 years, first manual techniques and later computer-based techniques have been developed in order to extract from the EMG signal information on how muscles are controlled by the central nervous system and the peripheral nervous system. One of these techniques, named the Precision Decomposition technique, has been developed by C. J. De Luca and colleagues since the late 1970s. It was first applied to intramuscular EMG signals (LeFever and De Luca, 1978; LeFever et al., 1982a, b), and later modified for surface EMG signals (De Luca et al., 2006; Nawab et al., in press). Special electrodes, both surface electrodes and intramuscular electrodes (needle or wire electrodes), were designed to accomplish this task. This introductory chapter provides a brief description of the EMG signal, the techniques used to record and decompose it, and the main findings from the use of the Precision Decomposition technique during the past three decades.

The EMG signal

The action potential that causes the muscle to contract is an electric pulse generated in the motoneurons, neural structures whose cell body is located in the anterior horn of the spinal cord and that synapse with the muscle fibers. A single motoneuron may synapse with one or more muscle fibers, whereas each muscle fiber is innervated by only one motoneuron. The motoneuron and all the muscle fibers it innervates is called a motor unit (MU). It is the functional unit of muscles since all the fibers that comprise it will contract when the pulse from the motoneuron is received. The EMG signal is the sum of the action potentials caused by the membrane depolarization that starts at the motor end plate (the connecting point between the motoneuron and the muscle fibers) and propagates in both directions along the fibers. All the action potentials from the fibers innervated by a specific motoneuron superimpose to form the motor unit action potential (MUAP) and, when the motoneuron is repeatedly excited, a motor unit action potential train

(MUAPT) is formed. The MUAPTs of the fibers located in the vicinity of the electrode are captured by the electrode and constitute the EMG signal.

Signal detection

The EMG signals that were acquired for this project were recorded with specially designed electrodes that simultaneously detect three channels of EMG signal. Some of the data presented in this thesis were previously collected in other projects with a quadrifilar fine wire intramuscular sensor (see Adam, 2003; Adam and De Luca, 2003, 2005). (See Chapter 3.) Data acquired in this project were recorded with a special surface sensor. (See Chapter 4.)

The wire sensor was composed by four Nichrome or Platinum wires coated with nylon. The distal end (1 mm) of the wires was curved so that the electrode was anchored into the muscle. The diameter of each wire was 50 or 75 μm, depending on the desired detection selectivity. The wires were inserted into the muscle using a disposable hypodermic needle which was removed after the electrode had been inserted. The signals were band passed from 1 kHz to 10 kHz and sampled at a rate of 50 kHz. The filtering process purposefully distorted the shapes of the action potentials, rendering them particularly suitable to the decomposition algorithms. The sampling rate was also chosen in such a way to provide the required resolution to the decomposition algorithm.

The surface sensor was comprised of four pins (0.5 mm in diameter) with blunted ends that protruded from the housing so that, when pressed against the skin, they made a surface indentation. Pins were located at the edges of a 5 x 5-mm square. These surface EMG signals were band padded from 20 Hz to 1750 Hz, and the signals are sampled at 20 kHz.

Signal decomposition

The term decomposition has been commonly used to describe the process whereby individual MUAPs are identified and uniquely classified from a set of superimposed motor unit action potential trains (MUAPTs) belonging to concurrently active motor units. The concept of decomposition is depicted in Figure 1. It involves the breaking down of the interference EMG signal that is recorded when more than one motor unit is active in the vicinity of the detection

electrode. The process of decomposing an EMG signal may be a trivial task when only two MUAPTs with distinctly different MUAP shapes are present; but it may become a challenge when many MUAPTs with nearly similar and unstable MUAP shapes are present. A completely decomposed EMG signal provides all the information available in the signal.

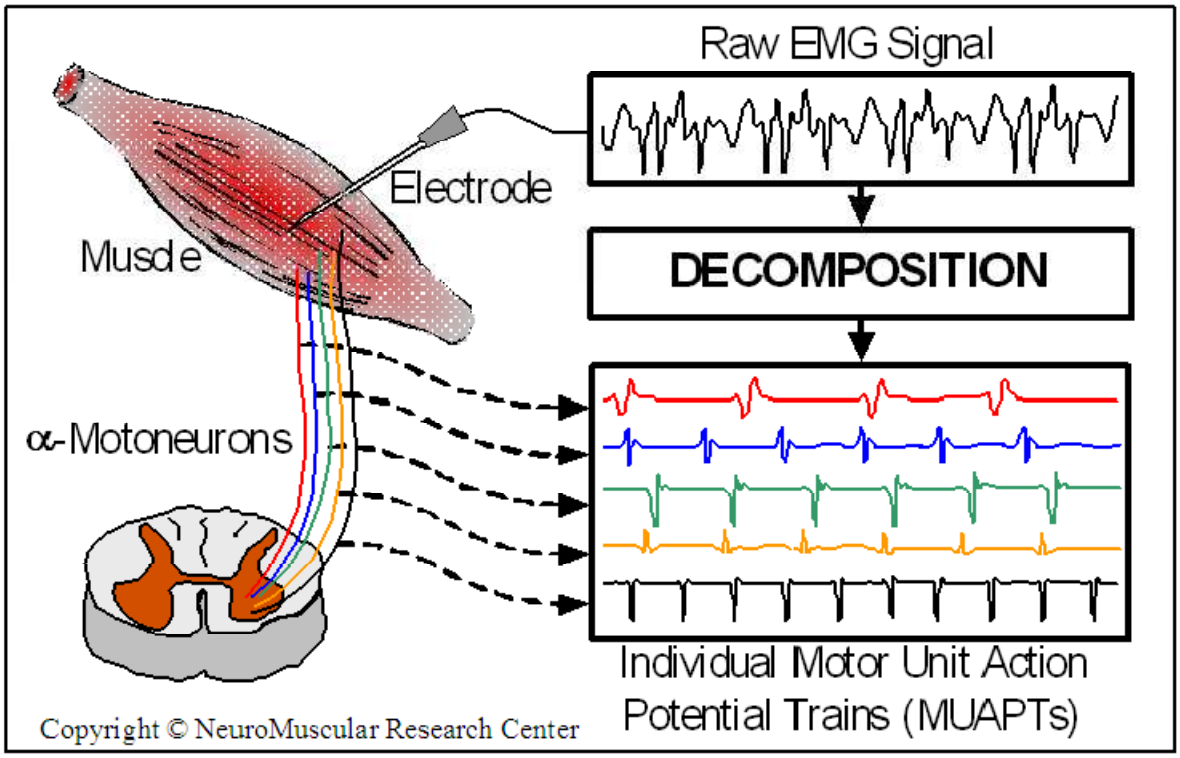

Figure 1: Decomposition of EMG signals. Pictorial outline of the decomposition of the EMG signal into its constituent MUAPs (From De Luca et al., 1982a).

The decomposition algorithm, first developed for intramuscular EMG signals, is a complex procedure that classifies the individual action potentials by using template matching and probability of firing statistics, resolves superpositions, and allocates the action potentials to motor units (Le Fever et al., 1982; Mambrito and De Luca, 1984; Stashuck and De Luca, 1989; De Luca, 1993). Decomposition is often a difficult task since the EMG signal may present a high level of superposition from different MUs. The shape may also change across the different action potentials of each MU (arising from slight movements between the sensor and muscle fibers and/or intracellular processes), and shapes from different MUs may appear very similar to each other at various times among the action potentials. These phenomena may also act in concert with each

other to make the decomposition task all the more difficult. The algorithm can be run automatically, but sometimes interaction with an operator is required to achieve higher accuracy (from 85% up to 100%) in the MUAPs detection when decomposing intramuscular EMG signals; therefore automatic decomposition is followed by manual decomposition. Recently, the decomposition algorithm has been modified and made suitable for surface EMG signals (De Luca et al., 2006; Nawab et al., in press). The task of resolving the motor unit action potential trains is even more difficult in the case of surface EMG signals since superposition, similarity of shape, or change of shape of the action potentials are accentuated. Decomposition accuracy ranges from 85% to 97% (on average 92.6%) for surface files (Nawab et al., in press).

When an action potential has been identified as belonging to a specific motor unit, the algorithms seek the instance of the greatest value of the amplitude of the action potential and store it as its firing time. In so doing, a time series of all the firings of each motor unit is obtained. All the firings of each decomposed train can then be displayed with bars as a function of the contraction time as pictured in Figure 2B. Each horizontal line contains the firings of a single motor unit and the firing time instants are presented with vertical bars. The time intervals between firings (the time interval between the firing of a motor unit and the previous firing of the same motor unit) are plotted as a function of contraction time in Figure 2A. Figure 2C shows the mean firing rates of the motor units, computed by low-pass filtering each firing time impulse train with a unit-area Hanning window. The width of the window determines the amount of smoothing applied to the mean firing rate curves.

Results of the decomposition algorithm

Several properties of the control of motor units have been revealed by the decomposition of EMG signals during the past years. A more detailed description may be found in De Luca and Adam (1999) and more recent papers (Adam and De Luca, 2003, 2005).

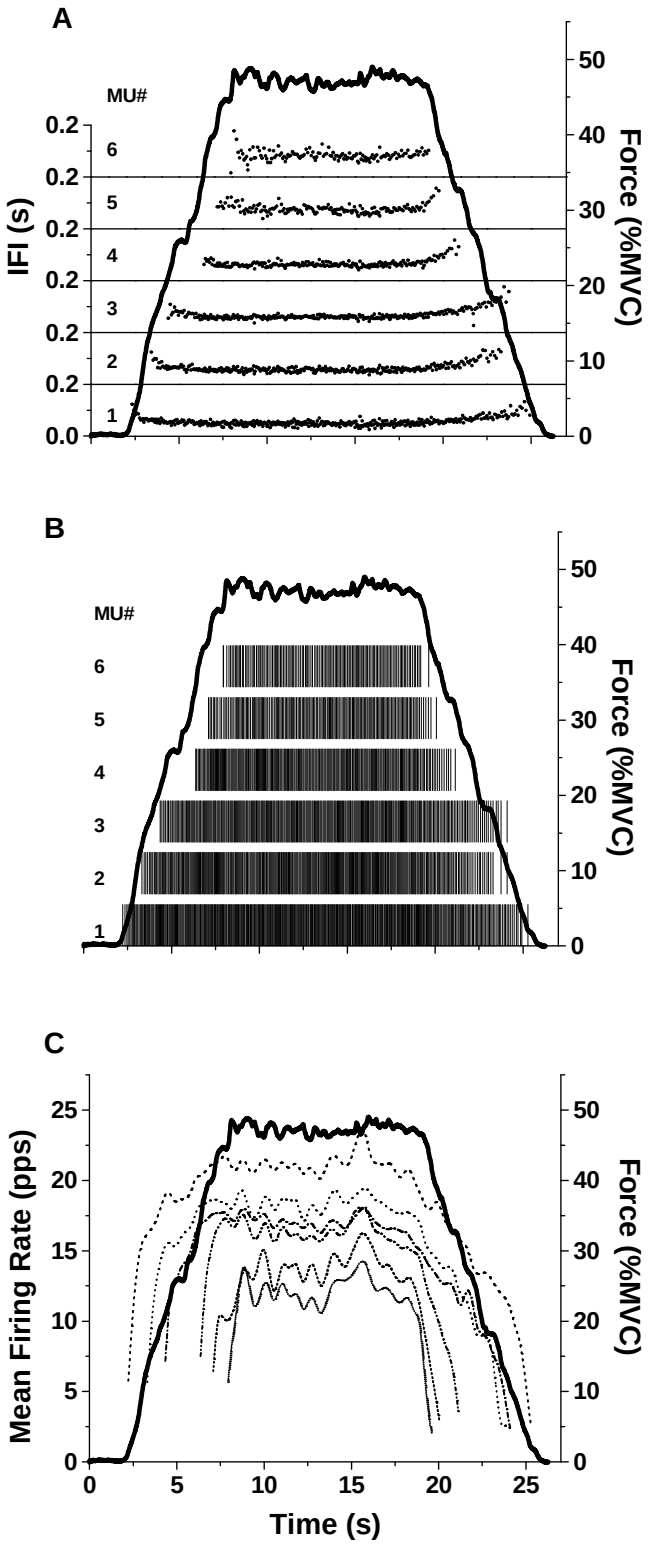

Figure 2: Results of the decomposition algorithm. Contraction time is measured on the horizontal axis and contraction force (solid line), normalized to the maximum voluntary contraction (MVC), is measured on the right vertical axis. A) Dot Plot: each inter-firing interval (IFI) of a MUAPT is plotted sequentially on the vertical scale. B) Bar Plot: a bar is placed in the location of each motor unit action potential (MUAP). C) Firing Rate Plot: the mean number of pulses per second of each motor unit is plotted as a function of time. (From Adam, 2003.)

Firing Rate Decay

The first observation directly resulting from the Precision Decomposition analysis was the firing rate decay (De Luca and Forrest, 1973; De Luca et al, 1982b; De Luca, 1985; De Luca et al., 1996). During isotonic isometric contractions at 30%, 50% and 80% MVC in the first dorsal interosseous (FDI) and in the tibialis anterior (TA) muscle, the firing rate of the motor units decreased as a function of time (see Figure 3A). It was first suggested (De Luca, 1979) and later interpreted (De Luca et al., 1996) that the observed decrease may be due to either an intrinsic property of the motoneuron to exhibit a firing rate decay over time when stimulated with a DC current (this phenomenon was first described in an animal preparation by Kernell, 1965a,b); or that it may be a consequence of twitch potentiation, which refers to the increase in the amplitude and duration of the force twitch upon repeated firing. The last hypothesis has later found further evidences in the work of Adam and de Luca (2005).

Common Drive

Another property of motor unit firing rates, that was observed thanks to the decomposition technique, is the common drive (De Luca et al., 1982a, b). It refers to the tendency of motor unit firing rates to fluctuated in unison, with minor time delay between them. The common fluctuations of four concurrently active motor units are clearly visible in Figure 3A. Common modulation in the firing rates of motor units has been verified by several investigators (Miles, 1987; Stashuk and de Bruin, 1988; among others); and indicates that the central nervous system does not control the firing behavior of each individual motor unit, but instead, modulates the behavior of the entire motoneuron pool of a muscle in the same way. The existence of common drive does not mean that motor units fire synchronously, but it indicates a similar control of motor units over a larger time scale than the one related to individual firings. The amount of common input received by concurrently active motor units can be quantified by computing the cross-correlation function between their firing rates (see Figure 3B). High values for the cross-correlation between firing rates and force indicate that firing rates are correlated with the force output of a muscle, too. The peaks occurring at positive time lags indicate that the firing rates lead the force as is expected due

to the time required to build up the force in the muscle after the fibers have been activated. (See Figure 3C.)

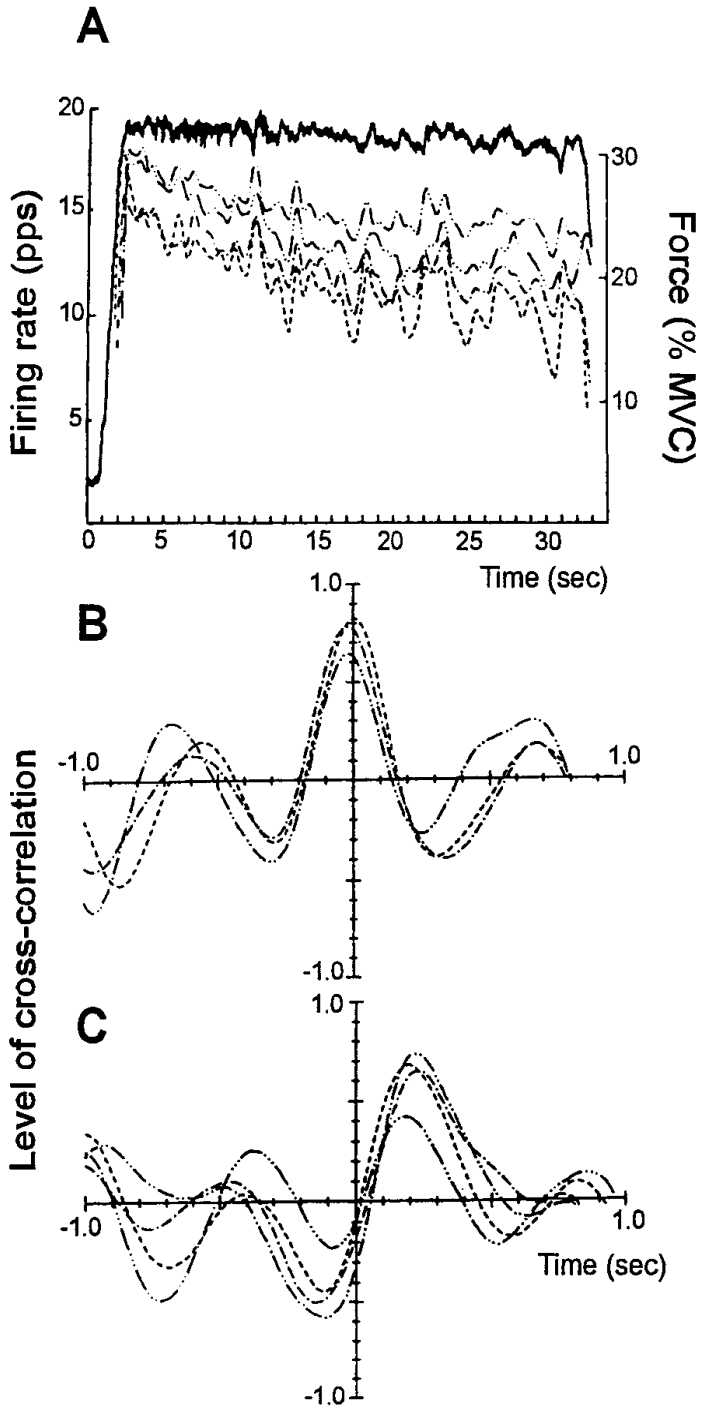

Figure 3: Common drive. A) Firing rate records of four concurrently active motor units (dashed lines) are shown superimposed on the force output (solid line) recorded during an isometric constant-force contraction of the deltoid muscle. The force level is given as a percentage of MVC on the right. B) The cross-correlations of the mean firing rates of a motor unit with those of the other units. Note that the peaks occur at zero time. C) The cross-correlations of the firing rates of all four motor units with the force output of the muscle. Peaks occurring at positive time lags indicate that the firing rate leads the force as is expected due to the time required to build up the force in the muscle after the fibers have been activated. (From De Luca et al., 1982b).

Synchronization

Synchronization refers to the tendency of motor units to fire at fixed time interval with respect to each other more often than would be expected if the motor units fired independently. Synchronization occurs in two modalities: short-term and long-term. The cross-interpulse histograms for two motor unit pairs characterized respectively by short-term (Figure 4A) and long-term (Figure 4B) synchronization are shown in Figure 4. The cross-interpulse histogram is a plot that collects the time difference between each firing of a reference motor unit (motor unit A) and the first previous and subsequent firing of a concurrently active motor unit (motor unit B). If the histogram has a peak at 0 ms, the two motor units tend to fire together. In contrast, if the two MUs are not synchronized, the cross-interval histogram will appear as a uniform distribution function. Synchronization has often been associated with force smoothness, with a higher degree of synchronization causing the force to be more variable (Yao et al., 2000). It has also been reported that synchronization increases after eccentric exercise (Dartnall et al., 2008). A study of motor unit pairs detected during isometric isotonic contractions in six muscles revealed that only a very small percentage of the firings were synchronized: an average of 8% of the firings were short-term synchronized and only 1% long-term synchronized (De Luca et al., 1993), suggesting that synchronization of motor unit firings is likely to be an epi-phenomenon with no physiological design of its own. More recently, it was shown that the degree of synchronization did not change during 20% MVC contractions performed to exhaustion in the vastus lateralis (VL) muscle, and thus, it cannot be related to the increase in force fluctuation observed during the development of muscle fatigue (Contessa et al., 2009).

Onion Skin

De Luca et al. (1982a) were among the first to document the onion skin phenomenon, together with Person and Kudina (1972) and Tanji and Kato (1973). It refers to the orderly hierarchy of motor unit firing rates: lower threshold motor units always display a greater firing rate than higher threshold motor units. Thus, when the firing rates are plotted as a function of time, they form overlapping layers resembling the structure of the skin of an onion. De Luca et al. (1982)

suggested that the control of motor units may have developed so as not to maximize the force-generating

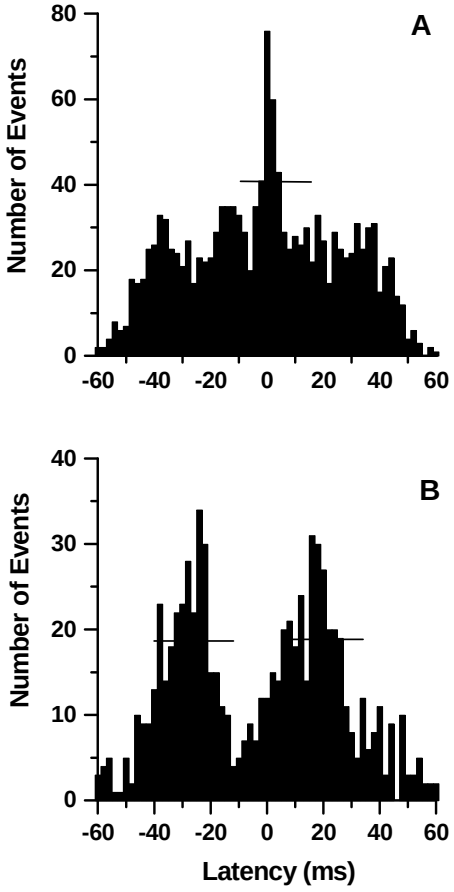

Figure 4: Synchronization. The amount or synchronization between two pairs of motor units is studied by calculating a cross-interval histogram. A) Example of a cross-interval histogram which displayed short-term synchronization. B) Example of long-term synchronization. (From Adam, 2003.)

capacity of a muscle, but instead seem to have a reserve capacity of force generation. The later recruited motor units are fast-twitch motor units and require a greater firing rate to fuse than the earlier recruited slower-twitch motor units. If the later recruited MUs maintain a lower firing rate, they will be less likely to tetanize. In contrast, if they fired faster, they would likely become exhausted in a very short time. In this way, a reserve capacity of force-generation is probably kept within the muscle, and it cannot be used during sustained voluntary contractions (even very strong contractions). They also suggested that the control system is probably organized in such a way as

to maximize not only the contraction force, but a combination of contraction force and contraction time. An evident example of the onion skin phenomenon is reported in Figure 5.

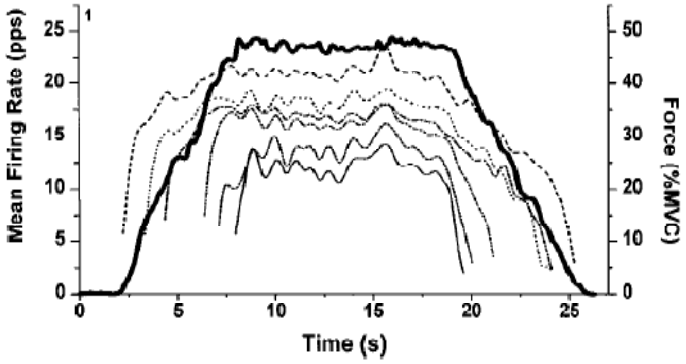

Figure 5: Onion Skin phenomenon. Firing rate records of six concurrently active motor units are shown superimposed on the force output (solid line) recorded during an isometric constant-force contraction. The force level is given as a percentage of MVC on the right.

Diversification

Diversification of the control properties refers to the diverse characteristics of the behavior of motor units in different muscles (De Luca et al., 1982a). The motor units of smaller, distal muscles, such as the FDI muscle, tend to be recruited in the force range up to 50 % MVC and have mean firing rates which reach relatively higher values when compared with those from larger, proximal muscles such as the deltoid and the trapezius muscles, which however recruit their motor units in a wider force range (up to 80 % MVC). A similar observation in the adductor pollicis and biceps brachii muscles was reported independently by Kukulka and Clamann (1981). The diverse control properties in different muscles might be useful in the generation of smooth muscle force: smaller muscles have less motor units and, therefore, force gradation due to recruitment would be coarser throughout the full range than in larger muscles which have many more motor units. Furthermore, the larger more proximal muscles tend to be more postural and are required to produce sustained contractions more often. The lower firing rates in these muscles may help delaying the progression of fatigue.

Exercise

Adam et al. (1998) reported that the firing rates and the recruitment thresholds of motor units are modified by long-term exercise. The FDI muscle of both the dominant and non-dominant hands was studied during isometric isotonic contractions performed at the same force level. Results indicated that long-term preferential use of the dominant hand, that can be regarded as a moderate form of exercise, decreased the firing rates of motor units. Also, a larger number of motor units was recruited at lower force levels. This finding is in accordance with previously known fact that the dominant hand has slower twitch muscle fibers (Tanaka et al., 1984; Zijdewind et al., 1990), probably due to the life-long preferential use, and this allows twitch fusion and force build up to occur at lower firing rates.

Aging

Erim et al. (1999) analyzed the firing rates and recruitment thresholds in the FDI muscle of young and elderly subjects (above 65 years of age), and reported that aging influences the control properties of motor units. Average firing rates were decreased, probably reflecting the slowing of the muscle, and recruitment thresholds were also lower, maybe due to a the greater percentage of slow-twitch fibers in muscles of elderly subjects. The common drive phenomenon and the onion skin phenomenon were disrupted: firing rates were often out-of phase, and they exhibited different trends (some were increasing at the same time as others were decreasing during an isometric, isotonic contraction). (See Figure 6.) These results suggested that these modifications may lead to an inefficient force generation scheme.

Motor Unit Substitution

De Luca and Westgaard (1999) reported the occurrence of motor unit substitution during very-low level (< 4% MVC), long-duration contractions (10 min) in the trapezius muscle: when the activity level decreased slightly, a motor unit stopped firing, and, in response to a subsequent slight increase in the force output, a new motor unit was recruited in place to the one that was derecruited. Motor unit substitution was not observed during the first few minutes of a contraction,

even among units that later displayed this phenomenon. They suggested that this phenomenon is the result of an adaptation process, so that the recruitment threshold of the already active motor unit may have become greater than that of the next ones in the hierarchy, which is then recruited in place of the "old" one.

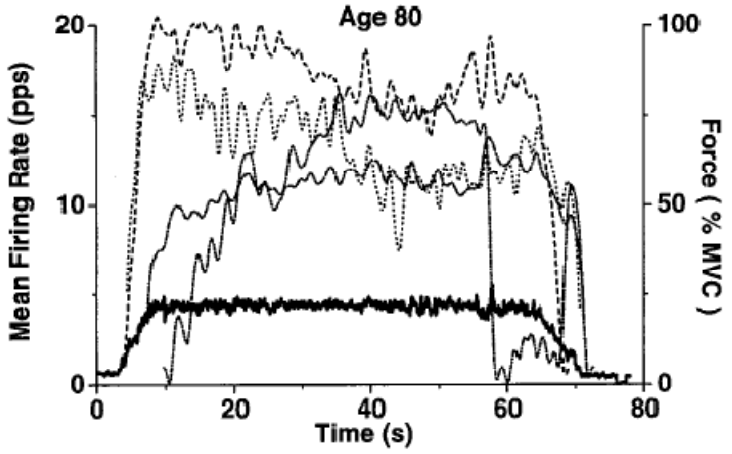

Figure 6: Aging. Firing rate behavior in an elderly subject: onion skin phenomenon is clearly violated. Firing rate records of five concurrently active motor units are shown superimposed on the force output (solid line) recorded during an isometric constant-force contraction. The force level is given as a percentage of MVC on the right. (From Erim et al., 1999.)

Fatigue

Motor unit firing patterns were studied in the VL muscle of three young subjects during a series of isometric knee extensions sustained at 20% MVC and performed to exhaustion (Adam and De Luca, 2003, 2005). The main findings were a monotonic decrease in the recruitment threshold of all motor units and the progressive recruitment of new units, all without a change of the recruitment order. Furthermore, the firing rates of motor units first decreased and then increased with time, complementing the changes in the elicited twitch, which first increased and then decreased. (See Figure 7.) The inverse relationship between motor unit firing rate and recruitment threshold was maintained throughout the fatigue series, suggesting that the way the CNS controls muscle force is invariant with fatigue. The observed common firing rate and recruitment adaptations complemented the mechanical changes of the muscle, indicating that the

firing rate of motor units adapts to counteract the change in the force produced by the muscle fibers during the contraction series. With fatigue, an increase in central drive to the motor unit pool was necessary to compensate for the loss in force output from the motor units whose muscle fibers were actively contracting.

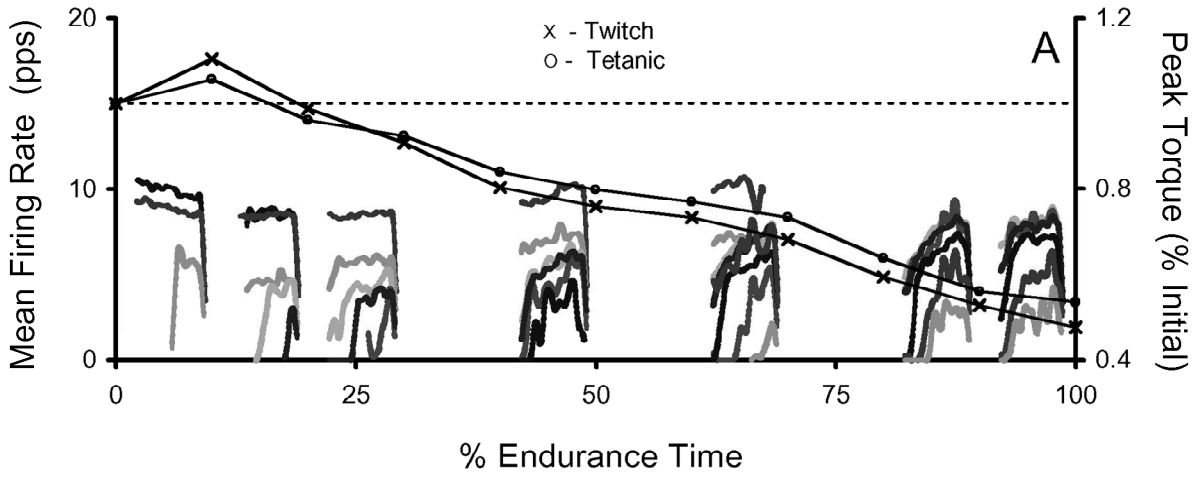

Figure 7: Fatigue. Overlay of time course of firing rate adaptations and elicited torque responses during the fatiguing contractions. Shown are mean firing rates of motor units (shaded lines, left vertical axis) and the peak torque of a single twitch and of the tetanic stimulation at 50 Hz (crosses and open circles, right vertical axis). (From Adam and De Luca, 2005.)

CHAPTER 3

MOTOR UNIT CONTROL AND FORCE FLUCTUATION DURING FATIGUE

(paper published in the Journal of Applied Physiology, 107: 235-243, 2009)

Abstract

During isometric contractions, the fluctuation of the force output of muscles increases as the muscle fatigues, and the contraction is sustained to exhaustion. We analyzed motor unit firing data from the vastus lateralis muscle to investigate which motor unit control parameters were associated with the increased force fluctuation. Subjects performed a sequence of isometric constant-force contractions sustained at 20% maximal force, each spaced by a 6-s rest period. The contractions were performed until the mean value of the force output could not be maintained at the desired level. Intramuscular EMG signals were detected with a quadrifilar fine-wire sensor. The EMG signals were decomposed to identify all of the firings of several motor units by using an artificial intelligence-based set of algorithms. We were able to follow the behavior of the same motor units as the endurance time progressed. The force output of the muscle was filtered to remove contributions from the tracking task. The coefficient of variation of the force was found to increase with endurance time ($p < 0.001$, $R^2 = 0.51$). We calculated the coefficient of variation of the firing rates, the synchronization of pairs of motor unit firings, the cross-correlation value of the firing rates of pairs of motor units, the cross-correlation of the firing rates of motor units and the force, and the number of motor units recruited during the contractions. Of these parameters, only the cross-correlation of the firing rates ($p < 0.01$, $R^2 = 0.10$) and the number of recruited motor units ($p = 0.042$, $R^2 = 0.22$) increased significantly with endurance time for grouped subjects. A significant increase ($p < 0.001$, $R^2 = 0.16$) in the cross-correlation of the firing rates and force was also observed. It is suggested that the increase in the cross-correlation of the firing rates is likely due to a decrease in the sensitivity of the proprioceptive feedback from the spindles.

Introduction

Contracting muscles do not produce a smooth or steady force. The cause of the force fluctuation has been a topic of some interest during the past 60 years (Halliday and Redfearn, 1956; among others). It has been further reported (Furness et al., 1977; Gottlieb and Lippold, 1983; among others) that these fluctuations increase both during and after sustained contractions as the muscle is fatigued.

When a muscle contracts, the central nervous system regulates muscle force production by varying two main motor unit parameters: the recruitment of new motor units and the modulation of firing rates of active motor units. The firing behavior of motor units can be assessed by parameters such as the firing rate, firing variability, synchronization of motor unit firings, and the common modulation of motor unit firings. The literature contains varying reports on the behavior, influence and causality of these parameters on the increasing force fluctuation during fatigue. For instance, De Luca and Forrest (1973) and Garland et al. (1994) reported a decrease in the firing rate of most motor units during a short-lasting fatiguing task. Adam and De Luca (2005) later found that this initial decrease was followed by an increase as the muscle continued to contract and progress towards exhaustion. After eccentric exercise the firing rate increases (Dartnall et al., 2008).

There have been contrasting reports on the changes of firing rate variability with fatigue. Variability of the firing rate was found to increase after a fatiguing exercise by Garland et al. (1994) in the biceps brachii muscle and by Enoka et al. (1989) in the first dorsal interosseus muscle (FDI). In contrast, Macefield et al. (2000) observed no systematic change in firing rate variability of the extensor hallucis longus muscle when fatigued during a sustained maximum voluntary contraction (MVC). A causal relationship between the firing rate variability and force variability was highlighted in a simulation study by Moritz et al. (2005). However, contrasting reports have been published. Firing variability was regarded as a likely contributor to the increased force fluctuations observed in elderly subjects at low forces by Tracy et al. (2005) and Laidlaw et al. (2000), but another study of some of the same authors (Galganski et al., 1993) reported an increase in force variability but not in firing rate variability in elderly subjects. Additionally, Semmler and

Nordstrom (1998) reported that increased force variability was not accompanied by a change in firing rate variability when comparing skill-trained and strength-trained subjects.

Controversial reports can also be found for synchronization and common modulation of motor unit firings. In a simulation study, Yao et al. (2000) found that synchronization had a substantial effect on the amplitude of force fluctuations, and the authors suggested that it may explain some of the experimentally observed increases in the amplitude of the surface EMG (sEMG) signal, such as those which occur during fatiguing contractions. Both synchronization and low-frequency coherence of motor unit firings were found to increase after eccentric exercise by Dartnall et al. (2008). In contrast, Semmler and Nordstrom (1998) reported no relation between either synchronization or common modulation of firings and force fluctuations when comparing skill-trained and strength-trained subjects. Synchronization did not contribute to the increased force fluctuations during low-force isometric contractions in elderly subjects in a study by Semmler et al. (2000). Similarly, Nordstrom et al. (1990) noted no change in the strength of synchronization in the masseter muscle during a fatiguing contraction. Interestingly, Holtermann et al. (2008), using a novel sEMG method, noted an increase in both synchronization and force variability, but no causal dependency between these two parameters, during a fatiguing contraction. There can be many reasons for the discrepancies among the reported observations. Some differences may be due to the measurement of the force variability; others to the analysis of grouped motor units from different contractions and/or subjects.

In this study we were interested in investigating if modifications occurred in the neural control of motor units. In our protocol we requested the subjects to use visual feedback in order to follow a ramp trajectory up to 50% MVC and then maintain a force output constant at 20% MVC for approximately 50 s. This protocol requires the subjects to track the visually displayed force output about a mean value. This tracking process per se introduces a force-variability due to the innate ability of the subjects to modulate the force output on the basis of the processed visual cue. We removed this tracking fluctuation from the data and focused on the force variability caused by the intrinsic force production. In this study we investigated the behavior of the control properties of

motor units during fatiguing contractions sustained to exhaustion and related the behavior to the increasing force fluctuation. Our approach enabled us to follow the firings of individual motor units throughout a sequence of sustained contractions. In this fashion we could document the alterations in the firing characteristics in the motor units and did not need to rely on observations made on the group behavior of different motor unit populations.

Methods

The experiments performed to collect the data for this study have been previously reported by Adam and De Luca (2003, 2005). They are described here in brief; additional details may be obtained by referring to the previous papers.

Subjects -- Four healthy men reporting no known neurological disorder participated in the study. The mean ± SD for the age of the subjects was 21.25 ± 0.96 yr (range 20 - 22). An informed consent form approved by the Institutional Review Board at Boston University was administered to all subjects before participation in the study.

Force measurement -- Subjects were seated in a chair designed to restrain hip movement and immobilize their dominant leg at a knee angle of 60° flexion. Isometric knee extension force was measured via a load cell attached to lever arm and a pad positioned against the tibia 3 cm above the medial malleolus. Visual feedback of the knee extension force was displayed on a computer screen. The force signal was band-pass filtered from DC – 100 Hz and digitized at 2 kHz.

EMG recording -- Intramuscular EMG signals were recorded from the vastus lateralis (VL) muscle of the dominant leg by use of a quadrifilar fine wire sensor. The electrodes of the sensor were comprised of four 50 µm diameter nylon-coated Ni-Cr wires glued together and cut to expose only the cross section of the wires (De Luca and Adam, 1999). The sensor was inserted into the muscle via a 25 gauge disposable hypodermic needle, which was removed after the wires were inserted. Three combinations of pairs of wires were selected and differentially amplified to yield three separate intramuscular EMG channels. The signals were amplified, band-pass filtered (1 kHz – 10 kHz), sampled at 50 kHz, and stored on a PC for offline data analysis.

Protocol -- At the beginning of the experimental session, subjects performed three brief maximal knee extension contractions of approximately 3 s in duration. The greatest value of the three trials was chosen as the maximal voluntary contraction (MVC) force. The subjects were then asked to follow a series of force trajectories, which were displayed on a computer screen, by isometrically extending the knee joint. The tracking task was practiced a few times to ensure subjects were able to smoothly follow the trajectories. The subjects performed 7-10 contractions separated by at least 3 min of rest before proceeding to the fatigue protocol.

After the practice session, subjects proceeded to the fatigue protocol where they were asked to track repeated contractions, separated by 6 s of rest, until they could no longer maintain the target level. (See Figure 8.) Each contraction began with a ramp up to 50% MVC (at a rate of 10% MVC/s) and a brief hold phase; the target value was then decreased to 20% MVC and maintained at this level for 50 s. At the end of the cycle, the force level was decreased at the same rate as the initial ramp. Strong verbal encouragement was given when the force traces dipped below the 20% MVC target value by more than 1% MVC (5% of target value) and the fatigue sequence was terminated at the end of a contraction, when the dips in the force occurred at a rate of more than 2 per 10 s of constant target force.

Although the interval for analysis was the plateau region, that is, the 50 s where the force was held constant at 20% MVC, the ramp at the beginning of each cycle allowed us to observe changes in the recruitment threshold of each motor unit throughout the contraction series. The inclusion of the higher-force ramp was part of a force paradigm designed for other data collection requirements in previously published work. In this work, it proved useful for identifying the recurrence of specific motor units in separate contractions. For additional information refer to Adam and De Luca (2003).

Data Analysis -- Five contractions for each subject were analyzed: the first, the second, the middle, a contraction between the middle and the last, and the last contraction. A 30 s interval in the middle of the 20% MVC part of the contraction was chosen for all computations. This interval was chosen because it allowed analysis of the data in a region where many motor units were firing continuously and new ones were recruited.

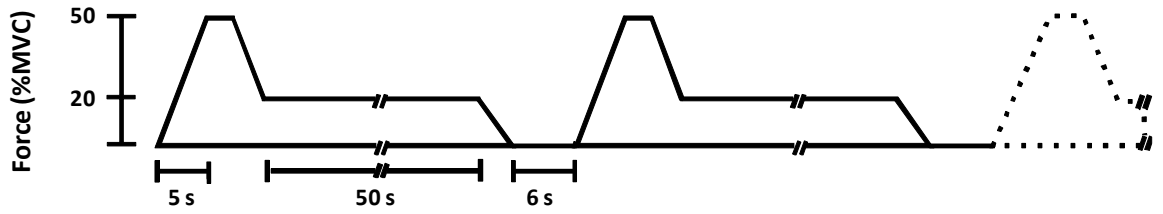

Figure 8: Fatiguing protocol. Successive isometric contractions were tracked to exhaustion, separated by 6 s of rest. Each contraction started with a ramp up to 50% MVC (at a rate of 10% MVC/s) and a brief hold phase; the target value was then decreased to 20% MVC and maintained at this level for 50 s. At the end of the cycle, the force level was decreased at the same rate as the initial ramp. (Modified from Adam and De Luca, 2003.)

The force data were analyzed after detrending the signals with a high-pass filter having a corner frequency at 0.75 Hz. The detrending was necessary to remove the low-frequency components caused by the trajectory tracking component of the force and maintain the higher-frequency components resulting from the motor unit firing behavior. The standard deviation (SD) and the coefficient of variation (CV = SD/mean value*100) of the force were computed in the same time range used for the motor unit analysis.

The intramuscular EMG signals were decomposed into their constituent motor unit action potential trains by means of the Precision Decomposition technique (LeFever and De Luca 1982a; Nawab et al., 2008). This is an artificial intelligence driven automatic technique that uses template matching, template updating and probability of firing statistics to separate and identify the individual action potentials with up to 85% accuracy. The accuracy can be improved to over 97.5% with an operator-assisted editor (Nawab et al., 2008). In this study, we used the technique to process three channels of intramuscular EMG signals detected via a quadrifilar fine wire sensor. The shapes of the action potentials belonging to an individual motor unit appear differently on each channel. This distinction was instrumental in identifying the occurrence of the individual firings of the individual motor units as well as enabling some of the individual motor unit action potentials to be followed amongst contractions (see also Adam and De Luca, 2003). An example of the results of the decomposition process can be seen in Figure 9A which present the timing of the individual firings of 6 motor units that were identified during the contraction that produced the force plotted

in the figure. (Note that the inter-pulse intervals are plotted vertically.) Only motor units that could be identified for at least two successive contractions were considered for further analysis. The time-varying mean firing rate of each motor unit was computed by low-pass filtering the impulse train representing the time occurrence of each motor unit firing with a Hanning window of 400 ms duration. Figure 9B shows the time-varying firing rates of the same motor units shown in Figure 9A. The firing rates were detrended to remove the slow variations by filtering the signals with a high-pass filter having a corner frequency at 0.75 Hz. An example may be seen in Figure 9C. The SD and CV (SD/mean value*100) of the mean firing rates were computed from the detrended signals.

The level of common drive between pairs of concurrently active motor units was computed by calculating the cross-correlation function of the detrended mean firing rates of all motor unit pairs within a contraction. An example is shown in Figure 9E. The degree of common drive was obtained by measuring the maximum of the cross-correlation function in the interval of +/- 100 ms. Please see De Luca et al. (1982) and De Luca and Adam (1999) for details. In order to determine if the common fluctuations in the mean firing rates are also reflected in the force output of the muscle, the detrended mean firing rate of each motor unit (Figure 9C) was cross-correlated with the detrended force output (Figure 9G). The degree of cross-correlation was determined by measuring the maximum that occurred with a lag of 100 to 200 ms. An example may be seen in Figure 9F.

Synchronization between the firings of pairs of motor units was calculated according to the technique described in De Luca et al. (1993). The cross-interval histogram was calculated for each pair of motor units in a contraction. An example may be seen in Figure 9D. For each pair, the motor unit with the least number of firings was chosen as the reference motor unit and the other as the alternate. For each firing in the reference motor unit, the forward and backward latencies between it and the nearest firing in the alternate motor unit were accumulated in the cross-interval histogram. To find latencies where synchronization occurred, the count of each latency bin was compared to a statistically determined threshold, determined by using a binomial distribution and a confidence level set at 95%. The strength of synchronization was then computed for each peak in

the histogram that surpasses the threshold by means of the Synch Index (SI), which represents the percentage of synchronized firings beyond that which would be expected if the two motor units were firing independently.

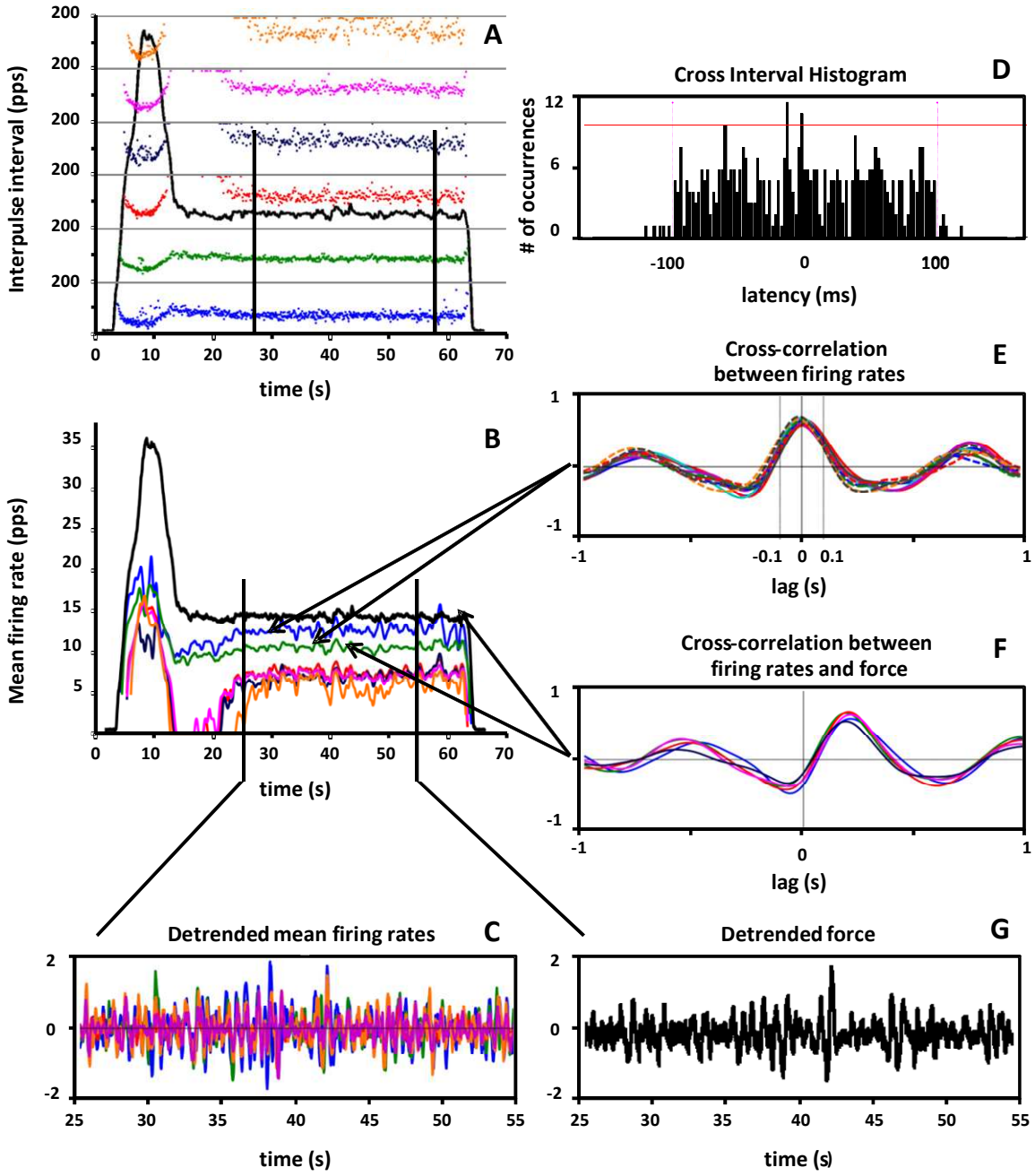

Figure 9: Data analysis. A traced force trajectory is shown superimposed on the inter-pulse intervals (A) and on the mean firing rates (B) of the active motor units. The black vertical lines indicate the 30 s interval used for all data analysis. The detrended mean firing rates (C) and the detrended force (G) in this time interval are shown. From these signals, the following parameters were computed: the strength of synchronization (D), the cross-correlation (E) between the detrended firing rates of all active motor unit pairs and the cross-correlation (F) between the detrended firing rates of each motor unit and the detrended force. Note that in (A) when the inter-pulse intervals of the motor units are greater than 200 ms, a fixed value of 200 ms is displayed.

Results

Subjects were able to track from 6 to 10 consecutive trajectories (7.75 ± 2.06 contractions) prior to reaching the limit of their endurance capacity as measured by their ability to maintain the 20% MVC force level. The pre-fatigued knee extension MVC values measured at the beginning of the experimental session ranged from 206.01 to 220.89 N (213.12 ± 7.8 N)**.** As the contraction sequence progressed, all subjects showed a decreased proficiency in smoothly tracing the force trajectories and an increase in force fluctuations. This phenomenon is evident in Figure 10 which presents three samples of the force profile tracked by subject #2. The last contraction of subject #2 could be used only for force analysis due to a considerable degree of motor unit superposition and changes in shape.

The analyzed data from one individual subject (subject #3) are presented in Figure 11. The change in parameter values as a function of endurance time is evident and representative of the grouped patterns shown in Figure 12, which shows the behavior of all the subjects. In order to determine if the parameter values varied as a function of the contraction number, they were plotted on a normalized scale for endurance time, where the first contraction was designated as 0% endurance time and the last contraction of the series for each subject was designated as 100% endurance time. A linear regression analysis was performed on each parameter and the slope of the regression was tested for significant difference from the value 0 according to the two-tailed t-statistic using a threshold $\alpha = 0.05$. If the slope is not significantly different from 0, it would indicate that there was no influence of endurance time. Table I contains the equation of the regression line, the R^2 value, the significance level of the slope and the number of data points used in the regression.

Force variability -- The variability in the force, computed as the CV of the detrended force, increased from an average value of 0.67% ± 0.18% in the first contraction to an average value of 2.10% ± 0.99% in the last contraction prior to exhaustion. Subjects #2 and #3 showed the greatest increase in the CV of the force. Significant positive relations were found for the CV of the force as a function of endurance time for each subject. (See Table I.) A significant positive relation

was found for the CV of the force as a function of endurance time for grouped subjects. (See Table I and Figure 12.)

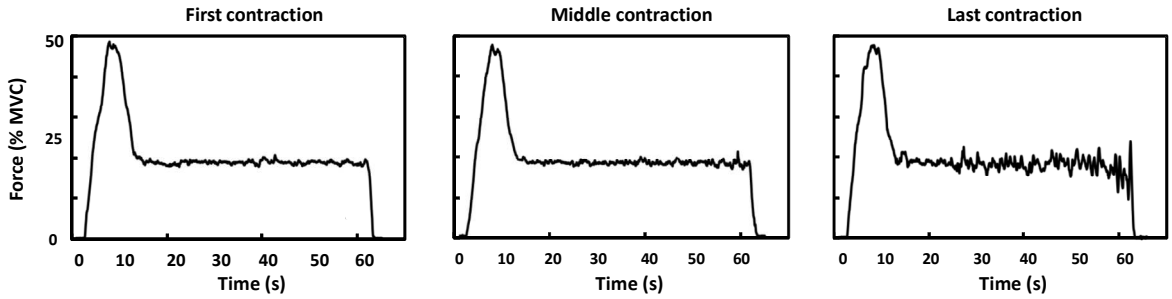

Figure 10: Force variability. The first, middle and last traced force trajectories for subject #2 are presented in order to show the increase in the force fluctuations with the progression of fatigue.

Firing rate variability -- The CV of the detrended mean firing rates were computed for 26 motor units throughout the sequence of contractions. The CV of the firing rates of motor units which were active in the plateau region of the first contraction did not change significantly (see Table I) as the contraction sequence progressed, whereas, the CV of the mean firing rates of motor units which began firing in the plateau region in successive contractions almost always decreased while they stabilized their firing pattern. These later recruited motor units were always characterized by a greater variability in their firing rate with respect to the previously active motor units. No significant relation between the CV of the mean firing rates of the motor units firing from the first contraction and the CV of the force was found ($R^2 = 0.02$, p=0.65 for subject #1; $R^2 = 0.3$, p=0.21 for subject #2; $R^2 = 0.06$, p=0.51 for subject #3; $R^2 = 0.09$, p=0.34 for subject #4).

Cross-correlation of firing rates -- The cross-correlation functions were computed on the firing rates in the plateau region between pairs of concurrently active motor units. Forty-two (42) pairs of motor units were followed throughout at least two, and in some cases all of the contraction sequence. All subjects showed some degree of cross-correlation of the firing rates between the value of the common drive (computed as the maximum of the cross-correlation function in the interval of +/- 100 ms) and endurance time for three of the four subjects. (See Table I.) Only subject #4 did not show a significant increase. On average, the common drive increased from 0.25 ± 0.13 in the first contraction to 0.39 ± 0.20 in the last contraction. Subjects #2 and #3, which

exhibited higher variability in the force, also showed higher common drive values than the other two subjects. When the cross-correlations of all the subjects were grouped together, the R^2 value decreased slightly, as would be expected from the inter-subject variability, but the slope value remained significant. A significant relation between the value of the common drive and the CV of the force was found for three out of four subjects ($R^2 = 0.76$, $p<0.0001$ for subject #1; $R^2 = 0.14$, $p=0.029$ for subject #2; $R^2 = 0.33$, $p=0.01$ for subject #3). Only subject #4, which did not show a significant increase of common drive with endurance time, was not characterized by a significant increase ($R^2 = 0.01$, $p = 0.74$).

Cross-correlation of firing rates and force -- The same trend was found for the maximum value of the cross-correlation functions between individual motor unit firing rates and force, computed for 26 different MUs throughout the contraction sequence. The values increased as the number of performed contractions increased and a positive linear trend was found for all subjects. (See Table I.) On average, the maximum increased from 0.32 ± 0.09 in the first contraction to 0.45 ± 0.16 in the last contraction. Again, subjects #2 and #3 had the highest values. When the cross-correlations of all the subjects were grouped together, the R^2 value decreased, as would be expected from the inter-subject variability, but the slope value remained significant. A significant relation between the cross-correlation of firing rates and force and the CV of the force was found for all subjects ($R^2 = 0.72$, $p<0.0001$ for subject #1; $R^2 = 0.24$, $p=0.028$ for subject #2; $R^2 = 0.66$, $p=0.0001$ for subject #3; $R^2 = 0.30$, $p=0.024$ for subject #4).

Synchronization of motor units -- A total of 100 motor unit pairs were analyzed. They were obtained from all the contractions of all the subjects. Most of them (73 out of 100) showed some minor degree (average SI < 4%) of synchronization and most of the synchronized pairs (69 out of 73) presented long-term synchronization (time lag > 6 ms), while a smaller group (34 out of 73) presented short-term synchronization (time lag ≤ 6 ms). The average Synch Index was always in the range between 2 to 4% in all contractions and for all subjects. This indicates that when synchronization of motor unit firings was noted, only 2 to 4% of the firings were synchronized beyond that expected by random chance. Table I indicates that there is no clear trend suggesting that the Synch Index varies systematically as a function of contraction sequence (endurance time).

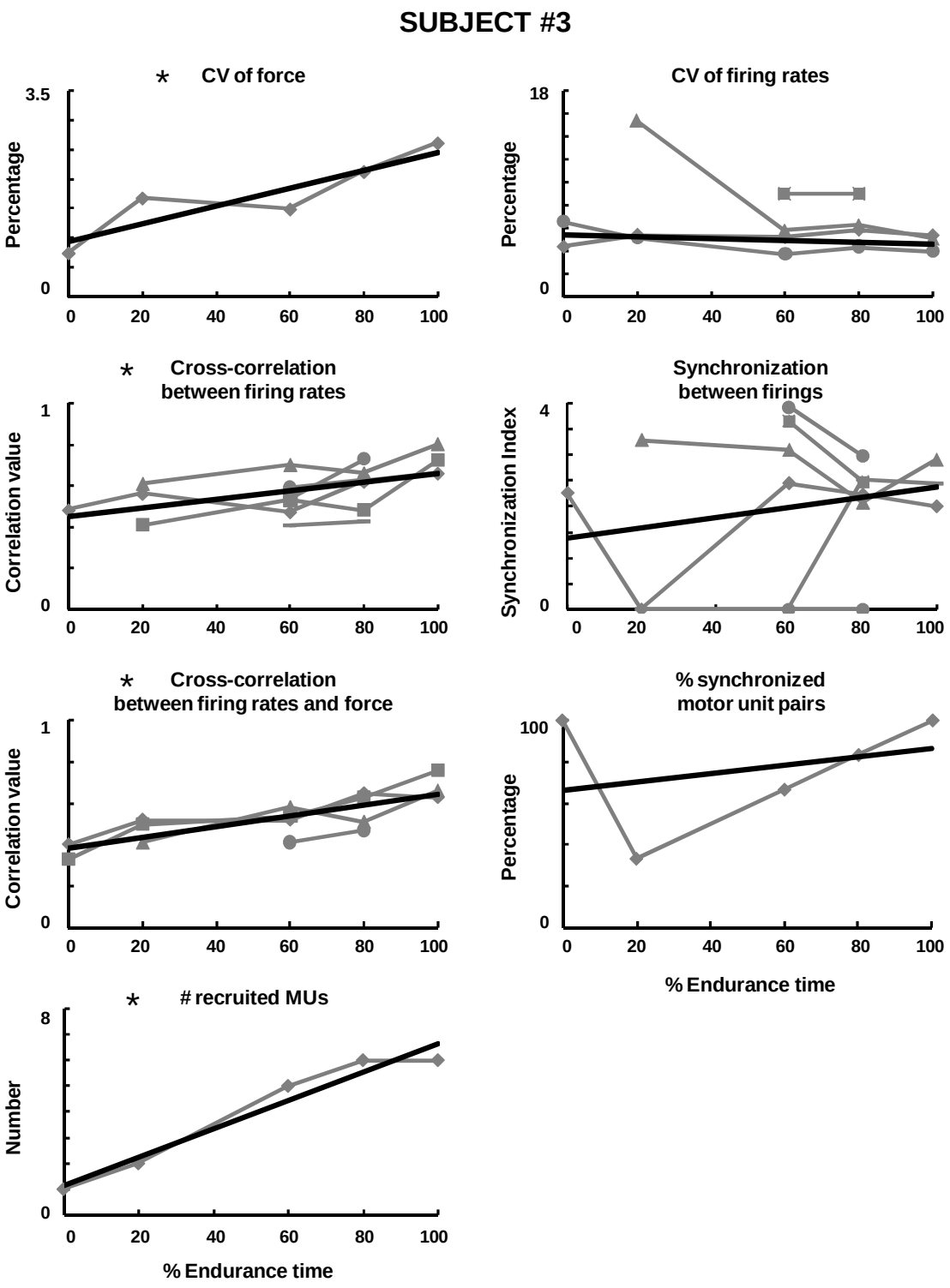

Figure 11: Results individual subject. The behavior of all the analyzed variables with endurance time is presented for subject #3: the coefficient of variation (CV) of the detrended force, the Common Drive defined as the maximum value of the cross-correlation function between the detrended motor unit firing rates in the interval +/- 100 ms, the maximum valued of the cross-correlation function between the detrended motor unit firing rates and the force, the number of recruited motor units during the analyzed interval, the CV of the detrended mean firing rates, the strength of synchronization (Synch Index (SI)) (see text), and the percentage of synchronized motor unit pairs. The first four parameters were significantly increasing with endurance time (this is indicated by the * symbol). The first plot on the right hand side shows the CV of the detrended mean firing rates as a function of endurance time for all motor units. Only motor units that were active in the first and subsequent contractions were used for the regression analysis.

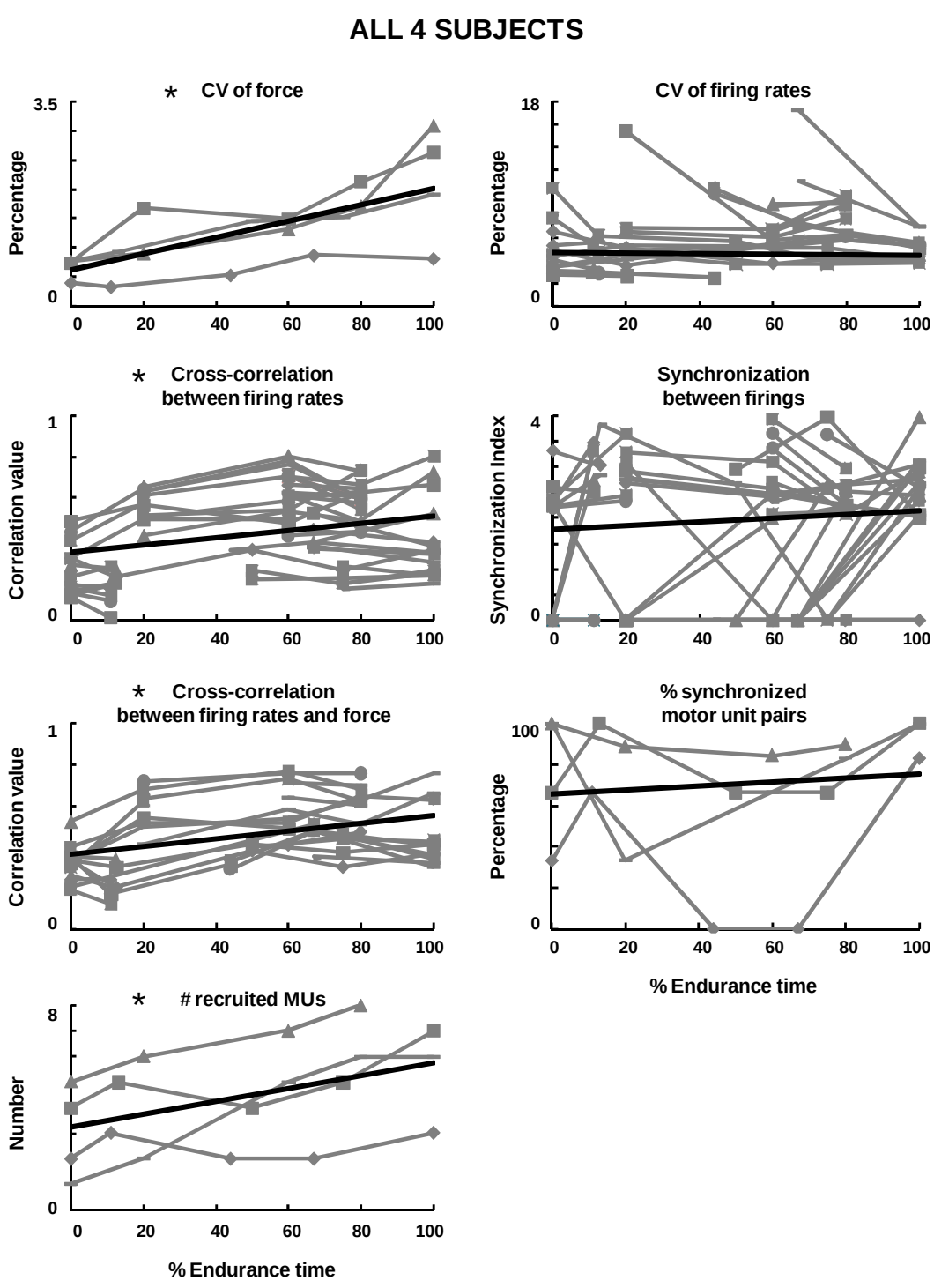

Figure 12: Results all subjects. The behavior of all the analyzed variables with endurance time is presented for all subjects grouped: the CV of the detrended force, the Common Drive defined as maximum value of the cross-correlation function between the detrended motor unit firing rates in the interval +/- 100 ms, the maximum values of the cross-correlation function between the detrended motor unit firing rates and the detrended force, the number of recruited motor units during the analyzed interval, the CV of the detrended mean firing rates, the strength of synchronization, and the percentage of synchronized motor unit pairs. The first four parameters were significantly increasing with endurance time (this is indicated by the * symbol). The first plot on the right hand side shows the CV of the detrended mean firing rates as a function of endurance time for all motor units. Only motor units that were active in the first and subsequent contractions were used for the regression analysis.

Table I: Parameters influencing force fluctuation: statistics. Statistics from the regression analysis performed on single subjects and on grouped subjects for each analyzed parameter. The equation of the regression lines, the R^2 value, the p value and the number n of data points used for the regression are reported. In each case, the independent variable x is the endurance time. In the case of the CV of the firing rates, the regression lines were drawn considering only motor units active from the first contraction.

Parameters	Subject #1	Subject #2	Subject #3	Subject #4	Grouped subjects
CV force	y=0.53x+0.35 R^2=0.81 p=0.036* n=5	y=1.99x+0.51 R^2=0.80 p=0.042* n=5	y=1.53x+0.93 R^2=0.81 p=0.039* n=5	y=1.10x+0.79 R^2=0.97 p=0.002* n=5	y=1.38x+0.62 R^2=0.51 p<0.001* n=20
Cross-correlation between firing rates	y=0.27x+0.15 R^2=0.64 p<0.0001* n=25	y=0.19x+0.5 R^2=0.23 p=0.004* n=35	y=0.2x+0.45 R^2=0.27 p=0.024* n=19	y=0.22 R^2=0 p=0.92 n=21	y=0.18x+0.33 R^2=0.10 p=0.001* n=100
Cross-correlation between firing rates and force	y=0.19x+0.23 R^2=0.43 p=0.001* n=21	y=0.25x+0.51 R^2=0.33 p=0.009* n=20	y=0.26x+0.38 R^2=0.62 p<0.001* n=16	y=0.09x+0.32 R^2=0.29 p=0.026* n=17	y=0.19x+0.36 R^2=0.16 p<0.001* n=74
# Recruited MUs	y=0.32x+2.26 R^2=0.06 p=0.70 n=5	y=3.50x+5.10 R^2=0.98 p=0.01* n=4	y=5.52x+1.13 R^2=0.95 p=0.004* n=5	y=2.15x+3.97 R^2=0.54 p=0.16 n=5	y=2.51x+3.26 R^2=0.22 p=0.042* n=19
CV mean firing rate	y=-0.21x+4.47 R^2=0 p=0.93 n=11	y=2.46x+3.44 R^2=0.26 p=0.24 n=7	y=-0.73x+5.35 R^2=0.11 p=0.35 n=10	y=-1.62x+5.35 R^2=0.10 p=0.33 n=12	y=-0.26x+4.63 R^2=0 p=0.72 n=40
Synchronization between firing rates	y=0.54x+1.03 R^2=0.02 p=0.48 n=25	y=-0.51x+2.48 R^2=0.03 p=0.36 n=35	y=0.98x+1.39 R^2=0.05 p=0.38 n=19	y=0.01x+2.31 R^2=0 p=0.99 n=21	y=0.36x+1.77 R^2=0.01 p=0.34 n=100
% Synchronized MU pairs	y=0.14x+30.52 R^2=0.02 p=0.81 n=5	y=-0.12x+95.7 3R^2=0.46 p=0.32 n=4	y=0.2x+66.09 R^2=0.09 p=0.62 n=5	y=0.09x+75.95 R^2=0.04 p=0.75 n=5	y=0.10x+65.39 R^2=0.01 p=0.64 n=19

Also, no trend was found for the number of synchronized motor unit pairs as a function of the contraction sequence. When the subjects were grouped, the SI and the number of synchronized pairs were statistically independent of the endurance time. (See Table I for details.)

Number of newly recruited motor units -- As it was previously noted by Adam and De Luca (2005), motor units were recruited during the successive contractions to partially compensate for the decrease in the amplitude of the force twitches of the active motor units. For each subject there was a trend for the number of observed recruited motor units to increase during the contraction sequence. In subjects #2 and #3 the trend was significant, whereas for subjects #1 and #4 it was not. (See Table I.) Nonetheless, when all subjects were grouped, the increasing trend was significant. A significant relation between the number of newly recruited motor units and the CV of the force was found only for subject #2 ($R^2 = 0.96$, $p= 0.018$). No significant relation was found for the other subjects ($R^2 = 0$, $p=0.91$ for subject #1; $R^2 = 0.67$, $p=0.092$ for subject #3; $R^2 = 0.50$, $p=0.18$ for subject #4).

Discussion

A muscle does not produce a smooth or constant force, even when it is attempted to do so. In our earlier work we have shown that the firing rates of motor units are not constant and that fluctuations in the firing rates are correlated with the fluctuations in the force output of the muscle (De Luca et al., 1982). The question raised in this work is why the force fluctuation increases during a fatiguing contraction, as it has been reported by Furness et al. (1977), among others. In this study we considered only the intrinsic force fluctuations, that is, those that were caused by the motor unit firing behavior. We did so, by filtering the force and removing any influence of force corrections resulting from attempts at maintaining the force constant.

We investigated the behavior of the motor unit control parameters during constant-force isometric contractions and found only one that presented a significant relationship (in 3 out of 4 subjects) with the observed increase in the force fluctuation. It was the Common Drive derived from the cross-correlation value of the firing rates of motor units. The number of motor units that were recruited tended to increase with endurance time, even if the increase was not significant for

each of the subjects, but was significant when the subjects were grouped. The relation between the number of newly recruited motor units and the coefficient of variation (CV) of the force was not significant for all subjects. The lack of significance may be due to the limited number of motor units that we were able to track.

The firing rate variability remained unaltered for all the motor units which were recruited during the first contraction and could be followed throughout subsequent contractions. Most of the motor units that were recruited during subsequent contractions decreased their CV as their firing rate increased and stabilized; as is typical of newly recruited motor units. With the minor exception of the short-term contribution of the unstable firing rates of newly recruited motor units which is overwhelmed by the unaltered CV of the rest of the active motor units, it does not seem possible for firing rate variability to cause the increase in the force variability. Our finding differs from those of other authors, who relate the force variability, during an isometric contraction, mainly to the variability in the firing rates of the active motor units. Moritz et al. (2005) was able to improve the performance of a motor unit model to predict force variability by acting on the firing rate variability, suggesting that this is a major determinant of the fluctuation in isometric force. This observation may be so, but the fact remains that in reality we found a significant increase in force variability without any significant increase in the firing variability throughout the endurance time that fatigued the muscle to exhaustion. Laidlaw et al. (2000) compared the firing behavior in the FDI muscle between young and old subjects, and found that firing variability has a role in steadiness. However, that finding only held for the lowest force levels contractions (2.5% and 5% MVC) and not for higher force levels (7.5% and 10% MVC). This finding is not unexpected because at force levels below 5% MVC, motor units have firing rates typically less than 10 pulses per second and in the absence of many other motor units the individual pulses and associated force twitches can influence the variability of the force output. Their finding would only apply to fatiguing contractions if the firing rate decreased to the low values associated with a 5% MVC contraction. Such a decrease in the firing rates, however, was not observed in VL motor units during repeated, submaximal contractions according to the fatigue protocol of this study. Instead, our findings are consistent with those of Semmler and Nordstrom (1998), who found no difference

in the firing variability of motor units in the FDI muscle of skilled-trained subjects compared to strength-trained subjects, even though the skilled subjects produced lower force variability; those of Macefield et al. (2000), who reported no change in firing variability of motor units in the extensor hallucis longus during a sustained MVC; and those of Galganski et al. (1993), who found no difference in the firing variability of motor units in the FDI muscle of young and elderly subjects, despite an increased force variability in elderly subjects.

Another firing parameter that has been associated with increasing force variability is the synchronization of motor unit firings. In a computer simulation study, Yao et al. (2000) showed that motor unit firing synchronization increased the amplitude of the fluctuations in the simulated force without altering the magnitude of the average force. In another simulation study, Taylor et al. (2003) reported that an increasing level of short-term synchronization with excitatory drive provided the closest fit to the experimentally observed relation between the coefficient of variation of the force and the mean force. Our findings are consistent with those of Semmler et al. (2000) who showed that an increased force-variability in older subjects was not coupled with higher levels of motor unit firing synchronization. Admittedly, their results could be influenced by the different profile of the motor unit force twitches of the young and elderly subjects nonetheless they raise the question as to the existence of a causal relationship between synchronization and the force variability. In the present study, we found that the degree of synchronization of motor unit pairs that could be tracked across contractions was remarkably low (Synch Index between 2 and 4%, see Figure 12), a value that is consistent with that of previous reports (De Luca et al., 1993; Semmler et al., 2000; Taylor and et al., 2003). Furthermore, both the degree of synchronization and the number of synchronized motor unit pairs did not change significantly as a function of sustained contractions. (See Table I.) Consequently, synchronization cannot account for the increase in the force variability during fatigue.

A motor unit parameter that was found to be altered during fatigue is the Common Drive, defined as the maximum value of the cross-correlation function of the firing rates between pairs of concurrently active motor units. It was found to increase significantly with endurance time in 3 out of 4 subjects. The increase was seen in all motor units and in all subjects. The cross-correlation

between firing rates and the force also increased. These observations are consistent with the prediction of the Lowery and Erim (2005) model. In a simulation study, they superimposed low-frequency oscillations (<5 Hz) to the input of a model that generated motor unit firings (to simulate the Common Drive) and found that both common in-phase fluctuations of mean firing rates and force variability increased, while common oscillatory inputs at frequencies close to the mean firing rate were most effective in inducing short term synchronization. The question remains as to why the Common Drive increases during sustained isometric contractions.

It has previously been proposed by De Luca et al. (2009) that during a sustained contraction, the cross-correlation of motor unit firing rates is influenced by motor unit recruitment via the feedback from the spindles and possibly the Golgi Tendon Organs, with the spindles being the more dominant factor. Muscle spindles respond to the mechanical excitation of the non-fused muscle fibers and provide a discordant excitation to the homonymous motoneurons. Spindles in the proximity of the contracting muscle fibers either slacken or stretch depending on their orientation with respect to the fibers (Binder and Stuart, 1980; Edin and Vallbo, 1990). Thus, Ia firings either decrease or increase until the recruited muscle fibers become fused or quasi-fused. With motor unit recruitment, some motoneurons will be facilitated and some will be disfacilitated due to the discordant afferent input. Consequently, the firing rates of the motor units will vary in a discordant manner and the amplitude of their cross-correlation will decrease. Even if the alignment of the spindles with respect to the muscle fibers was uniform, a discordant afferent input could result from inhomogeneous changes in the sensitivity of the spindles during sustained contractions. In this study, we found a relationship between the number of newly recruited motor units and the cross-correlation value of all motor unit firing rates with endurance time. Thus, it is reasonable to postulate that a decreased spindle influence would result in an increase in the cross-correlation value of the firing rates when motor units are recruited during a fatiguing contraction. We are not aware of any evidence of differential changes in the excitation of individual spindle outputs, but there is evidence for a global change in the spindle firing rates during a sustained contraction. Macefield et al. (1991) reported a decrease in muscle spindle firing rate during voluntary contractions sustained for 1 minute. Hill (2001) suggested that the decrease could be explained by

a progressive fatigue of the intrafusal fibers induced by a prolonged γ-drive to these fibers. Additional support is provided by the work of Avela et al. (1999, 2001) which showed a reduction in the stretch reflex and in the H-reflex amplitude after the performance of a fatiguing repeated passive stretching exercise, and suggested that this was a consequence of a reduction in the activity of the large diameter Ia afferents, resulting from the reduced sensitivity of muscle spindles.

The increasing number of motor units that were recruited during the successive contractions would also provide an increasing force-variability. As the new motor units are recruited they fire with lower firing rates, are not fused, and the individual force twitches increase the force variability. The data would suggest that there is such an influence, but the relationship is significant only for grouped subjects. Perhaps with improved technology, it might be possible to observe more recruited units and provide a data set that could establish significance for the individual subjects as well.

In conclusion, we found that during a sequence of sustained isometric force contractions performed at 20% MVC and repeated until the targeted level could no longer be maintained, the fluctuation of the force about the targeted value increased progressively. The behavior of the force was found to be correlated to the Common Drive of the motor units which increased in progressive contractions. The increasing number of newly recruited motor units is also likely to produce the increasing force-fluctuation. The coefficient of variation of the firing rates and the synchronization of the motor unit firings were not found to alter as a function of endurance time, and consequently could not account for the increase in variability of the force during fatigue.

CHAPTER 4

THE EXCITATION PLANE

Introduction

When a muscle contracts, motor units are recruited and modulate their firing rate according to the force demand. It is well known that motor units are activated in order of increasing size and excitability (Henneman, 1957), and that the range of forces where motor units are recruited differs for different muscles (De Luca et al., 1982a, 1996). Animal studies employing steady injected currents that directly stimulate the motoneurons have shown that the frequency versus current relation may be represented by a single straight line for all currents up to those causing inactivation (Granit et al., 1963; Kernell, 1965a). The firing rate at recruitment has often been associated to the time course of the after-hyperpolarization (AHP), so that earlier recruited motor units, which are characterized by slower AHP, also display lower minimum firing rates (Kernell, 1965c). In human studies, a positive relation between recruitment threshold and initial firing rate has been found by more recent studies (De Luca and Erim,1994; Erim et al., 1996; Moritz et al., 2005); whereas other authors indicate that motor units start firing with approximately the same firing rate regardless of their recruitment threshold (Tanji and Kato, 1973; Freund et al., 1975; among others). However, the different observations on the initial firing rates are highly dependent on the available technology and the methods used for estimating the first firings of a motor unit. Contrasting reports also exist for the maximal firing rates: firing rates have been observed to either converge to the same value near maximal force levels (De Luca and Erim, 1994; Erim et al., 1996), or to reach lower values for later recruited motor units (Tanji and Kato, 1973; De Luca et al., 1982). Moritz et al. (2005) reported that high-threshold motor units might be able to fire faster than low-threshold motor units.

In this study we were interested in studying the firing rate behavior of motor units during linearly increasing force contractions up to maximum voluntary contraction force (MVC), at different rates of force increase. In our protocol, we requested the subjects to use visual feedback in order to follow ramp trajectories up to either maximal force (100% MVC) at a rate of 10% MVC/s,

or up to 80% MVC at a rate of 4% MVC/s, or up to 50% MVC by tracking a slower ramp trajectory, at a rate of 2% MVC/s. A newly developed decomposition technique applicable to surface EMG signals (De Luca et al., 2006; Nawab et al., in press), was used to observe a large number of motor units recruited on almost the entire range of recruitment in two different muscles, and to follow their behavior from recruitment up to maximal force levels. The aim of the project was to model the behavior of the firing rates as a function of excitation during isometric force contractions.

Methods

Two muscles were studied: the vastus lateralis (VL) muscle and the first dorsal interosseous (FDI) muscle.

Subjects -- Eight healthy subjects (3 males and 5 females) reporting no known neurological disorder participated in the study. The age of the subjects was 21.29 ± 2.36 yr (range 19 – 26 yr). An informed consent form approved by the Institutional Review Board at Boston University was read and signed by all subjects before participation in the study.

Force measurements -- For the VL experiments, subjects were seated in a chair designed to restrain hip movement and immobilize their dominant leg at a knee angle of 60° flexion. Isometric knee extension force was measured via a load cell attached to a lever arm and a pad positioned against the tibia, 3 cm above the medial malleolus. For the FDI experiments, subjects were seated with their upper limb extended. Their dominant hand was immobilized with straps so that the FDI was constrained to contract isometrically. The abduction force was measured by placing a strain-gauge force transducer against the proximal interphalangeal joint of the index finger. Isometric force was band-pass filtered from DC – 450 Hz and digitized at 20 kHz, the sampling rate of the Decomposition system.

EMG recording -- Surface EMG signals were recorded from the muscle of the dominant limb by using a surface sensor array comprised of five pins (0.5 mm in diameter) with blunted ends that protrude from the housing so that, when pressed against the skin, they make a surface indentation. Pins are located at the edges of a 5 x 5-mm square, and in the center of the square.

Four differential combinations of signals from the detection surfaces were selected and amplified to yield four separate EMG channels. The signals were band-pass filtered (20 Hz – 1750 Hz), sampled at 20 kHz, and stored on a PC for offline data analysis.

The sampling rate of 20 kHz was required to provide sufficient time resolution for the decomposition algorithms.

Protocol -- At the beginning of the experimental session, three brief maximal contractions of approximately 3 s in duration were performed with a rest period of 3 min between the contractions. The greatest value of the three trials was chosen as the maximal voluntary contraction (MVC) force. In this fashion, all contractions were produced at the same relative force level. The subjects were then asked to follow a force trajectory presented on a computer screen by isometrically contracting the muscle. Three different trajectories were tracked: a force trajectory up to 100% MVC (with a ramp up at a rate of 10% MVC/s), a trapezoidal force trajectory up to 80% MVC (comprised of a ramp up at a rate of 4% MVC/s and a hold phase of approximately 5 s), and a trapezoidal force trajectory up to 50% MVC (with a ramp up at a rate of 2% MVC/s and a hold phase of approximately 5 s). The three different force paradigms were designed to highlight differences in the firing rate generation process at different rates of force increase. Two repetitions were performed for each trajectory, and rest period of at least 10 min was given in between trials. During the recording sessions, because the contractions were performed at a force rate lower than that chosen by the subjects when being tested for the 100% MVC value, subjects were not usually able to reach the MVC force. They were then asked to follow the trajectory up to the highest possible force level. The three different trajectories tracked by one of the subjects during the VL experiments are presented in Figure 13.

Data analysis -- Surface EMG signals were decomposed into their constituent motor unit action potential trains by means of a set of algorithms that uses a specially developed knowledge-based artificial intelligence framework (De Luca et al., 2006; Nawab et al., in press). The accuracy ranges from 85% to 97%, with an average of 92.6% (Nawab et al., in press). The decomposition procedure yielded a train of firing instances for all the motor units that were identified during the contraction.

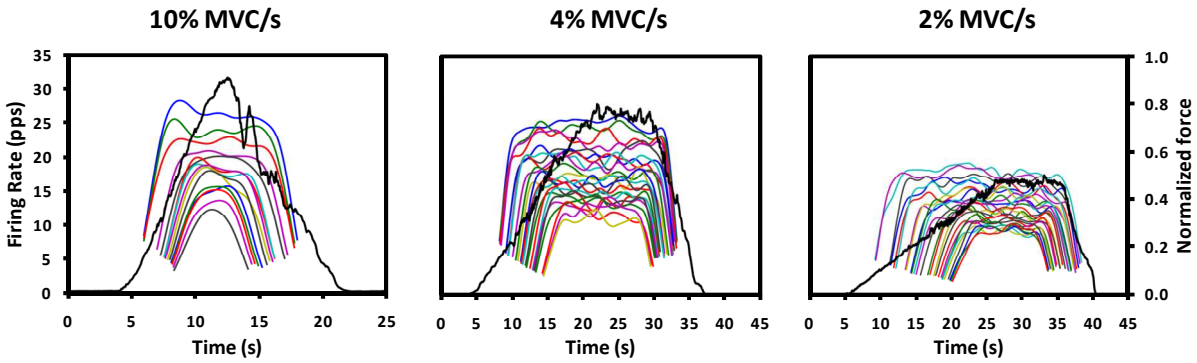

Figure 13: Protocol. Three types of contractions were performed: a linearly increasing force contraction at 10% MVC/s up to 100% MVC (on the left-hand side), a linearly increasing force contraction at 4% MVC/s up to 80% MVC followed by a 5-s hold phase (middle plot), and a linearly increasing force contraction at 2% MVC/s up to 50% MVC followed by an approximately 5-s hold phase (on the right-hand side).

The time-varying mean firing rate of each motor unit was computed by low-pass filtering the impulse train, representing the time occurrence of each motor unit firing, with a unit-area Hanning window of 4-s duration (LeFever and De Luca, 1982a). For each motor unit, four parameters were extracted from the mean firing rate data: the recruitment threshold (τ_r), the firing rate at recruitment (λ_r), the maximal firing rate (λ_m), and the slope of initial firing rate increase with time (ν). The recruitment threshold was calculated as the force level at which the motor unit began to fire. The firing rate at recruitment was estimated from the average of the first three interpulse intervals, and the maximal firing rate was computed as the maximum of the mean firing rate curve in the 100% MVC contractions, and as the mean firing rate over an approximately 5-s interval during the constant part of the force in the 80% MVC contractions. The slope (velocity) of the initial firing rate increase was computed as the slope of a regression line fitted to the initial approximately linear increase of the mean firing rate curve. The force signal was low-pass filtered by using a 4-s unit-area Hanning window, and the mean firing rates during the linearly increasing part of the contraction (ramp up) were plotted as a function of force. Again, the velocity of the firing rate increase was computed as the slope of a regression line fitted to the initial part of the mean firing rate curve plotted as a function of force. Firing rates at recruitment, maximal firing rates, and the velocity of the firing rates were plotted versus the recruitment thresholds of the motor units and a linear regression analysis was performed. The slope of the regression was tested

for significant difference from the value 0 according to the two-tailed t-statistic using a threshold $\alpha = 0.05$.

Results

Recruitment Threshold -- The VL muscle and the FDI muscle were characterized by different recruitment ranges: motor units were recruited up to 60% MVC in the FDI muscle and up to 76% MVC in the VL muscle.

Firing rate at recruitment -- Firing rates at recruitment ranged approximately from 4 to 14 pps in the FDI muscle, and from 4 to 13 pps in the VL muscle. A linear relation between firing rates at recruitment and recruitment threshold was found, so that earlier recruited motor units always displayed greater initial firing rates ($R^2 = 0.46$, $p<0.0001$ for the FDI muscle; $R^2 = 0.25$, $p<0.0001$ for the VL muscle in the faster contractions; $R^2 = 0.46$, $p<0.0001$ for the FDI muscle; $R^2 = 0.35$, $p<0.0001$ for the VL muscle in the intermediate contractions; $R^2 = 0.42$, $p<0.0001$ for the FDI muscle; $R^2 = 0.13$, $p<0.0001$ for the VL muscle in the slower contractions). (See Table II and Figure 14 and 15.) Similar values for the slope and the intercept of the regression lines were found when analyzing the faster, intermediate, and the slower contractions. (See Table II.)

Maximal firing rate -- Maximal firing rates ranged from approximately 7 to 35 pps in the FDI muscle, and from 5 to 30 pps in the VL muscle. In the same way as for the firing rate at recruitment, an inverse linear relation was found between maximal firing rates and recruitment thresholds ($R^2 = 0.65$, $p<0.0001$ for the FDI muscle; $R^2 = 0.51$, $p<0.0001$ for the VL muscle in the faster contractions; $R^2 = 0.68$, $p<0.0001$ for the FDI muscle; $R^2 = 0.49$, $p<0.0001$ for the VL muscle in the intermediate contractions; $R^2 = 0.79$, $p<0.0001$ for the FDI muscle; $R^2 = 0.48$, $p<0.0001$ for the VL muscle in the slower contractions). (See Table II and Figure 14 and 15.) Lower values for the intercept of the regression lines were observed as the slope of the contractions was decreasing (the target force level was also decreasing from 100% MVC to 80% and 50% MVC). (See Table II.)

Velocity of the firing rate -- A negative linear relation between the velocity of the firing rate and the recruitment threshold was found contractions when the mean firing rates were plotted

as a function of time (R^2 = 0.64, p<0.0001 for the FDI muscle; R^2 = 0.49, p<0.0001 for the VL muscle in the faster contractions; R^2 = 0.76, p<0.0001 for the FDI muscle; R^2 = 0.38, p<0.0001 for the VL muscle in the intermediate contractions; R^2 = 0.76, p<0.0001 for the FDI muscle; R^2 = 0.32, p<0.0001 for the VL muscle in the slower contractions). (See Table II and Figure 14 and 15.)

Similar results were obtained when the mean firing rates were plotted as a function of force, since the force was linearly varying with time. (See Table II.) When the mean firing rate curves were plotted as a function of time, the slope and intercept of the regression lines were similar when comparing the results from contractions with different slopes. If they were plotted as a function of force, the slope and intercept of the regression lines computed from the contractions performed at a rate of 2% MVC/s and 4% MVC/s were approximately 5 and 2.5 times slower than the slope and intercept of the regression lines from the contractions performed at 10% MVC/s, given that the force was linearly varying with time. (See Table II and Figure 14 and 15.)

Table II: Firing rate behavior: statistics. Statistics from the regression analysis on the firing rates at recruitment (λ_r), the maximal firing rates (λ_m), and the velocity of the firing rates (ν) (for the firing rates (λ) plotted as a function of time (t) and as a function of force (ϕ)) versus the recruitment thresholds of the motor units (τ_r).

		FDI				**VL**			
		λ_r	**λ_m**	**ν (λ vs. t)**	**ν (λ vs. ϕ)**	**λ_r**	**λ_m**	**ν (λ vs. t)**	**ν (λ vs. ϕ)**
10% MVC/s	**Slope**	-11.20	-39.61	-19.54	-1.83	-5.69	-26.74	-9.47	-0.9
	Intercept	10.56	30.44	12.80	1.20	9.32	28.26	10.03	0.93
	R^2-value	0.46	0.65	0.64	0.61	0.25	0.51	0.49	0.45
4% MVC/s	**Slope**	-9.31	-30.61	-17.25	-4.57	-7.58	-25.75	-10.95	-3.03
	Intercept	9.62	27.01	11.20	2.74	9.39	25.89	9.74	2.39
	R^2-value	0.46	0.68	0.76	0.78	0.35	0.49	0.38	0.37
2% MVC/s	**Slope**	-10.86	-46.19	-17.96	-9.40	-5.68	-29.54	-12.58	-7.55
	Intercept	8.75	25.52	8.42	4.19	7.44	20.41	7.05	3.72
	R^2-value	0.42	0.79	0.76	0.68	0.13	0.48	0.32	0.32

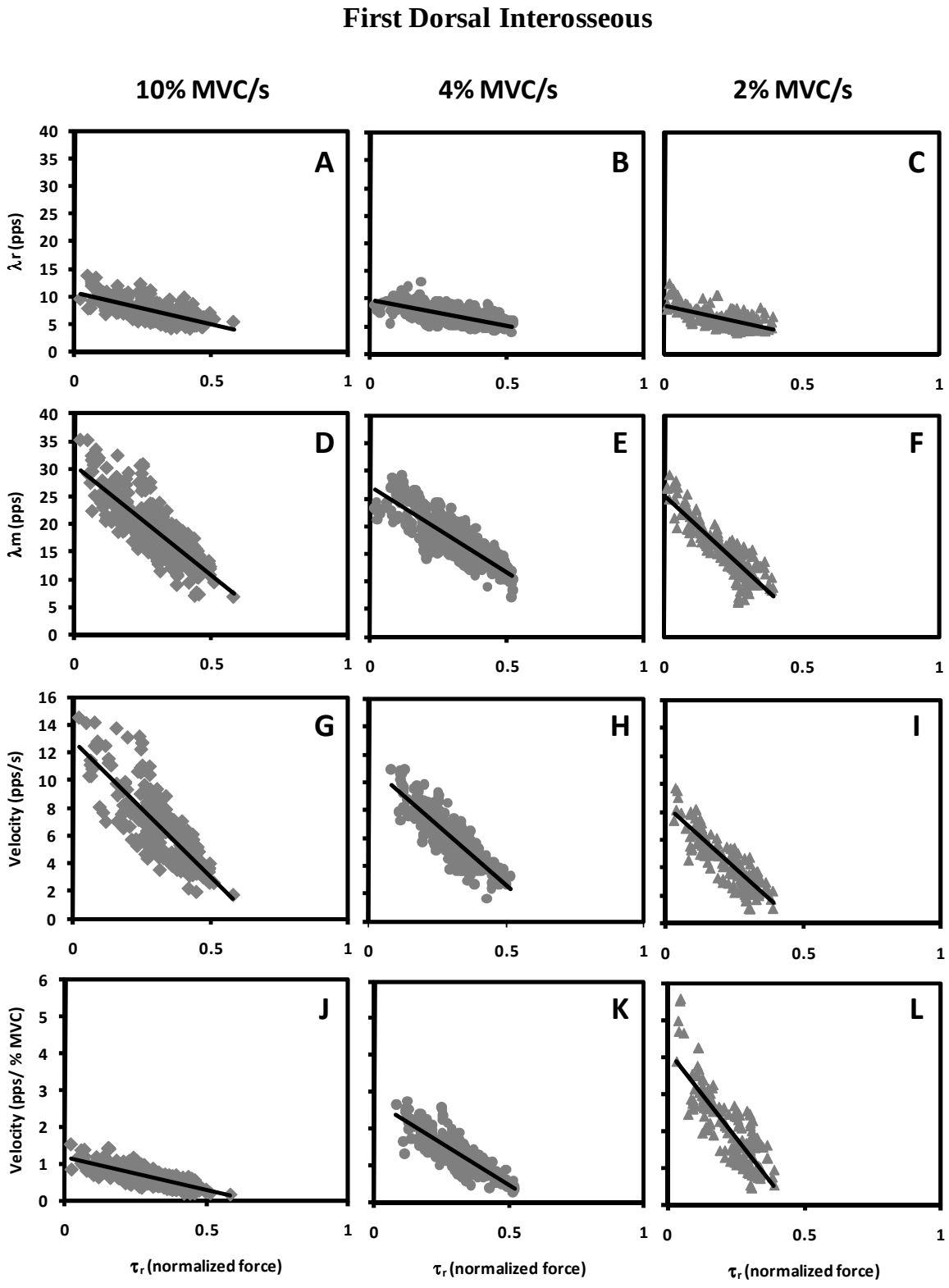

Figure 14: Experimental results: FDI. Firing rates at recruitment (λ_r) (A, B, C), maximal firing rates (λ_m) (D; E, F), velocity (ν) of the firing rate (firing rate as a function of time (G, H, I) and as a function of force (J, K, L)) versus recruitment thresholds (τ_r) for the FDI muscle. The left-hand side column reports the results from the faster contractions (performed at 10% MVC/s), the middle column shows the results from the intermediate contractions (performed at 4% MVC/s), and the right-hand side column shows the results from the slower contractions (performed at 2% MVC/s).

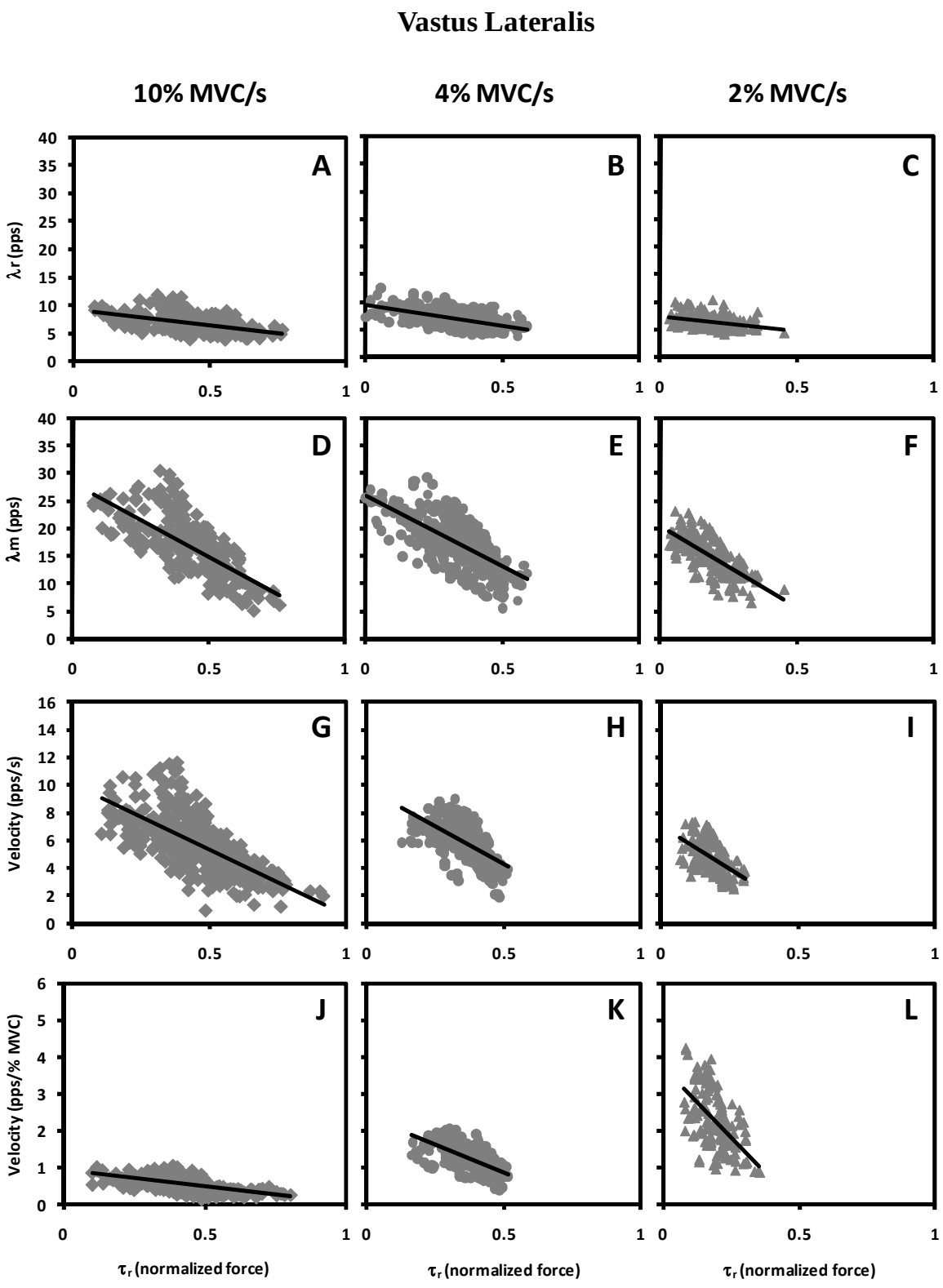

Figure 15: Experimental results: VL. Firing rates at recruitment (λ_r) (A, B, C), maximal firing rates (λ_m) (D, E, F), velocity (ν) of the firing rate (firing rate as a function of time (G, H, I) and as a function of force (J, K, L)) versus recruitment thresholds (τ_r) for the VL muscle. The left-hand side column reports the results from the faster contractions (performed at 10% MVC/s), the middle column reports the results from the intermediate contractions (performed at 4% MVC/s), and the right-hand side column shows the results from the slower contractions (performed at 2% MVC/s).

Model of firing rate behavior -- When a motor unit is recruited, it begins firing with an initial firing rate λ_r, which is characteristic of each motor unit and is linearly related to its recruitment threshold τ_r, so that earlier activated motor units always display a higher firing rate at recruitment.

When the force is increased, the motor unit increases its firing rate accordingly, up to a maximal value λ_m. This value is also linearly related to τ_r, so that earlier recruited motor units show higher maximal firing rates. Furthermore, the results of this study indicate that, during linearly increasing force contractions, earlier recruited motor units increase their firing rates faster than later recruited motor units, and that this increase is independent of the contraction type or of the rate of increase of the force. As the excitation is increased, the velocity of the mean firing rates decreases and they reach a maximal value, beyond which no further increase is observed. (See Figure 13.) This behavior may be fitted with an exponential equation:

$$\lambda_r + (\lambda_m - \lambda_r) * (1 - e^{(\frac{t_r - t}{\theta})})$$

where t_r is the recruitment time and θ is the time constant of the firing rate increase. This equation was chosen because it is able to describe the increase of the mean firing rates from the characteristic minimal value at recruitment up to the maximal value at or near maximal force, and it provides a good fit to the firing rate curves (R^2 values always greater than 0.95 for the contractions increasing at 10% MVC/s; R^2 values always greater than 0.84 for the contractions rising at 4% MVC/s; R^2 values always greater than 0.82 for the contractions rising at 2% MVC/s). In order to compute θ, the equation was fitted to the mean firing rate curves, given the already calculated values for λ_r, λ_m, and t_r. Similarly to the previous data analysis, the time constant of firing rate increase was plotted as a function of recruitment threshold, and a linear regression analysis was performed. A positive linear relation was found between θ and τ_r ($R^2 = 0.43$, $p<0.0001$ for the FDI muscle; $R^2 = 0.29$, $p<0.0001$ for the VL muscle in the 10% MVC/s contractions; $R^2 = 0.32$, $p<0.0001$ for the FDI muscle; $R^2 = 0.21$, $p<0.0001$ for the VL muscle in the 4% MVC/s contractions; $R^2 = 0.25$, $p<0.0001$ for the FDI muscle; $R^2 = 0.21$, $p<0.0001$ for the VL muscle in the 2% MVC/s contractions). (See Table III and Figure 16.)

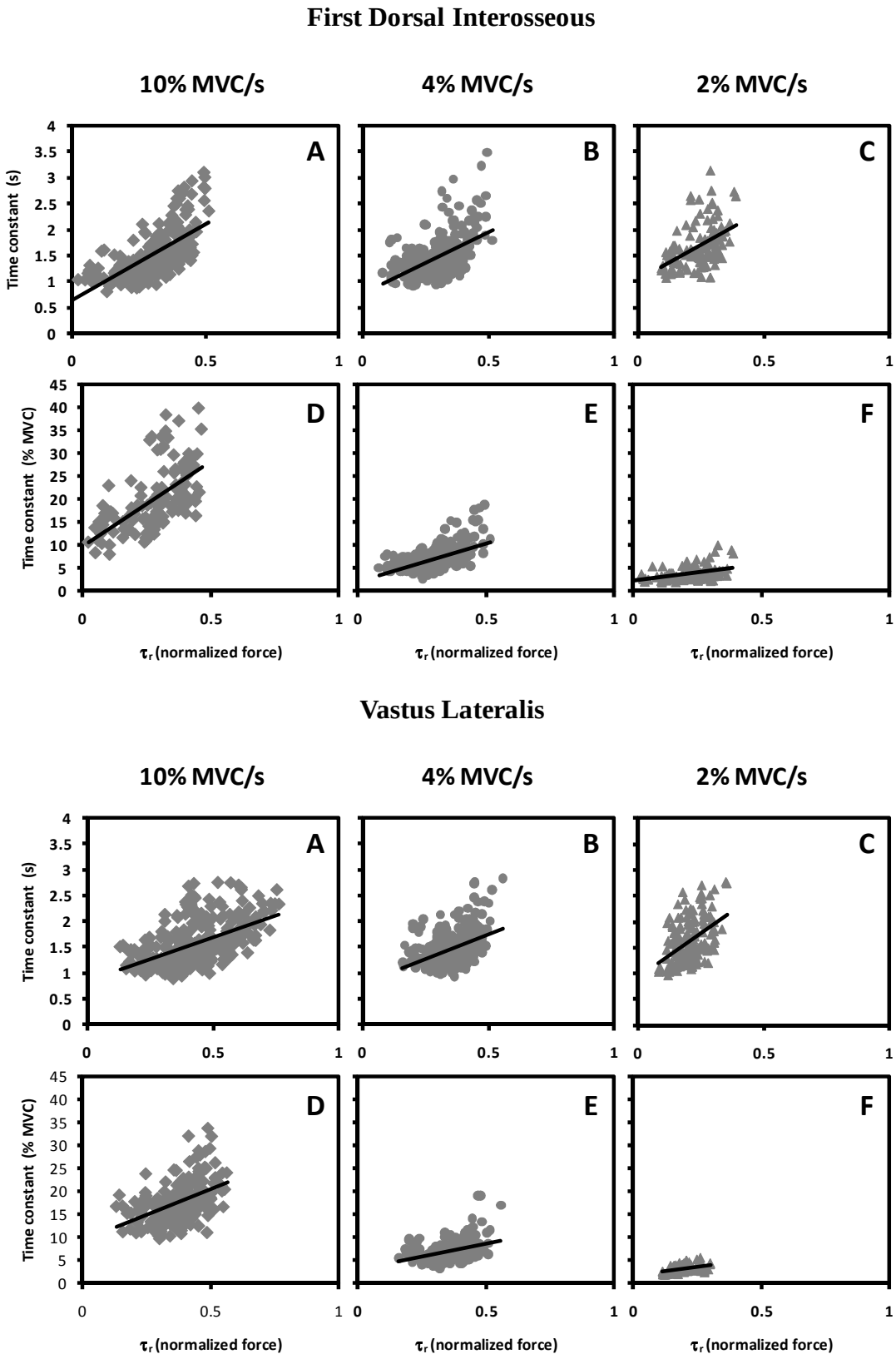

Figure 16: Experimental data: FDI and VL. The time constant of the exponential functions that were fitted to the curves are plotted versus the recruitment threshold of the motor units. In A, B and C the mean firing rates were plotted as a function of time, in D, E and F they were plotted as a function of force. The left-hand side column contains data from the faster contractions (ramp up at 10% MVC/s), the middles column shows data from the intermediate contractions (ramp up at 4% MVC/s), while the right hand side columns contains data from the slower contractions (ramp up at 2% MVC/s).

The same equation was fitted to the mean firing rate curves plotted as a function of force, where the variable t was replace by ϕ, the output force, and the time of recruitment t_r was replaced by the recruitment force τ_r. Again, a linear relation exists between θ and τ_r ($R^2 = 0.38$, $p<0.0001$ for the FDI muscle; $R^2 = 0.22$, $p<0.0001$ for the VL muscle in the 10% MVC/s contractions; $R^2 = 0.37$, $p<0.0001$ for the FDI muscle; $R^2 = 0.15$, $p<0.0001$ for the VL muscle in the 4% MVC/s contractions; $R^2 = 0.21$, $p<0.0001$ for the FDI muscle; $R^2 = 0.22$, $p<0.0001$ for the VL muscle in the 2% MVC/s contractions). (See Table III and Figure 16.) The equation was able to adequately fit the mean firing rate curves (the R^2 values of the fit was always greater than 0.94 for the contractions rising at 10% MVC/s; always greater than 0.93 for the contractions rising at 4% MVC/s; always greater than 0.87 for the contractions rising at 2% MVC/s).

Table III: Time constant of firing rate increase: statistics. Statistics from the regression analysis on the time constant of firing rate increase as a function of motor unit recruitment threshold.

		FDI		VL	
		θ (λ vs. t)	**θ (λ vs. ϕ)**	**θ (λ vs. t)**	**θ (λ vs. ϕ)**
10% MVC/s	**Slope**	2.89	36.62	1.72	22.93
	Intercept	0.65	9.92	0.83	9.12
	R^2-value	0.43	0.38	0.29	0.22
4% MVC/s	**Slope**	2.37	16.96	1.92	11.07
	Intercept	0.78	1.95	0.79	3.02
	R^2-value	0.32	0.37	0.21	0.15
2% MVC/s	**Slope**	2.74	7.63	3.48	8.14
	Intercept	1.02	2.22	0.92	1.58
	R2-value	0.25	0.21	0.21	0.22

Similarly to what was previously observed, the slope and intercept of the regressions were approximately the same when comparing the results for the faster and slower contractions if the mean firing rate curves were plotted as a function of time. If they were plotted as a function of force, θ was equivalent to that of the force slope values of the two contractions. An example of the mean firing rate curves fitted with the above equation for the two muscles is presented in Figure 17 for both contraction types.

The excitation plane -- During voluntary linearly varying isometric contractions, an association exists between the increasing muscle force and the increasing excitation to the motoneuron pool. In the absence of excitation (normalized excitation E = 0, equal to 0% of maximal excitation), there are no active motor units and no force is produced (normalized force ϕ = 0, equal to 0% of maximal force output). As the excitation increases, motor units are recruited and increase their firing rates. Consequently, the force output increases. The maximal level of excitation (normalized excitation E = 1, equal to 100% of maximal excitation) can be thought of as the excitation required in order to exert the maximal force output (normalized force ϕ = 1, equal to 100% of maximal force output). Thus, the motor unit firing rate behavior as a function of force can be thought of as the behavior as a function of excitation.

In this study, we showed that the range of the firing rates of all motor units is bounded from an initial value to a maximal value, when the excitation goes from zero to maximal level, and that this range is muscle dependent. We showed that the increase of the motor unit firing rates can be suitably described by an exponential function, whose time constant is greater for later recruited motor units. Furthermore, the rate of increase of the mean firing rates appeared to be independent of the slope of the force trajectory, and thus to be independent of the excitation received by the motoneuron pool. This result suggests that each motor unit has a characteristic rate of rise, and that, regardless of the excitation received, once it is activated above its recruitment threshold, it will start increasing its firing rate with a characteristic time constant and it will continue increasing as long as the excitation is provided. We introduced an exponential equation which models the

excitation-firing rate relation, together with the distributions of firing rates at recruitment, maximal firing rates, and time constant of firing rate increase.

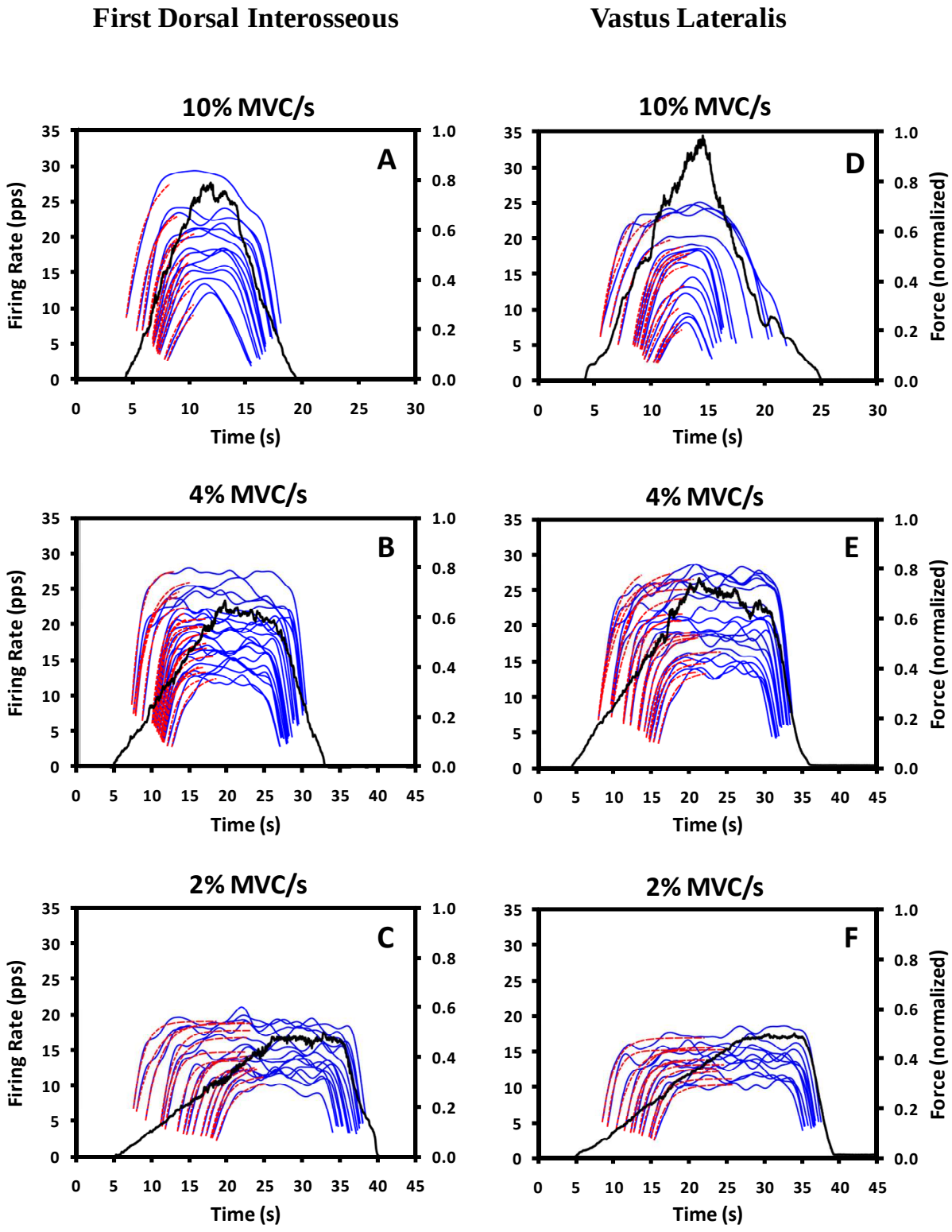

Figure 17: Results of the fit. The mean firing rate were fitted with the exponential function and the time constant of the exponential rise was computed.

If the equation is used to estimate the firing rate of all the motor units in a motor unit pool as a function of increasing excitation, from zero to maximum excitation, we obtain the "excitation plane" which spans the entire firing rate range for each motor unit. The excitation plane was drawn for the muscles analyzed in this study for a contraction increasing at a rate of 10% MVC/s using the experimentally obtained distributions (see Table IV) for the firing rates at recruitment, maximal firing rates, and time constant of firing rate increase. (See Figure 18.)

Table IV: Equation modeling the Excitation Plane. Modeled distributions of firing rates at recruitment, maximal firing rate, and time constants of firing rates increase for the two muscles of the study (*i* represents the motor unit number).

	First Dorsal Interosseous	Vastus Lateralis
Firing rate at recruitment	$\lambda_r(i) = -11.20 * \tau_r(i) + 10.56$	$\lambda_r(i) = -5.69 * \tau_r(i) + 9.32$
Maximal firing rate	$\lambda_m(i) = -39.61 * \tau_r(i) + 30.44$	$\lambda_m(i) = -26.74 * \tau_r(i) + 28.26$
Time constant	$\theta(i) = 36.62 * \tau_r(i) + 9.92$	$\theta(i) = 22.93 * \tau_r(i) + 9.12$

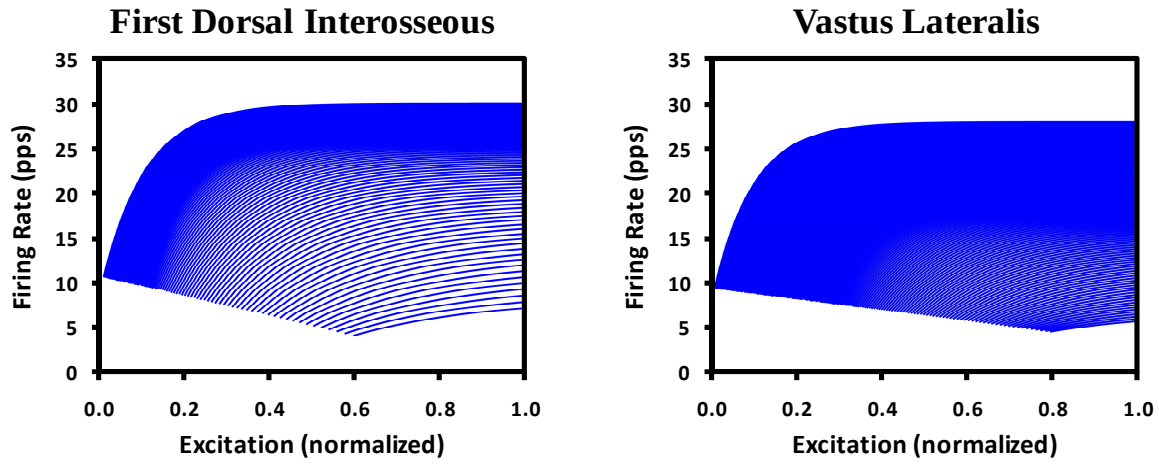

Figure 18: Excitation plane. Excitation plane drawn for the two muscles of the study for contractions where the force is increased at a rate of 10% MVC/s. Note that, for the VL muscle, only half of the motor units were displayed.

The number of motor units (*N*) was set to 120 for the FDI muscle (Feinstein et al., 1955), and to 600 in the VL muscle (data derived from the rectus femoris muscle, Christensen, 1959). A range of recruitment threshold was assigned to each muscle: 0-60% MVC for the FDI muscle, 0-80% MVC for the VL muscle; and the recruitment threshold was assumed to have an exponential distribution (Fuglevand et al., 1993). These excitation planes, drawn for contractions increasing at a rate of 10% MVC/s for the FDI and the VL muscles, will be used in the next chapter for the simulation of muscle force.

Discussion

Firing rate behavior has been studied extensively, both in animals and in human subjects. Discrepancies still exist on the ranges and distributions of firing rates at recruitment and at maximal force levels, and on the way they adapt to changes in the excitation received by the motoneuron pool.

In this study, we were able to detect a large number of motor units from two different muscles via a newly developed decomposition technique applicable to surface EMG signals and we were able to observe the firing rate behavior over the entire force range.

The ranges of the recruitment threshold differed for the two muscles, and results were consistent with previously reported values. In the FDI muscle, motor units were recruited approximately up to 60% MVC, as previously reported by other investigators (Freund et al., 1975 (0 - 58% MVC); Thomas et al., 1986 (0 - 54% MVC); Kamen et al., 1995 (0 - 60% MVC)). A wider range of recruitment was found for the VL muscle (up to 80% MVC).

Firing rates at recruitment had slightly wider ranges than what previously reported in the literature. In the FDI muscle, the range was 4 - 14 pps (8.4 ± 1.3 pps was the mean ± standard deviation observed by Milner-Brown et al., 1973; 8.9 ± 2.2 pps by De Luca et al., 1982; 4 - 10 pps (6.5 ± 13.6 pps) was the range observed by Duchateau and Hainaut, 1990). For the VL muscle, the range observed was 4 - 13 pps. Firing rates at recruitment have often been associated to the time course of the after-hyperpolarization (AHP), so that earlier recruited motor units, which are characterized by slower AHP, also display lower minimum firing rates (Kernell, 1965c). This

finding was in agreement with those of Erim et al. (1996, 1999), Moritz et al. (2005), and Clamann (1970), who observed a positive linear relation between recruitment threshold and initial firing rate. In this study, a significant negative linear relation was found between initial firing rates and recruitment threshold. It should be noted that differences in the range and distribution might derive from the difficulty in accurately detecting the first firings of a motor unit action potential train. Furthermore, results are highly dependent on the method employed to estimate the initial firing rate value: in this study, it was computed as the inverse of the average of the first three interpulse intervals.

The maximal firing rates ranged from 7 to 35 pps in the FDI muscle. A range of 17 - 47 pps (*) was reported by Duchateau and Hainaut (1990); 18 - 50 pps (*) by Bigland-Ritchie et al. (1992); 23 - 92 pps (*) by Kamen et al. (1995); 16 - 64 (*) by Seki et al. (2005); all during maximal voluntary contractions. (*) indicates that values were visually derived from plots. Our data suggest that the maximal firing rates vary over a smaller interval in the VL muscle (5 - 30 pps), whereas a range of 12 - 40 pps has been reported by Woods et al. (1987). A significant negative linear relation was observed between maximal firing rates and recruitment threshold, so that the "onion skin" phenomen (De Luca et al., 1982a) also holds at maximal force levels. A slightly negative correlation has been previously found in the FDI muscle, but not in the deltoid muscle by De Luca et al. (1982a). Tanji and Kato (1973) and Monster and Chan (1977) also found that some earlier recruited motor units reached higher maximal firing rates. In contrast, when approaching the highest force levels, firing rates tended to converge to similar values in the TA muscle (De Luca and Erim, 1994; Erim et al., 1996). Moritz et al. (2005) reported that high-threshold motor units reach higher peak firing rates than low-threshold motor units, as did Kosarov and Gydikov (1976). Again, differences might arise from the difficulty in accurately tracking motor unit firings at maximal force levels, due to movement of the electrode to or a higher degree of action potential superposition.

Kernell (1965a, b) studied the relation between the strength of the stimulus current and the firing rate in cat motoneurons, and suggested that the firing rate behavior can be considered a linear function of the current over a certain range ("the primary range", which goes to the initial

firing rates up to an average firing rate of 51 pps). With a further increase in the stimulus current, only some motoneurons were able to fire even faster, in the so called “secondary range”, and again the relation between current and firing rate was linear but with a steeper slope. Gydikov and Kosarov, 1974, and Monster and Chan, 1977, also observed that low threshold motor units tended to saturate as muscle force is increased in the biceps brachii and in the extensor digitorum communis muscles. Our data indicate that firing rate behavior is independent of the contraction type, suggesting that, once they are recruited, all motor units increase their firing rates following their own characteristic rate of rise up to a maximal firing rate value which depends on the excitation received. Finally, firing rate behavior can be modeled with a simple exponential function with different time constants of firing rate increase for each motor unit.

We can thus define an excitation plane, that describes the relation between the common excitation received by the entire motoneuron pool and the different electrical responses of each motor unit in the pool. The contours of the plane vary among muscles, since different muscles will present diverse control properties of motor units, such as different ranges of recruitment thresholds and of initial or maximal firing rates.

CHAPTER 5

MODEL OF MUSCLE FORCE GENERATION

Introduction

Muscle force is the mechanical response of the muscle fibers to the excitation received by the motoneuron. The muscle twitch is the response to a single stimulus of the motor unit (MU). The force is modulated by the increasing or decreasing the activation of the motor units within a muscle, which is accompanied by a modulation of the firing rates and recruitment of the motor units. As the firing rates of the MUs increase, the force from individual twitches summate to produce a prolonged contraction, this is commonly referred as tetanization. The objective of this work is to develop a muscle force model capable of explaining how the Central Nervous System and the Peripheral Nervous System control motor units to produce force. The model is a continuation of the work of Adam (2003) and was intended to improve upon a previous model (Erim and Aghera, 2001) by incorporating recent findings on the firing rate generation process (see Chapter 4); time-dependent changes in motor unit twitch parameters; and a feedback loop that enables the simulation of force production during the performance of constant force isometric contractions, which require the subject to follow a predetermined force trajectory. The model was used to simulate sustained constant-force contractions in the first dorsal interosseous (FDI) and the vastus lateralis (VL) muscles.

Methods

Model Layout

The model is based on the concept of the common drive (De Luca et al., 1982a; De Luca and Erim, 1994) and the onion skin phenomenon (De Luca and Erim, 1994). The common drive states that all the motoneurons in a pool receive a common excitatory signal that modulates the firing rate of the motor units in unison. This common excitation determines the number of active motor units and their firing rates. The onion skin phenomenon states that firing rate of motor units

are inversely related to their recruitment threshold. The electrical behavior of the motor units is then translated into force, given the mechanical characteristics of the individual motor units. Finally, the compound muscle force is obtained as the linear summation of the forces generated by each active motor unit. If the output force is kept constant, such as in a constant-force tracking task, the error between the output force and the target force is fed back to the input of the model to adequately modify the excitation signal. The layout of the model is depicted in Figure 19. The basic building blocks are: (1) the "excitation plane" block, which represents the relation between the common excitation received by the motoneuron pool and the electrical response of the motor units (number of active motor units and their firing rates); (2) the "force twitch" block, which translates the electrical behavior of the motor units into their mechanical response; and (3) the "feedback loop" block, which modifies the input signal in order to maintain the output force at a set constant level. Intermediate steps are introduced to faithfully model the force production process, such as the generation of the motor unit impulse trains; the introduction of noise and of a common oscillatory behavior in the firing rates of all active motor units; the time-dependent changes in the force twitches; the introduction of a gain to account for the non-linear summation of twitches; and the summation over time of the individual twitches to obtain the output motor unit force. All the intermediate steps will be described in the corresponding major building block paragraph.

Input

The input to the system is an excitation signal (E) common to all motor units, which represents the excitation required to attain a certain force level. During voluntary linearly-varying isometric contractions, an association exists between the increasing muscle force and the increasing excitation to the motoneuron pool. In the absence of excitation (normalized excitation $E = 0$, equal to 0% of maximal excitation), there are no active motor units and no force is produced (normalized force $\phi = 0$, equal to 0% of maximal force output). If the excitation is increased, more and more motor units are recruited, the firing rates of motor units increase, and the force output increases. The maximal level of excitation (normalized excitation $E = 1$) can be thought of as the excitation

required in order to exert the maximal force output (normalized force ϕ = 1, equal to 100% of maximal force output).

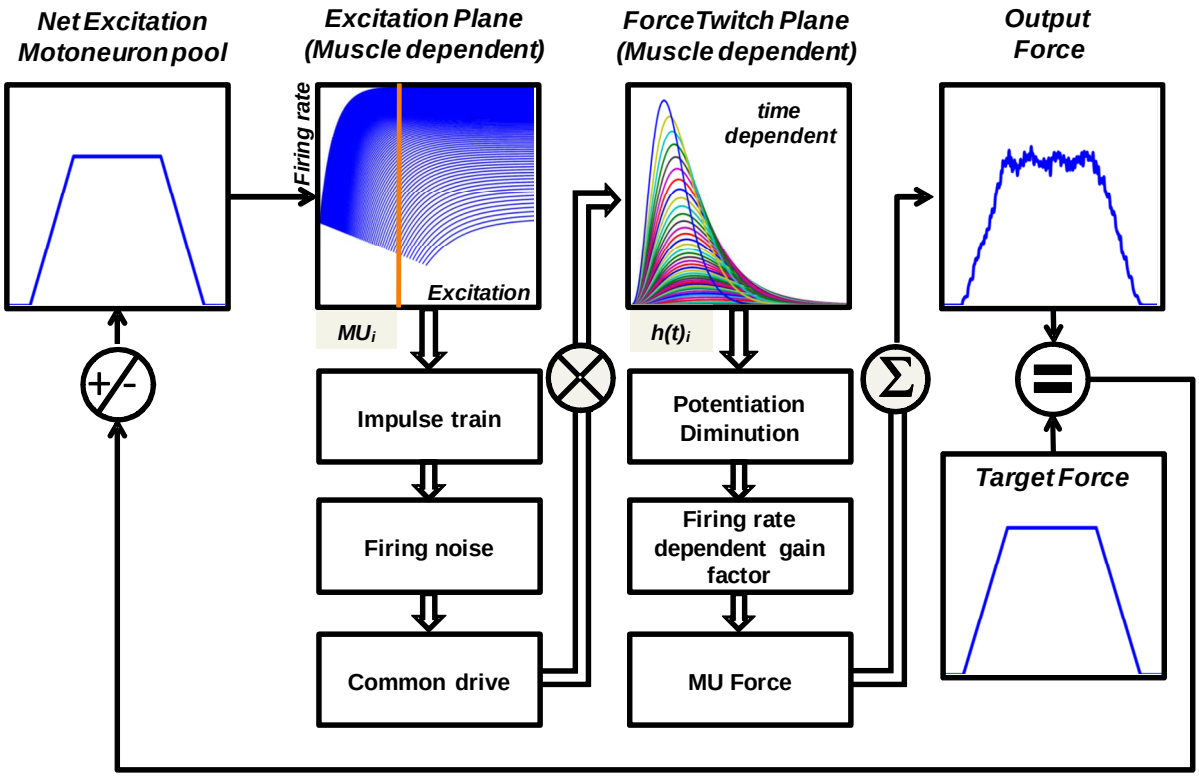

Figure 19: Model block diagram. The input to the muscle force model is the common excitation to the motoneuron pool, and the output is the muscle force. The basic building blocks are the "excitation plane" block and the "force twitch plane" block, which model the electrical and mechanical response of the motor units to the input signal; and the feedback loop, that enables the simulation of prolonged constant force contractions.

Excitation Plane block

The excitation plane block translates the common excitatory signal received by all motor units into their individual electrical response, that is, into their different firing rate values. Experiments on anesthetized cats have shown a linear relationship between the steady state injected current and the firing rate of motoneurons (Kernell 1965a, b). We showed in Chapter 4 that the range of firing rates of all motor units is bounded from an initial value and a maximal value, when the excitation goes from zero to maximal level; and that this range is muscle dependent. We observed that the increase in the motor unit firing rates can be suitably described by an exponential function, whose time constant is prolonged for later recruited motor units. Furthermore, we observed that the increase in the motor unit firing rates (time constant of the

exponential function) is independent of the excitation. Thus, we defined an excitation plane, whose boundaries are given by the initial and maximal firing rates, for which holds (see Chapter 4):

$$\lambda_r + (\lambda_m - \lambda_r) * (1 - e^{(\frac{\tau_r - \phi}{\theta})})$$

The dependent variables in this equation are: the recruitment threshold of motor units τ_r, the firing rate recruitment λ_r, the maximal firing rate λ_m, and the time constant of firing rate increase θ. These variables will assume different values in different muscles, and thus the excitation plane will be unique for each muscle.

It has already been demonstrated that motor units are recruited in order of increasing size and excitability (Henneman, 1957). Smaller, lower-conduction velocity, and higher-input resistance motor units are recruited earlier than larger, faster-conduction velocity, and lower-input resistance motor units, which are subsequently activated as the excitation to the motoneuron pool increases. It is also known that different muscles are characterized by diverse ranges of recruitment: the motor units of smaller, distal muscles, such as FDI muscle, tend to be recruited in the force range up to 50% maximal voluntary contraction (MVC); whereas larger, more proximal muscles, such as the deltoid muscle, recruit their motor units up to 80% MVC (De Luca et al., 1982a). The model was simulated for two different muscles: the FDI and the VL muscles. The FDI was assigned the recruitment range 0-50% MVC (De Luca et al., 1982a, 1996; Thomas et al., 1986; own observations (see Chapter 4)); the VL was assigned the range 0-80% MVC (own observation, see Chapter 4). Finally, the distribution of motor units within the recruitment range has been reported to be skewed such that the low-threshold motor units greatly outnumber the high-threshold motor units (Duchateau and Hainaut, 1990; Milner-Brown et al., 1973). Following the work of Fuglevand et al. (1993) the distribution of recruitment threshold was thus modeled as an exponential of the form:

$$\tau_r(i) = e^{ai}$$

$$a = \frac{\log(RR)}{N}$$

where τ_r is the recruitment threshold and *i* is the motor unit number. The coefficient *a* was used to establish a range of recruitment thresholds and *RR* is the recruitment range. *N* refers to the total number of motor units in the pool, and it was set to 120 for the FDI muscle (Feinstein et al., 1955), and to 600 in the VL muscle (data derived from the rectus femoris muscle, Christensen, 1959). The histogram and distribution of the calculated recruitment thresholds for the FDI and VL muscles are reported in Figure 20.

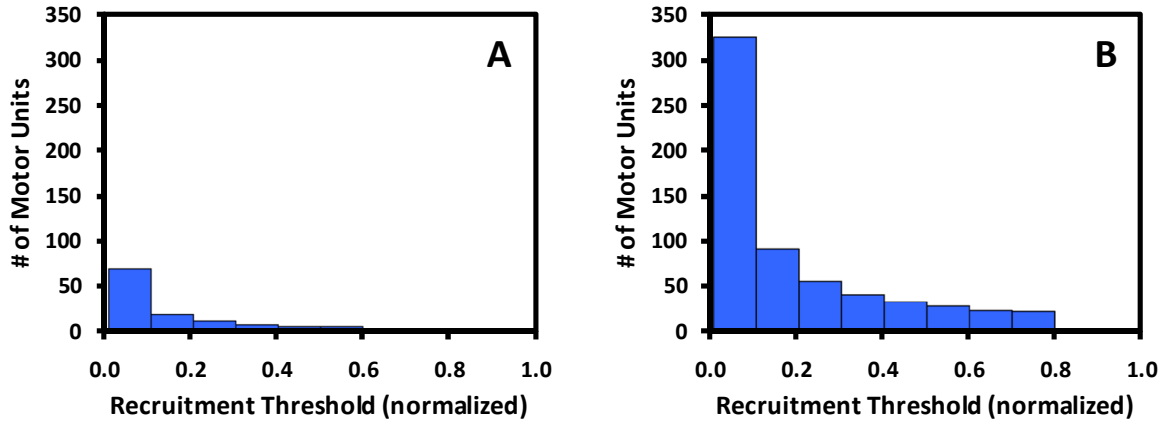

Figure 20: Recruitment Threshold. Histogram of the recruitment thresholds of the motor units in the model of the FDI motor unit pool (A) and of the VL motor unit pool (B). The total number of units is N=120 and N=600, the range of recruitment threshold is RR=60 and RR=80 for the FDI and VL muscle respectively.

Contrasting reports may be found in the literature about the distribution of the firing rates at recruitment and of the maximal firing rates. A positive linear relation or no correlation between recruitment threshold and firing rates at recruitment has been observed in previous studies (Milner-Brown et al., 1973; Erim et al., 1996, 1999). Maximal firing rates have also been reported either to be higher for earlier recruited motor units (De Luca et al., 1982a), or to be higher for later recruited motor units (Kosarov and Gydikov, 1976; Moritz et al., 2005), or to converge to similar values (De Luca and Erim, 1994; Erim et al., 1996). We observed a negative linear relation between recruitment threshold and both λ_r and λ_m (see Chapter 4), and we introduced this relation in the model to obtain the distribution of firing rates at recruitment and of maximal firing rates. (See equations in Table V.)

The time constant of the firing rate increase θ was also set for each motor unit based on the results presented in Chapter 4. We fitted the mean firing curve with a simple exponential function

and we computed the time constant of the increase. We found a negative linear relation between the time constant and the recruitment threshold of the motor units. The negative linear relation was employed in the model so that earlier recruited motor units were characterized by a much faster increase in their firing rates compared to later recruited motor units. (Equations are reported in Table V.) All distributions were derived from the analysis of contractions increasing up to almost maximal force level at a rate of 10% MVC/s. (See Chapter 4.)

A plot of the excitation plane derived for both the FDI and the VL muscle is shown in Figure 21.

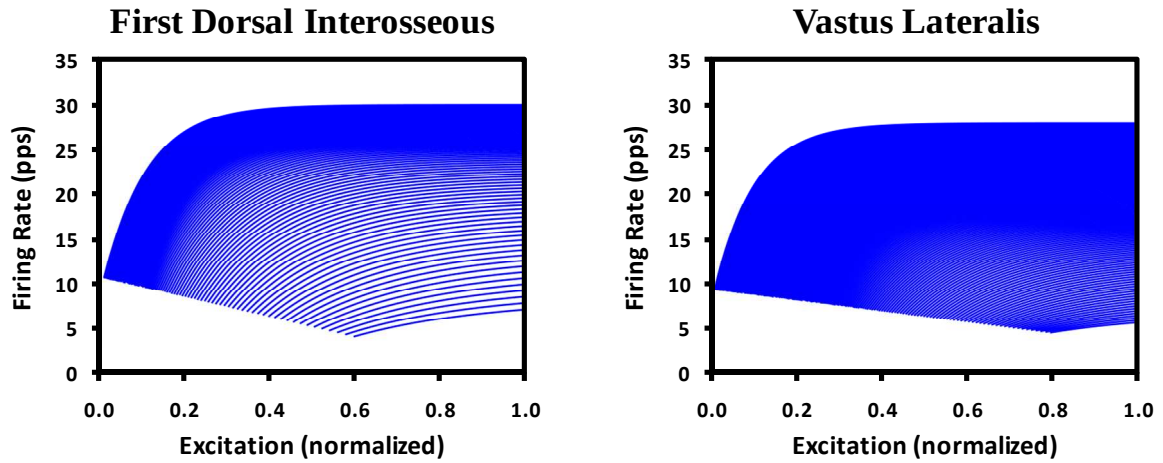

Figure 21: Excitation Plane. The modeled excitation planes for the FDI muscle and the VL muscle are presented.

Table V: Excitation Plane equation. Modeled distributions of the firing rate at recruitment, maximal firing rate, and time constant of firing rates increase for the two muscles of the study for a 10% MVC/s contraction. *i*=1:120 in the FDI muscle; *i*=1:600 in the VL muscle, and it represents the motor unit number. τ_r is the modeled recruitment threshold for each motor unit.

	First Dorsal Interosseous	Vastus Lateralis
Firing rate at recruitment	$\lambda_r(i) = -11.20 * \tau_r(i) + 10.56$	$\lambda_r(i) = -5.69 * \tau_r(i) + 9.32$
Maximal firing rate	$\lambda_m(i) = -39.61 * \tau_r(i) + 30.44$	$\lambda_m(i) = -26.74 * \tau_r(i) + 28.26$
Time constant	$\theta(i) = 36.62 * \tau_r(i) + 9.92$	$\theta(i) = 22.93 * \tau_r(i) + 9.12$

Impulse train generator -- The firing rate value of each motor unit is transformed into an impulse train by using the Integral Pulse Frequency Modulation (IPFM) method, which produces a spike train with a frequency equal to the numerical value of the firing rate input. This process is performed by integrating the signal input over time and generating an impulse every time the threshold value 1 is reached. At this point, the integrator resets back to zero and the process starts again. Simulated impulse trains for the first (MU #1) and the last (MU #91) recruited motor units during a 20% MVC contraction sustained for 10 s in the FDI muscle are shown in Figure 22A.

Noise in the impulse train -- The inter-pulse interval (IPI) between two adjacent firings of a motor unit can be regarded as a random variable (De Luca and Forrest, 1973). Moritz et al. (2005) computed the coefficient of variation (CV) of the firing rates at different force levels ranging from 2 to 95% MVC in the FDI muscle. The CV decreased exponentially as the force increased above recruitment threshold for each motor unit and, after recruitment, was approximately constant with force for all motor units at a mean value of 19.8 ± 2.5%. Other authors as well showed that the mean and standard deviation (SD) of the IPIs are related so that the CV of the IPIs has an approximately constant value for all motor units that ranges between 10% and 30% (Clamann, 1969; Nordstrom et al., 1992; Macefield et al., 2000).

There have been contrasting reports on the changes of firing rate variability with fatigue. Variability of the firing rate, computed as the CV of the unfiltered IPIs, was found to increase after a fatiguing exercise by Garland et al. (1994) in the biceps brachii muscle and by Enoka et al. (1989) in the FDI muscle. In a previous work (Contessa et al., 2009; see also Chapter 3), we were able to show that the coefficient of variation of the detrended mean firing rates remains unchanged with fatigue in the VL muscle during intermittent 20% MVC isometric contractions sustained to exhaustion. Our results are consistent with those of Macefield et al. (2000), who observed no systematic change in firing rate variability of the extensor hallucis longus muscle when fatigued during a sustained MVC.

Based on these results, the firing times of each motor unit impulse was manipulated similarly to Fuglevand et al. (1993). IPIs were generated from a normal distribution with mean

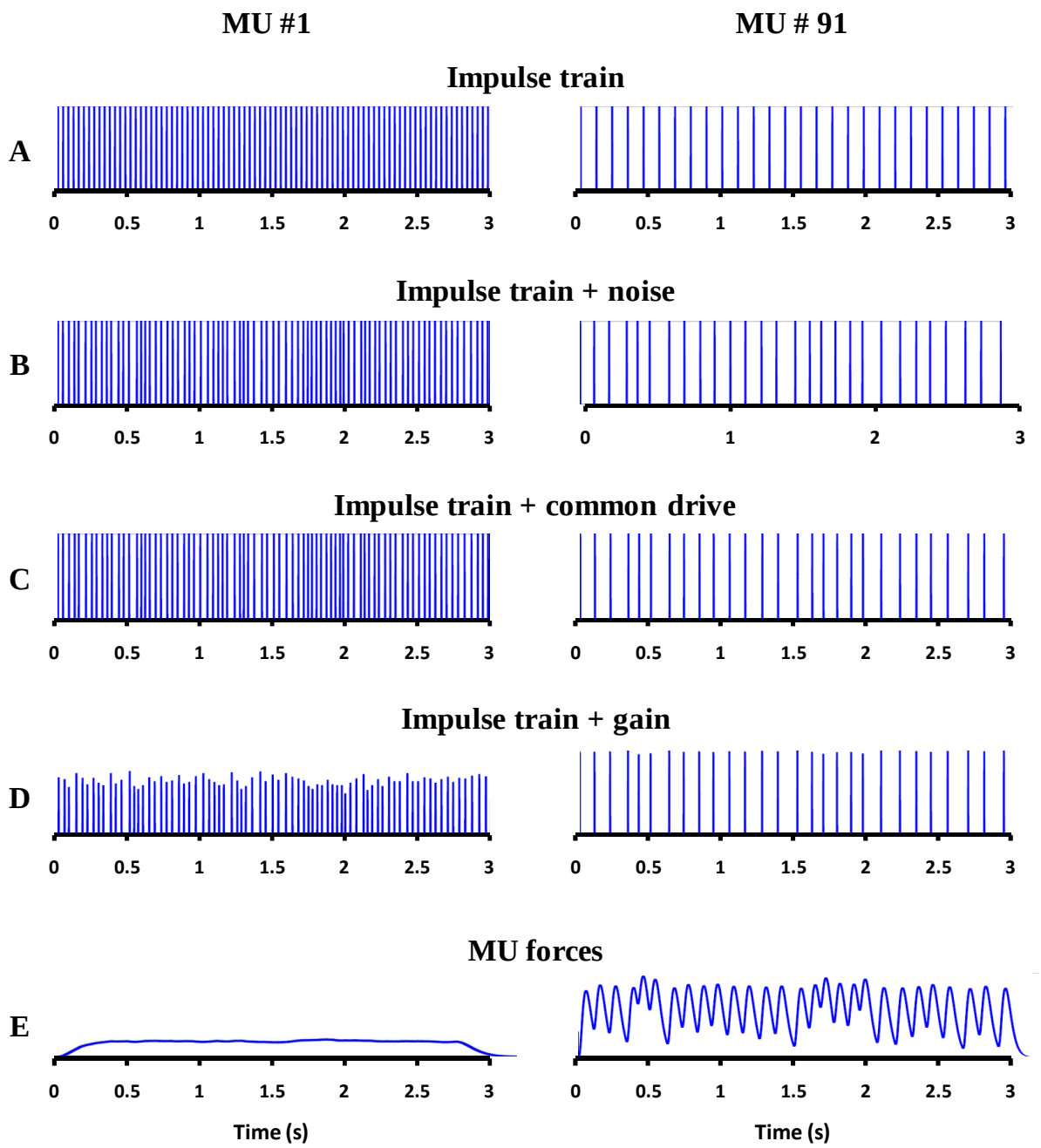

Figure 22: Impulse train and MU force generation. A) Impulse trains generated for the first (motor unit #1) and last (motor unit #91) motor unit recruited during a 20% MVC contraction. B) Impulse train with superimposed gaussian noise at 20% mean IPI. C) Impulse train with superimposed common drive, modeled by a 0.8 Hz sinusoid with amplitude equal to 20% of the mean IPI. D) Train of pulses scaled with a frequency dependent gain function. E) Output forces for the individual motor units.

equal to the inverse of the average firing rate and constant CV = 20%, and each firing in a motor unit impulse train was adjusted so that:

$$t_{i,j} = t_{i,j-1} + \mu + \sigma * Z$$

where $t_{i,j}$ is the time of the j-th firing of motor unit i; $t_{i,j-1}$ is the time occurrence of the preceding firing, μ is the mean firing rate of the impulse train, σ is the standard deviation of the IPIs (σ = CV*μ = 0.2*μ), and Z is the Z-score, representing how far a generated value of the IPIs deviates from the mean of the distribution. Z-score were randomly picked from the interval [-3.9 - 3.9], so that the instantaneous IPIs were allowed to deviates at most four standard deviations from the mean of the normal distribution. The effect of noise in two simulated trains of pulses is displayed in Figure 22B.

Common Drive -- It has been shown that motor units are controlled in unison, rather than individually, indicating that the central nervous system modulates the behavior of the entire motoneuron pool of a muscle in the same way. The effect of this common input to the motoneuron pool is a common modulation in the firing rates of motor units at a frequency of approximately 0.8 Hz, a phenomenon that has been verified by several investigators (Miles, 1987; Stashuk and de Bruin, 1988; De Luca et al., 1982b; De Luca and Erim, 1994; among others). This phenomenon can be visually illustrated by plotting the cross-correlation function between motor units, which shows a maximum at a time lag close to zero. The fluctuations in the firing rates are translated also in the muscle force output: the cross-correlation function between motor units and force usually presents a peak at positive time lags indicating that the firing rates leads the force as is expected due to the time required to build up the force in the muscle after the fibers have been activated.

Common drive was included in the model as a sinusoidal signal of frequency 0.8 Hz and amplitude equal to 20% of the mean IPI, that was used to adjust the firing times of all impulses in the motor unit trains after noise had been added. The amplitude of the sinusoid was chosen to be equal to 20% of the mean IPI because the maximum of the cross-correlation function between motor units (named the CDC, Common Drive Coefficient) showed to provide results similar to those observed in experimental studies (CDC between 0.2 - 0.6, De Luca and Erim, 2002; Contessa et al., 2009). (See also the results section.) The effect of the common drive on the impulse trains of MU #1 and MU#91 (during a 20% MVC contraction) are reported in Figure 22C.

Twitch Plane block

The twitch plane block generates the characteristic twitch forces of each motor unit and thus translates the electrical behavior of the motor unit (impulse) into its mechanical response (force twitch). The main parameters that are commonly used to characterize the force twitch are: the amplitude of the twitch, defined as the value of its peak; the rise time, defined as the time to the peak of the twitch; and the half-relaxation time, which is the time from the peak to the point where the amplitude is reduced to half of its maximal value. (See Figure 23.) The literature reports consistent data on the motor unit force twitches, both in animal and human studies. It is generally accepted that the amplitude of the force twitches vary over a wide range, typically ≥ 100-fold; that the contraction time varies over a smaller range, 4 to 5-fold; and that earlier recruited lower-threshold motor units produce lower-amplitude longer-duration force twitches (Henneman and Olson, 1965; Burke, 1967; Milner-Brown et al., 1973b; Burke et al., 1973; Monster and Chan, 1977; Calancie and Bawa, 1985).

The mechanical properties of human motor units have been studied with mostly four different techniques (see Chan et al., 2001, for a comprehensive review): spike-triggered averaging (STA); intramuscular stimulation (IMS); intraneural stimulation (INS); and percutaneous stimulation (PS). STA, first introduced by Buchthal and Schmalbruch in 1970, averages the isometric force recorded during the identified action potentials from a motor unit to estimate its contribution to the net force. A sampling bias towards low-recruitment threshold smaller-twitch tension motor units is often introduced, since low steady firing rates are necessary to enable identification of the action potentials. This method is also affected by twitch fusion (summation of mechanical responses) even at very low firing rates; and it can produce unreliable results if the shape of the twitch changes over time. STA has been reported to underestimate contraction time and half-relaxation time, and to overestimate peak tension (Thomas et al., 1990; Kossev et al., 1994; Elek and Dengler, 1995). IMS (first reported by Buchthal and Schmalbruch, 1970, and later refined by Taylor and Stephens, 1976) consists of weak stimuli at the terminal twigs of the motor axon that activates a whole motor unit. This method may yield a large number of motor units and presents no problem of twitch fusion, since the stimulus rate may be precisely controlled; but it is

susceptible to muscle movement since the stimulating electrode is seated in the muscle. INS, introduced by Westling et al. (1990), involves the stimulation of the motor axon in the nerve trunk with a needle electrode while using surface electrodes to record action potentials. Unlike IMS, the stimulating electrode is placed proximally in the nerve trunk, which ensures complete activation of the motor unit. It is a more invasive technique and may yield a lower number of motor units; furthermore, it is only applicable to nerves with a long superficial course that can be easily accessed beneath the skin surface. PS, adopted for example by Sica and McComas (1971) and Doherty and Brown (1994), again involves stimulating the motor axon in the nerve truck but with a bipolar surface electrode. As the INS technique, it yields a lower number of motor units and is only applicable to superficial and easily accessible nerves.

Data regarding the shapes of the force twitches were derived from the literature for the FDI muscle. A summary of the results is presented in the following paragraph and in Table VI. In order to derive an accurate estimate of the motor unit twitch parameters, studies employing spike-triggered averaging were not considered. No data were available for the VL muscle, and thus the distributions of the parameters assumed for the FDI muscle were used also for the VL muscle with a minor change in the parameters, as explained in a subsequent paragraph.

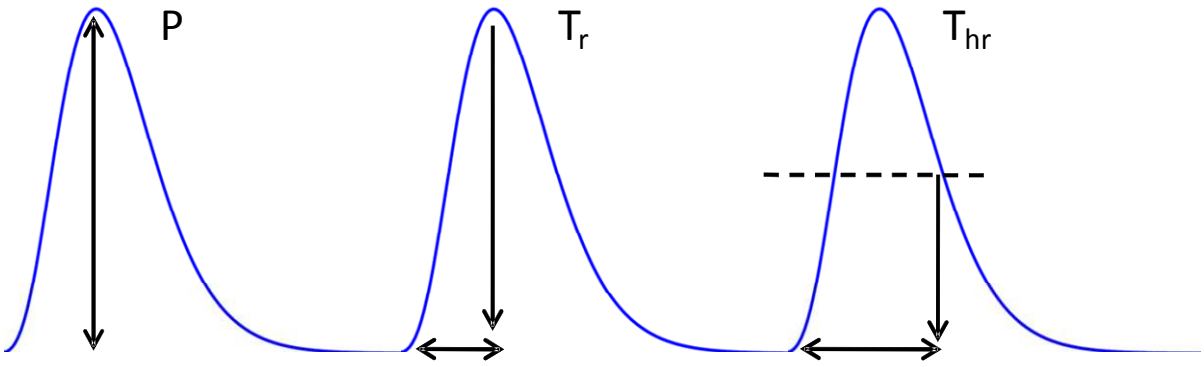

Figure 23: Motor unit twitch. The three parameters that characterize the motor unit twitch are the peak amplitude (P), that is the maximum value of the tension; the twitch rise time (T_r), which is the time to reach the maximal value; and the twitch ½ relaxation time (T_{hr}), that is the time it takes to the amplitude to decrease to half of its peak value P/2.

FDI twitch parameters -- The FDI muscle in humans has been studied extensively using either spike-triggered averaging, intramuscular stimulation, or intraneural stimulation.

Regardless of the technique employed, a positive correlation was always observed between recruitment threshold and twitch tension. An exponential distribution of tensions was reported in most studies, with the greatest number being in the early recruited, low-amplitude twitch tension motor units (Milner Brown et al., 1973b; Stephens and Usherwood, 1977; Thomas et al., 1986; Elek et al., 1992; Kossev et al., 1994; Elek and Dengler, 1995; McNulty et al., 2000; Gossen et al., 2003).

Results on the distributions of rise times and half-relaxation times are more sensitive to the technique employed. Rise times and half-relaxation times vary over a smaller range when compared to twitch tensions (Milner-Brown et al., 1973b; Stephens and Usherwood, 1977), and display a unimodal distribution (Young and Meyer, 1981; Elek et al.; 1992; Elek and Dengler, 1995; McNulty et al., 2000; Gossen et al., 2003). However, when STA is used, a linear relation between peak tension and the time parameters of the force twitch has been observed, for example by Thomas et al. (1986). In contrast, no correlation is reported when either IMS or INS are used. In general, fast twitch motor units have large twitch tensions, but there are also many motor units with small twitch tensions and fast rise times (Young and Meyer, 1981; Elek et al.; 1992; Elek and Dengler, 1995; McNulty et al., 2000; Gossen et al., 2003). A correlation between twitch rise times and half relaxation times has also been reported (Elek et al., 1992; McNulty et al., 2000).

Based on these results, we did not consider studies employing STA to obtain the values for the mean and standard deviation of the distributions of the force model.

In all studies, the range of twitch tensions is quite broad (on average 130-fold) and the distribution is skewed toward a greater number of low-force motor units (Elek et al., 1992, reported that approximately 70% of motor units have tensions < 14-fold). Furthermore, earlier recruited motor units tend to produce less force than later recruited motor units. An exponential distribution was thus chosen for modeling the peak twitch tensions (similarly to Fuglevand et al., 1993):

$$P(i) = e^{bi}$$

$$b = \frac{\log (RP)}{N}$$

where *N* is the number of motor units in the pool, *RP* is the range of peak twitch forces (set to 130, so that if 1 force unit corresponds to the first unit recruited, 130 force units is the force of the last recruited motor unit). Twitch rise times have on average a smaller range than peak forces (4-fold) and vary between 30-125 ms. They present an unimodal distribution skewed towards low rise times, with 89% of motor units having rise times between 45-85 ms (Young and Meyer, 1981), with an average of 65 ± 16 ms. Thus, lower force motor units tend to cover most of the range of rise times. The distribution of rise times was generated from a Weibull distribution with mean 65 ms and standard deviation 16 ms. The parameters for the distribution that matched these values were $k = 39.50$, $\beta = 2.32$, $\alpha = 30$:

$$p_x(x) = \frac{k}{\beta}\left[\frac{x-\alpha}{\beta}\right]^{k-1} e^{(-\frac{x-\alpha}{\beta})^k}$$

Half-relaxation times are correlated to rise times (Elek et al., 1992) and have a slightly broader range of values (5.5-fold, range 20-117, average mean 63 ± 20 ms). Again, the distribution for half-relaxation times was modeled as a Weibull distribution with a mean of 60 ms and standard deviation of 20 ms. The parameters for the distribution that matched these values were $k = 45.16$, $\beta = 2.23$, $\alpha = 2\ 0$. A plot of the distributions for all three parameters is showed in Figure 24.

VL twitch parameters -- While estimates of motor unit twitches in humans have been described for distal limb muscles including the FDI, no such data are available for the VL. We had some information on the mechanical characteristics of the whole muscle twitch from previously performed experiments. The twitch and the tetanic response to 50 Hz electrical stimulation of the VL muscle were recorded in a previous study (see Adam and De Luca, 2005, for details). The whole muscle twitch from three subjects had an average rise time of 90 ms and an average half-relaxation time of 60 ms. We assumed that the VL and the FDI were characterized by the same distribution for the parameters: that is, exponential for the peak twitch forces and weibull for the both the rise time and the half-relaxation time.

Table VI: Motor unit twitch parameters. Data on the peak twitch force, twitch rise time, half-relaxation time, and twitch duration are presented for several recording techniques. Data are presented as mean ± standard deviation, range and median.

Author (year)	Groups	Peak force (mN)	Rise time (ms)	½ Rel time (ms)	Duration (ms)	Method
Milner-Brown et al. (1973a)	Subject 1 Subject 2 Subject 3	14±16 13±14 23±28	51.5±12.6 55.6±11.4 59.1±16.9 30-100	42.8±10.3 44.9±14.6 40.5±7.7		STA
Stephens and Ushe. (1977)	13 subjects	1.8-300	32-122			STA
Thomas et al. (1986)	Subject 1 Subject 2 Subject 3 Subject 4	3-149 (36) 3-215 (64) 5-102 (36) 4-101 (31)	48-81 (65) 40-99 (69) 44-84 (65) 65-89 (77)			STA
Kossev et al. (1994)	12 subjects	17.7±19.8 0.2-105 10.3	47.3±12.8 20-90 44.8	33.9±10.3 14-75 33.6		STA
Carpentier et al. (2001)	RT<25% RT>25%	24.6±4.7 1-124 56.2±10 9-158	43.8±2.1 25-78 52.5±3.1 32-75	35.3±4 10-70 43.2±4.8 22-58		STA
Gossen et al. (2003)	8 subjects	15±15 1-75	57±8 42-76	45±8 33-59		STA
Young and Meyer (1981)	20 subjects	35±48 2.14-430	65±18 34-140			IMS
Elek (1992)	20 subjects	16±18.7 1-137 10.3	63±15 30-110 62	61±17 20-105 58		IMS
Kossev et al. (1994)	20 subjects	14.9±16.3 1-140 9.6	63.1±14.7 30-135 61.7	60.4±16.4 24-130 n 57.5		IMS
Elek and Dengler (1995)	25 subjects	14±15 9	64±14 63	61±16 59		IMS
McNulty et al. (2000)	22 subjects	2.2-72.8 14.7	70.3±5.0 32-111.3	70.2±6.5 20-115.9	101.3-468.8 183.8	INS

Force twitches for all motor units were generated using different combinations of values for the parameters characterizing the distribution of peak force, rise time and half-relaxation time. The force twitches were then summed to obtain the whole muscle twitch. The values that resulted in the closest fit for the experimentally observed values of rise time and half-relaxation time were chosen to model the VL force twitches.

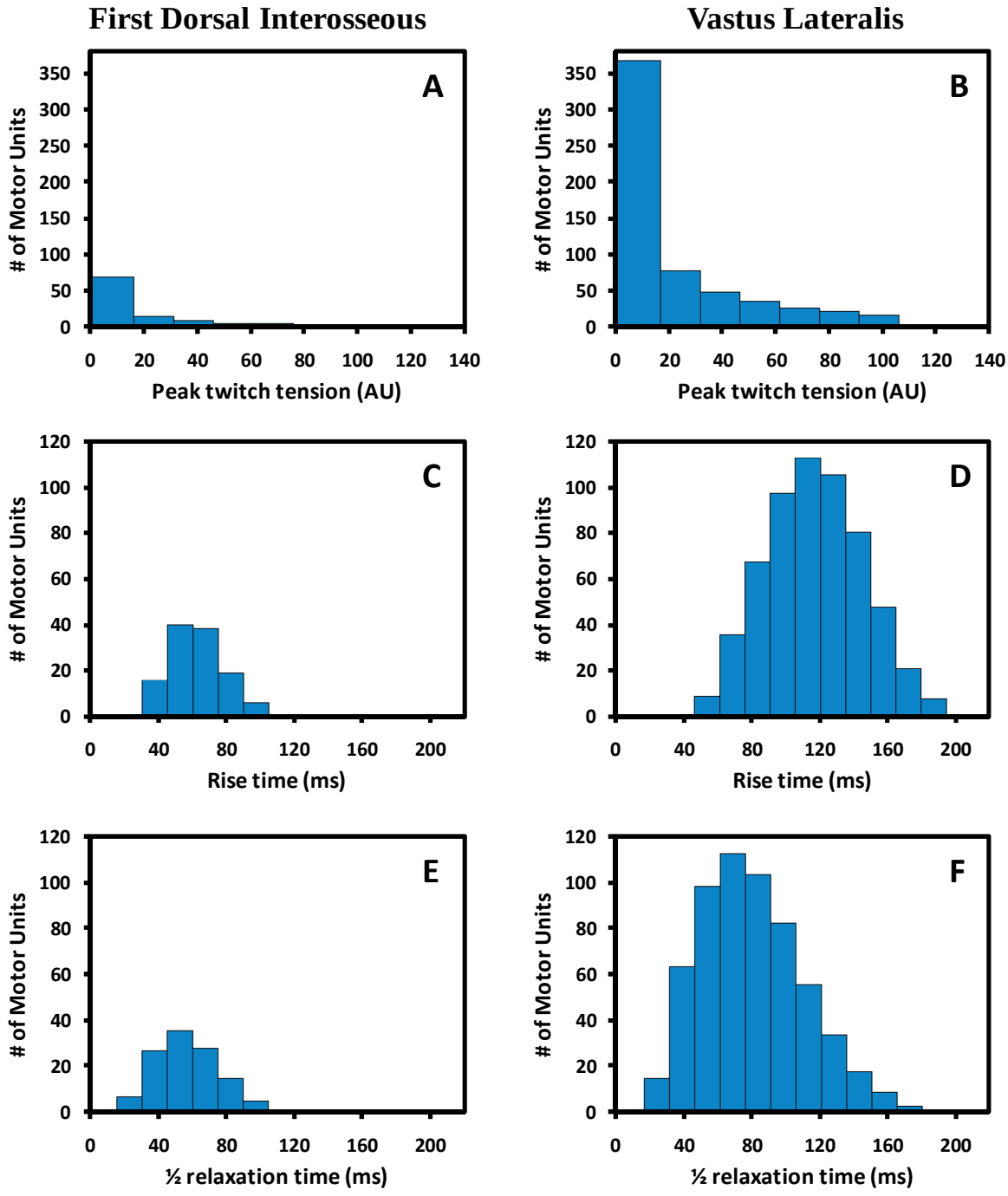

Figure 24: Force twitch parameters. The distribution for the force twitch parameters are shown for both the FDI (left-hand side) and the VL muscle (right-hand side). A) and B) peak tension; C) and D) rise time; E) and F) half-relaxation time.

A lower range of peak tensions was found (105-fold), whereas the parameters chosen to model the distribution of the time parameters were k = 97, β = 3.18, α =32 for the rise time, and k = 69, β = 2.05, α =21 for the half-relaxation time. A plot of the distributions for all three parameters is showed in Figure 24.

Motor unit force twitch equation -- The shape of the motor unit has previously been modeled as the response of a critically damped second-order filter (Fuglevand et al., 1993). This choice was motivated by earlier work on the frequency response on the cat hindlimb muscle (Stein et al., 1972; Mannard and Stein, 1973), and the approach was then confirmed in the human FDI (Miner-Brown et al., 1973a, c). Using this method the twitch half-relaxation time would be approximately 70% longer than the twitch rise time (Milner-Brown et al., 1973c). Experimentally observed data, though, show that the half-relaxation times are overestimated, since they are in the same range of the rise times or even shorter (see also Herbert and Gandevia, 1999). A different equation was thus chosen (Raikova and Aladjov, 2002), that enables to independently set not only the twitch peak tension and the rise time, but also the half-relaxation time:

$$f(t) = pt^m e^{-kt}$$

where

$$p = Pe^{-kT_r(\log T_r - 1)}$$

$$m = kT_r$$

$$k = \frac{\log 2}{T_{hr} - T_r - T_r \log\left(\frac{T_{hr}}{T_r}\right)}$$

where f(t) is the time dependent force twitch, P is the peak tension, T_r is the twitch rise time, and T_{hr} is the twitch half-relaxation time. T_{hr} in this equation is the time from the start of mechanical activity to the time where motor unit force decreases to half peak value. A plot of the motor unit force twitches modeled by these equation and the above obtain distributions for the parameters are reported in Figure 25.

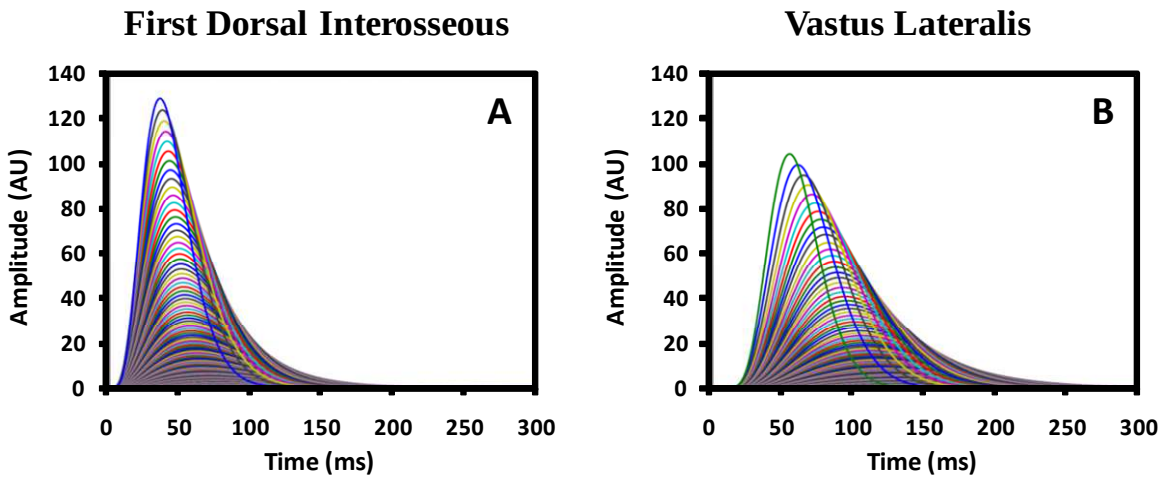

Figure 25: Motor unit twitches. Motor unit twitch forces modeled for both the FDI (A) and for the VL (B) muscles are displayed. Note that all motor units are shown for the FDI, whereas only 100 motor units out of 600 (1 every 6) are shown for the VL for clarity.

Time dependent changes in the force twitch -- The motor unit twitch force is known to change with time during a sustained contraction. Two phenomena have been reported: the potentiation of the motor unit twitch at the beginning of the contraction, followed by the diminution of the motor unit twitch as fatigue progresses (Burke 1981; Vandervoort et al. 1983; Dolmage and Cafarelli 1991; Macintosh et al. 1994; among others). Potentiation is associated with an increase in the amplitude of the motor unit force twitch, and thus with an increased force generation capacity. De Luca (1979), De Luca et al. (1996), and Adam and De Luca (2005) suggested that potentiation may be the cause for the observed decay in the firing rates of all motor units during the first 30-40 s of a contraction that is maintained at a constant force. In contrast, fatigue is accompanied by a decreased force generation capacity, and thus the motor unit twitch amplitude decreases. An association between the loss of force production and the increase in the firing rates during prolonged isometric contractions has been recently suggested by Adam and De Luca (2005): firing rates of motor units adapt to counteract the changes in the force produced by the muscle fibers during a sustained contraction.

While studies agree on the modifications in the amplitude of the twitch with potentiation and fatigue, the situation is less clear when considering the time parameters of the twitch, both the rise time and the half-relaxation time: several authors report that the parameters becomes either

slower, or faster, or do not change. Nordstrom and Miles (1990) followed the twitches of single motor units in the human masseter muscle using STA. In that study motor units displayed three main patterns: an initial increase in twitch amplitude (with the maximum reached at different times) followed by a slight decrease or no change; a continuous decrease; and a rapid decrease in the first 3 min that remained constant for the rest of the task. No relation between fatigability and initial peak tension or initial rise time was observed. In contrast, Thomas et al. (1991a) observed changes in twitches of thenar human motor units with INS when fatigued with a standard test (a 330 ms duration train of pulses at 40 Hz every second for 2 min). The motor units with the largest peak force before the fatigue test decreased their peak force and increased their rise time, but their relaxation rates tended to increase. Some motor units potentiated after the fatigue test, decreased their rise time and their relaxation rates. In Table VII and Table VIII, motor units from this study are classified into 3 groups: motor units with force loss (FI<0.75) and slowing (½ RT FI>1); motor units with little force loss (FI≥0.75) and slowing (½ RT FI>1); motor units with little force loss (FI≥0.75) and no slowing (½ RT FI≤1). INS was used also by Fuglevand et al. (1999) in five muscles of the hand: motor units potentiated after 3.1 s of tetanic stimulation and decreased their peak twitch force after the commonly used fatigue test (a 330 ms duration train of pulses at 40 Hz every second for 2 min). Motor units with the highest initial tensions tended to display the greatest decrease. The time course tended to get slower, but it was not related to initial peak force or fatigue index. The contractile properties of individual motor units in the FDI muscle were studied also by Carpentier et al. (2001) with the STA method, before and after fatiguing intermittent isometric contractions sustained at 50% MVC and repeated to the endurance limit. The mean twitch force increased with fatigue for low-threshold motor units (RT<25% MVC), whereas the twitch force decreased for high threshold (>25% MVC) motor units. Changes in the amplitude were accompanied by changes in the rise time but not in the half-relaxation time: motor units that decreased their peak force also decreased their rise time.

Many studies followed the changes in time of the whole muscle twitch, instead of those of individual motor units, during sustained voluntary isometric contractions. Bigland-Ritchie et al. (1983) analyzed the twitch response of the human adductor pollicis muscle before,during and after

Table VII: Potentiation data. Data on the peak twitch force, twitch rise time, half-relaxation time, and twitch duration are presented for several recording techniques. Data are presented as mean ± standard deviation and range.

Author	Muscle	Task	Peak force (mN)	Rise time (ms)	½ Rel time (ms)	Technique
Bigland-Ritchie et al. (1983)	Adductor pollicis	Initial value -5s MVC	 + 25-30%↑	59.9±6.7 56.8±5.9	 47.3±4.9	whole twitch
Vandervoort et al. (1983) -peak force in Nm-	Plantar flexor	Initial value -1s MVC -10s MVC	17.8±5.5 +4±13% 25.5±7.2↑ +45±17%	133±7.6 117±5.7↓	114±26.3 95±22.9	whole twitch
Vandervoort et al. (1983) -peak force in Nm-	Tibialis anterior	Initial value -1s MVC -10s MVC	1.7±1 +43±36%↑ 3.5±1.3↑ +142±102%	93±16.4 83±19.2	99±31.5 69±11.9↓	whole twitch
Thomas et al. (1991a)	thenar	Initial value 1) stimulation Initial value 2) stimulation Initial value 3) stimulation	20±8 (mN) 31±6 10±5 20±7 7±2 9±3	49±8 54±10 47±7 53±6 54±13 54±13	60±12 89±9 57±13 70±14 71±23 63±19	INS
Vollestand et al. (1997) -peak force in N-	Knee extensors	Initial value -30% MVC Initial value -45% MVC Initial value -60% MVC	31±3 ~ 110%↑ 35±2 ~ 120%↑ 35±4 ~ 135%↓	41.4±3 ~ 78%↓ 38.5±0.7 ~ 80%↓ 40.9±2.2 ~ 80%↓	50.9±5.7 ~ 85%↓ 61.2±9.8 ~ 110%↑ 53.9±5.5 ~ 120%↑	whole twitch
Fuglevand et al. (1999)	Hand muscles	-3.1s tetanic stim	+29±3.7%			
Klein et al. (2001)	Triceps brachii	Initial value -6s 30% MVC -±6s 20% MVC -±6s 10% MVC -±5s 75% MVC	29±9 35±9↑ 32±9 30±9 142.9±26.7%↑	unchanged unchanged unchanged 98.2±10.3	unchanged unchanged unchanged 89±11.8%↓	whole twitch

Table VIII: Fatigue data. Data on the peak twitch force, twitch rise time, half-relaxation time, and twitch duration are presented for several recording techniques. Data are presented as mean ± standard deviation and range.

Author	Muscle	Task	Peak force (mN)	Rise time (ms)	½ Rel time (ms)	Technique
Bigland-Ritchie et al. (1983)	Adductor pollicis	Initial value -60s MVC	 -29.6±14%↓	56.8±5.9 54.1±9.1	47.3±4.9 65.1±8↑	whole twitch
Vandervoort et al. (1983)	Tibialis anterior	Potentiated -30s MVC -60s MVC	+142±102% ~+70±30%↓ ~-15±30%↓			whole twitch
Vandervoort et al. (1983)	Plantar flexor	Potentiated -10s MVC -60s MVC	+45±17% ~+45±17% ~+25±15%↓			whole twitch
Thomas et al. (1991a) -Fatigue Index-	Thenar	1)stimulation 2)stimulation 3)stimulation	0.49±0.17 1.05±0.32 1.43±0.42	1.22±0.23 1.08±0.14 1.09±0.14	1.07±0.29 1.22±0.25 1.18±0.40	INS
Binder MacLeod and McDermond (1993)	Quadriceps	Initial value -8s 60Hz Initial value -8s MVC	 -50% -30%	93±24.22 77±22.85↓ 73±17.35 71±12.21	78±22.87 123±50.34↑ 90±30.79 89±42.65	whole twitch
Vollestand et al. (1997)	Knee extensors	Initial value -30% MVC Initial value -45% MVC Initial value -60% MVC	31±3 ~ 75%↓ 35±2 ~ 65%↓ 35±4 ~ 45%↓	41.4±3 unchanged 38.5±0.7 unchanged 40.9±2.2 unchanged	50.9±5.7 ~ 60%↓ 61.2±9.8 ~ 70%↓ 53.9±5.5 ~ 75% ↓	whole twitch
Carpentier et al. (2001)	1) FDI RT<25% 2) FDI RT≥25%	Initial value -50%MVC Initial value -50% MVC	1-124 24.6±4.7 3-131 32.7±4.4↑ 9-158 56.2±10 7-92 31.4±5↓	25-78 43.8±2.1 29-105 53.1±3.2↑ 32-72 52.5±3.1 30-62 42.9±2.4↓	10-70 35.3±4 17-62 39.5±3 22-58 43.2±4.8 28-48 35±3	STA

maximal contractions sustained for 60s. Motor units potentiated after a short MVC (5s) and fatigued (the twitch amplitude decreased) after a fatiguing sustained MVC. Rise time remained unchanged, whereas relaxation time increased significantly. Vandervoort et al. (1983) reported greater potentiation in the tibialis anterior muscle than in the planterflexor muscle after maximal voluntary contractions. When the MVC was sustained for more than 10 s, potentiation was partially supressed by fatigue. Rise times and half-relaxation times tended to decrease with potentiation, although not always significantly. Binder MacLeod and MacDermond (1993) followed the changes in the twitch response when the quadriceps muscle was electrically and voluntarily fatigued. In both cases the peak force declined. The rise time and the half-relaxation time remained unchanged after voluntarily induced fatigue, whereas, after electrically induced fatigue, the rise time decreased whereas the half-relaxation time increased. Vollestand et al. (1997) observed the changes in twitch during isometric contractions of the knee extensors at 30%, 45% and 60% MVC repeated to exhaustion. Force loss increased with increasing target force. An initial potentiation was observed in the first 3 min, higher with increasing target force. Twitch rise time decreased in all experiments of about 20% after the first contraction (when the force potentiated), and then remained unchanged with fatigue. Half-relaxation times decreased with fatigue. For the 45% and 60% MVC contractions, half-relaxation time initially increased with potentiation before decreasing. Klein et al. (2001) reported that the whole muscle twitch of the triceps brachii muscle potentiated after 6 s of a 30% MVC constant force contraction, and remained stable after the following 20% and 10% MVC contractions. Time to peak and half-relaxation time did not change. After a conditioning contraction (5 s contraction at 75% MVC) the peak force increased to 1.3-2-fold approximately, and half-relaxation time decreased, whereas rise time was still unchanged. Changes in peak force were dependent on the intensity of the contraction.

This review of the literature clearly shows that all studies agree on the changes of the twitch peak force over time, with an initial increase with potentiation and a later decrease with fatigue. The modifications in the time parameters of the twitch, both the rise time and the half-relaxation time, are more debated. Results from one of our previous studies performed on the VL muscle (Adam and de Luca, 2005) showed that the peak twitch force initially increased to

approximately 1.08 of the initial value in the first 40 s of a 20% MVC isometric contraction, and then decreased to 0.53 of the initial value as the contractions were repeated to exhaustion (6-10 min). Rise time and half-relaxation time appeared to decrease with fatigue, but not significantly. The same study was performed on the FDI muscle (unpublished data): peak force increased on average up to 1.2 of the initial value in approximately 60 s, and then decreased to 0.4 of the initial value at endurance time (around 14 min). Rise time and half-relaxation time showed a decline to approximately 85% and 95% of the initial value, but the trend was not consistent in all subjects.

In order to introduce the time dependent changes of the motor unit force twitch into the model, peak twitch forces of the individual motor units were adjusted with time so that the whole muscle response simulated for a sustained contraction at 20% MVC mimicked the experimentally observed changes (Adam and De Luca, 2005). An exponential distribution of maximal peak values was generated, since a linear relation is often reported between changes in the peak value and the initial peak value, which in turn is linearly related to recruitment threshold. An exponential distribution was assumed also for the time to reach the peak potentiated value. The minimum peak value at endurance time was set to 0.2 of the initial value for all motor units, in order to obtain the experimentally observed decrease in the whole muscle twitch. Again, an exponential distribution was assumed for the time to reach the endurance limit. For the moment, a linear rate of increase or decrease was modeled for all motor units. Rise time and half-relaxation time were maintained constant with time, since no clear trend was suggested either by the literature or by the previous experimental results. More detailed studies and/or simulation are needed in order to more accurately model the time dependent changes in the muscle force production capacity. Figure 26 presents the modification in the twitches of two motor units active during a 20% MVC contraction in the FDI muscle.

Firing rate dependent gain factor -- The summation of force during tetanic contractions is highly nonlinear and depends on the firing rate (Cooper and Eccles, 1930; Mannard and Stein, 1973; Bawa and Stein, 1976). The relationship between isometric force and stimulus rate has a well know sigmoidal shape (Bigland and Lippold, 1954; Rack and Westbury, 1969), which depends on the contractile properties of the motor units; but if the stimulus rate is normalized as a

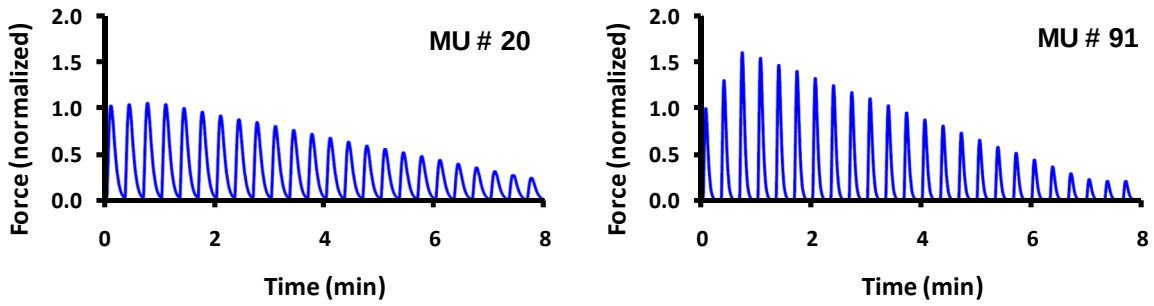

Figure 26: Time dependence of motor unit force twitch: FDI. The changes in time of two motor units (MU #20 and MU #91) active in a sustained 20% MVC contraction are presented.

function of the contraction time of the twitch, the shape of this force-frequency relation is similar for all motor units (Kernell et al., 1983; Thomas et al., 1991b). Furthermore, for normalized stimulus rate lower than 0.4, the gain is almost constant and similar to that of an isolated twitch (Burke, 1981).

We used previously collected data from both the FDI muscle and the VL muscle in order to obtain the force-frequency relation and consequently the gain of the relation for these two muscles (Adam, 2003). The muscles were electrically stimulated at 1, 5, 10, 15, 20, 30, 50, and 100 Hz and the response was recorded. The protocol was administered to 3 subjects in the VL muscle and to 7 subjects in the FDI muscle. The experimentally obtained force-frequency curves were fitted to the following exponential function (Herbert and Gandevia, 1999; Studer et al., 1999; Adam, 2003) for normalized stimulus rates f_n higher than 0.4:

$$y = 1 - r * e^{\frac{(0.4 - f_n)}{c}}$$

At normalized frequency lower than 0.4 the gain was assigned a value of 1. The resulting equation was subsequently normalized to 1 at the stimulus rate of 0.4 and divided by the normalized stimulus rate, so that the gain was evaluated by using the formula:

$$g_{ij} = \begin{cases} 1, & 0 < f_{n_{ij}} \leq 4 \\ \dfrac{0.4}{f_{n_{ij}}(1 - r)}\left[1 - r * e^{\frac{(0.4 - f_{n_{ij}})}{c}}\right], & f_{n_{ij}} > 4 \end{cases}$$

where g_{ij} is the gain assigned to the j-th firing of motor unit i and fn_{ij} is the normalized instantaneous firing rate T_i/IPI_j (T_i is the rise time of motor unit i and IPI_j is the j-th interpulse interval). The fitting parameters r and c represents the twitch to tetanus ratio (1-r) and the steepness of the force-stimulation rate curve. The values obtained from the experimental data and used in the model are r = 0.87 and c = 2.82 for the FDI muscle, r = 0.85 and c = 2.13 for the VL muscle. The force-frequency relation and the corresponding gain function obtained for both muscle are shown in Figure 27.

The gain was used to scale the amplitude of each motor unit impulse in the train depending on the corresponding IPI (see Figure 22D).

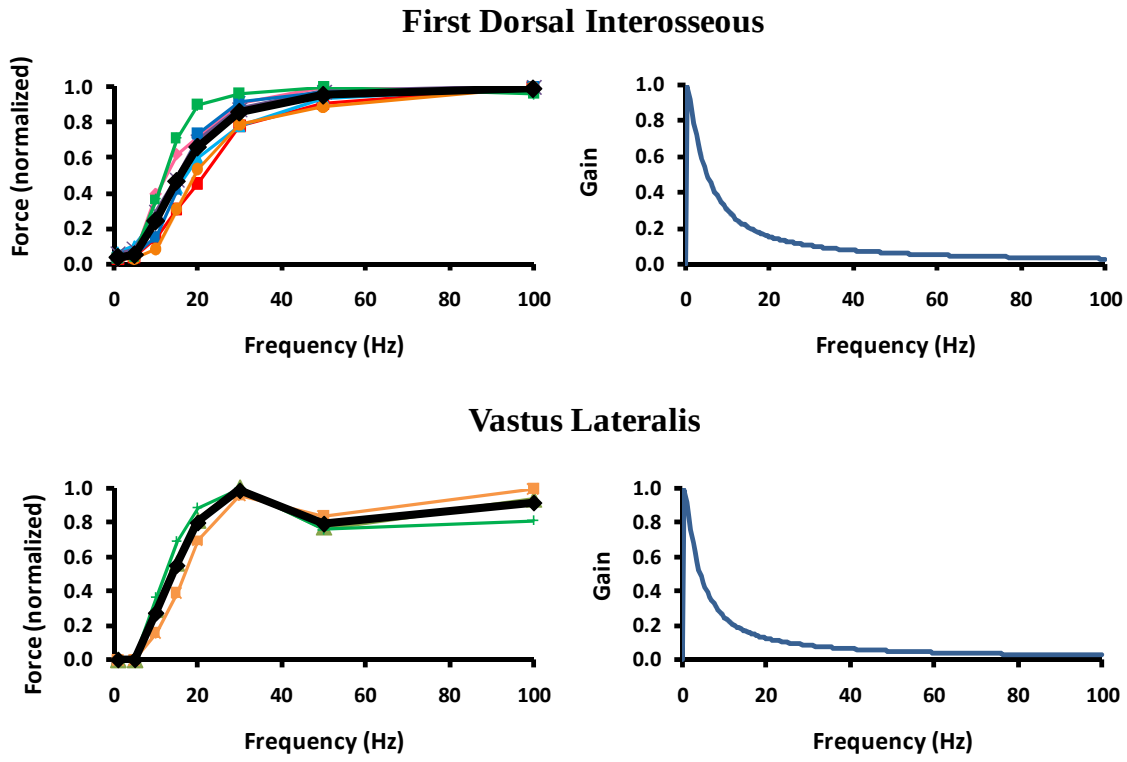

Figure 27: Firing rate dependent gain factor. The force-frequency curves obtained from previously performed experiment and the correspondingly gain function is presented for the FDI (top row) and for the VL (bottom row) muscles.

Motor unit force -- For each motor unit, the internal force produced over a train of firings was computed by convolving the scaled impulse train with the time dependent force twitch. The force was thus given by the sum of individual impulse responses shifted in time:

$$F_i(t) = \sum_j f_{ij}(t - t_{ij})$$

where t_{ij} is the j-th firing time of motor unit *i*, f_{ij} is the force twitch of motor unit *i* at the time of the j-th firing, and $F_i(t)$ is the resulting force output. (See Figure 22E).

Output force -- The compound muscle force was then obtained by summation of all internal forces produced by the active motor units, *k*:

$$F_{tot}(t) = \sum_k F_k(t)$$

Lastly, the force was low-pass filtered at a cutoff frequency of 5 Hz in order to mimic the tissue filtering effect.

Feedback Loop

The motor unit force twitches change over time as a result of potentiation first and then fatigue. Thus, the force produced by each motor unit will change and, if the force is voluntarily maintained consequently, the excitation (input of the model) must be adjusted to compensate. In the simulation this is achieved by comparing the output of the model (compound muscle force) to the target force; the error is fed back to the input. If the error surpasses a predetermined threshold, the excitation is increased or decreased until the force matches the target. The feedback loop was implemented as follow (see also Adam, 2003): the target force was segmented into time intervals of length d = 1 s during which all the parameters were kept constant. The length of the time step was chosen to balance the tracking accuracy and tracking time. Sufficient time was provided for the algorithm to produced trains of firings and not individual pulses, while adjusting the excitation at a suitable rate given the time duration of the potentiation and the fatigue processes. During each time step, the output force was simulated. Motor unit firing rates were computed and translated into their corresponding impulse trains. Trains were adjusted with the noise and with the common

drive and scaled by the firing rate dependent gain factor. Internal forces were produced for each motor unit which were summed together and filtered to obtained the compound muscle force as described above. The compound muscle force was calibrated by the MVC force value, computed at the beginning of the simulation when the excitation and the force production capacity are maximal (input = 100% maximal excitation, twitch amplitude = maximal potentiated twitch amplitude). The mean value of the output force was then compared to the target value. If the error in tracking the force trajectory was smaller than a fixed threshold, set to 5% of the target force, the simulation could proceed to the following time interval. If the error was greater than the threshold, the excitation value was adjusted accordingly: if the error was negative, the excitation was increased; otherwise the excitation was decreased. The minimum increment/decrement in excitation was set to the smallest threshold difference in the pool of motor units. This step was repeated until the error between output force and target force was within limits, at which point the simulation could proceeds to the following time interval *d*.

Results

Influence of Common Drive

To check the influence of common drive on the simulated force and firing rates, a 30s force trajectory at 20% MVC was simulated with different amplitudes of the 0.8 Hz sinusoid superimposed on the motor unit impulse trains. Force twitches were kept constant during the 30 s contraction. Six simulations were run and the amplitude of the common drive was 0, 5%, 10% 15%, 20%, and 25% of the mean IPI. Results are presented for the FDI muscle. 10 motor units, the first and last five motor units recruited during the simulated contraction, were chosen for the computation (MU #1-5 and MU #87-91). Mean firing rates were computed by low-pass filtering the impulse trains with a unit-area Hanning window of 1-s duration. Both the firing rates and the force were detrended to remove the slow variations by filtering the signals with a high-pass filter having a corner frequency at 0.75 Hz. The standard deviation (SD) and the coefficient of variation (CV = SD/mean value * 100) of the firing rates and the force were computed in the middle 20 s interval of the simulation. The level of common drive between pairs of concurrently active motor

units was computed by calculating the cross-correlation function of the detrended mean firing rates of all motor unit pairs within a contraction. The degree of common drive was obtained by measuring the maximum of the cross-correlation function in the interval of +/- 100 ms. Please see De Luca et al. (1982b) and De Luca and Adam (1999) for details. In order to determine if the common fluctuations in the mean firing rates are also reflected in the force output of the muscle, the detrended mean firing rate of each motor unit was cross-correlated with the detrended force output. The degree of cross-correlation was determined by measuring the maximum that occurred with a lag of 100 to 200 ms.

Results showed that the cross-correlation function tended to increase with the amplitude of the common drive sinusoid. There was also a trend for the correlation value to be lower when the cross-correlation function was computed between earlier recruited motor units than between later recruited motor units. Firing rates of later recruited motor units varied over a broader range than firing rates of earlier recruited motor units (27.67 ± 0.13 pps is the mean and SD of the mean firing rates for earlier recruited motor units, 10.52 ± 1.58 is the mean and SD for the later recruited motor units). A much clearer relation was seen when cross-correlating the firing rates with the force: the maximum of the cross-correlation function increased with the amplitude of the common drive sinusoid. The maximum value was always higher for later-recruited higher-amplitude force twitch motor units. (See Table IX, Figures 28, and 30.) A trend for the CV of the force to increase with common drive was observed.

Given the noise level with a CV equal to 20% of the mean IPI value, we chose an amplitude of the common drive sinusoid of 20% of the mean IPI, since this value provided a degree of common drive observed in previously experimental studies (CDC between 0.2 - 0.6, De Luca and Erim, 2002; Contessa et al., 2009).

Table IX: Influence of common drive: FDI. The coefficient of variation (CV) of the mean firing rates and of the force, the degree of cross-correlation between firing rates (CDC), and the degree of cross-correlation between firing rates and force (CDC force) were computed for 10 motor units in the FDI muscle for different values of the amplitude of the common drive sinusoid. The first and last five motor units recruited in a 20% MVC contraction were chosen. The mean values of the parameters for the motor unit groups indicated in column #1 are reported.

	Mean CV					
	CDC = 0	**CDC = 0.05**	**CD = 0.1**	**CD = 0.15**	**CD = 0.2**	**CD = 0.25**
Force	1.02	1.13	1.27	1.71	2.11	2.49
MU 1-5	3.39±0.49	4.01±0.45	3.79±0.14	3.68±0.21	3.68±0.34	3.86±0.27
MU 87-91	5.63±0.49	6.62±1.26	5.78±0.61	6.44±0.61	7.40±1.19	7.27±0.44
All MUs	4.51±1.27	5.31±1.64	4.79±1.13	5.06±1.52	5.54±2.13	5.56±1.83
	Mean correlation value between firing rates					
	CD = 0	**CD = 0.05**	**CD = 0.1**	**CD = 0.15**	**CD = 0.2**	**CD = 0.25**
MU 1-5	0.09±0.14	-0.02±0.23	0.10±0.14	0.14±0.22	0.12±0.09	0.13±0.12
MU 87-91	0.03±0.17	0.05±0.14	0.10±0.18	0.29±0.11	0.32±0.08	0.42±0.12
MU 1-5 and 87-91	0.02±0.13	0.07±0.17	0.09±0.16	0.16±0.17	0.19±0.13	0.26±0.14
All MU	0.04±0.14	0.04±0.18	0.09±16	0.18±0.18	0.21±0.13	0.27±0.16
	Mean correlation value between firing rates and force					
	CD = 0	**CD = 0.05**	**CD = 0.1**	**CD = 0.15**	**CD = 0.2**	**CD = 0.25**
MU 1-5	0.08±0.04	0.14±0.06	0.17±0.08	0.34±0.10	0.35±0.07	0.40±0.13
MU 87-91	0.13±0.11	0.17±0.04	0.32±0.11	0.46±0.09	0.52±0.07	0.64±0.06
All MU	0.11±0.08	0.15±0.05	0.24±0.12	0.40±0.11	0.43±0.11	0.52±0.16

Influence of Noise

To check the influence of noise on the simulated force and firing rates, a 30 s force trajectory at 20% MVC was simulated with different CV of the noise superimposed on the motor unit impulse trains. Force twitches were kept constant during the 30 s contraction. Six simulations were run and the

level of noise took values 0, 5%, 10% 15%, 20%, and 25% of the mean IPI. 10 motor units, the first and last five motor units recruited during the simulated contractions, were chosen for the

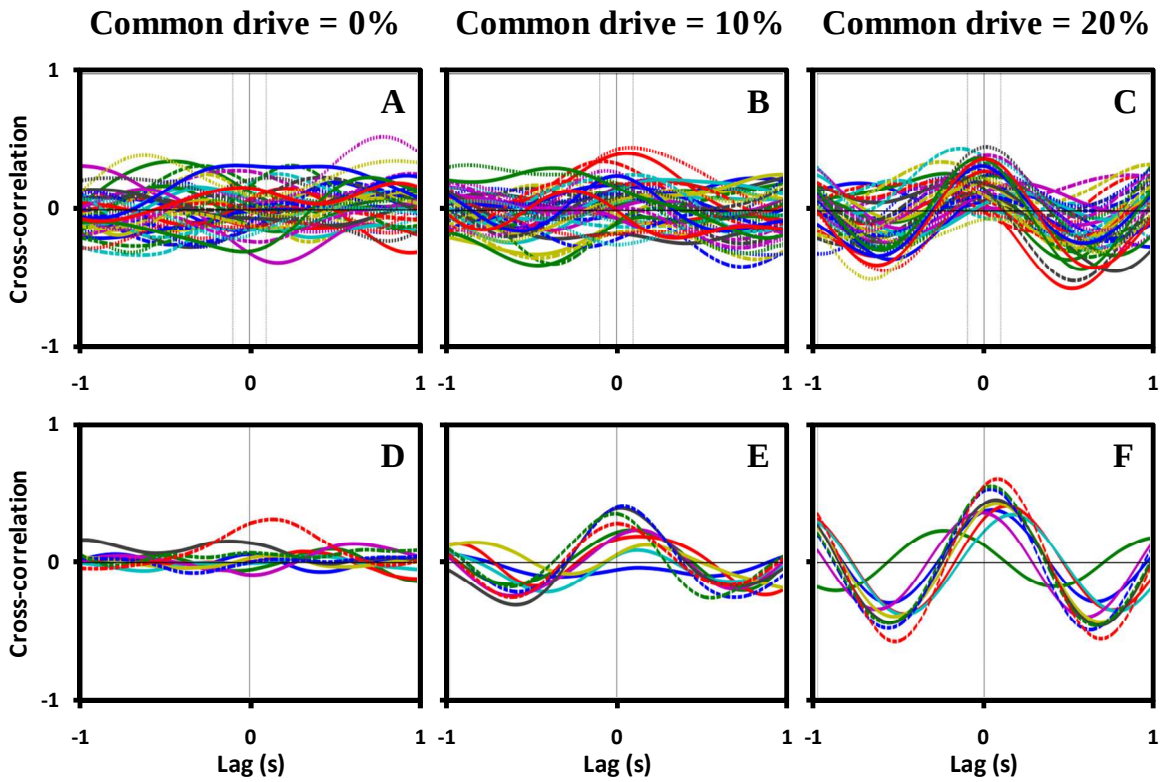

Figure 28: Influence of common drive: FDI. A), B), and C) Cross-correlation functions computed for pairs from 10 motor units of the FDI muscle during contraction simulated with increasing amplitude of the common drive sinusoid superimposed on the impulse trains. D), E), and F) Cross-correlation functions computed between 10 motor units of the FDI muscle and the force during the same contractions.

computation (MU #1-5 and MU #87-91). Mean firing rates were computed by low-pass filtering the impulse trains with a Hanning window of 1-s duration. Both the firing rates and the force were detrended to remove the slow variations by filtering the signals with a high-pass filter having a corner frequency at 0.75 Hz. The SD and the CV of the firing rates and the force were computed in the middle 20 s interval of the simulation. The level of common drive between pairs of concurrently active motor units was computed by calculating the cross-correlation function of the detrended mean firing rates of all motor unit pairs within a contraction. The degree of common drive was obtained by measuring the maximum of the cross-correlation function in the interval of +/- 100 ms. Please see De Luca et al. (1982b) and De Luca and Adam (1999) for details. In order to determine if the common fluctuations in the mean firing rates are also reflected in the force output of the muscle, the detrended mean firing rate of each motor unit was cross-correlated with the detrended force output. The degree of cross-correlation was determined by measuring the maximum that occurred with a lag of 100 to 200 ms.

Results showed that the cross-correlation function tended to decrease with the increase in the CV of the noise. There was also a trend for the correlation value to be lower when the cross-correlation function was computed between earlier recruited motor units than between later recruited motor units. The same behavior was seen when cross-correlating the firing rates with the force: the maximum of the cross-correlation function decreased with increasing noise. Again, the maximum value was usually higher for later-recruited higher-amplitude force twitch motor units. (See Table X and Figure 29 and 30.) The CV of force remained unchanged throughout all the different simulations.

Table X: Influence of noise: FDI. The CV of the mean firing rates and of the force, the degree of cross-correlation between firing rates (CDC), and the degree of cross-correlation between firing rates and force (CDC force) were computed for 10 motor units in the FDI muscle for different values of the CV of the noise. The first and last five motor units recruited in a 20% MVC contraction were chosen. The mean values of the parameters for the motor unit groups indicated in column #1 are reported.

	Mean CV					
	CV = 0	**CV = 0.05**	**CV = 0.1**	**CV = 0.15**	**CV = 0.2**	**CV = 0.25**
Force	1.71	1.74	1.87	1.93	2.11	2.19
MU 1-5	1.33±0.00	1.64±0.12	2.17±0.21	3.03±0.13	3.68±0.34	4.63±0.40
MU 87-91	3.52±0.38	3.77±0.34	4.95±0.34	5.74±0.59	7.40±1.19	7.86±1.03
All MUs	2.42±1.18	2.71±1.15	3.56±1.49	4.38±1.48	5.54±2.13	6.24±1.85
	Mean correlation value between firing rates					
	CV = 0	**CV = 0.05**	**CV = 0.1**	**CV = 0.15**	**CV = 0.2**	**CV = 0.25**
MU 1-5	1.00±0.00	0.75±0.04	0.30±0.11	0.25±0.20	0.12±0.09	0.09±0.11
MU 87-91	1.00±0.00	0.86±0.02	0.64±0.07	0.40±0.13	0.32±0.08	0.15±0.12
MU 1-5 and 87-91	1.00±0.00	0.80±0.04	0.44±0.11	0.31±0.09	0.19±0.13	0.10±0.14
All MUs	1.00±0.00	0.80±0.05	0.45±0.15	0.32±0.14	0.21±0.13	0.11±0.13
	Mean correlation value between firing rates and force					
	CV = 0	**CV = 0.05**	**CV = 0.1**	**CV = 0.15**	**CV = 0.2**	**CV = 0.25**
MU 1-5	0.95±0.00	0.83±0.02	0.53±0.09	0.46±0.06	0.35±0.07	0.23±0.03
MU 87-91	0.99±0.00	0.92±0.01	0.80±0.04	0.64±0.04	0.52±0.07	0.39±0.09
All MUs	0.97±0.02	0.87±0.05	0.66±0.16	0.55±0.10	0.43±0.11	0.31±0.11

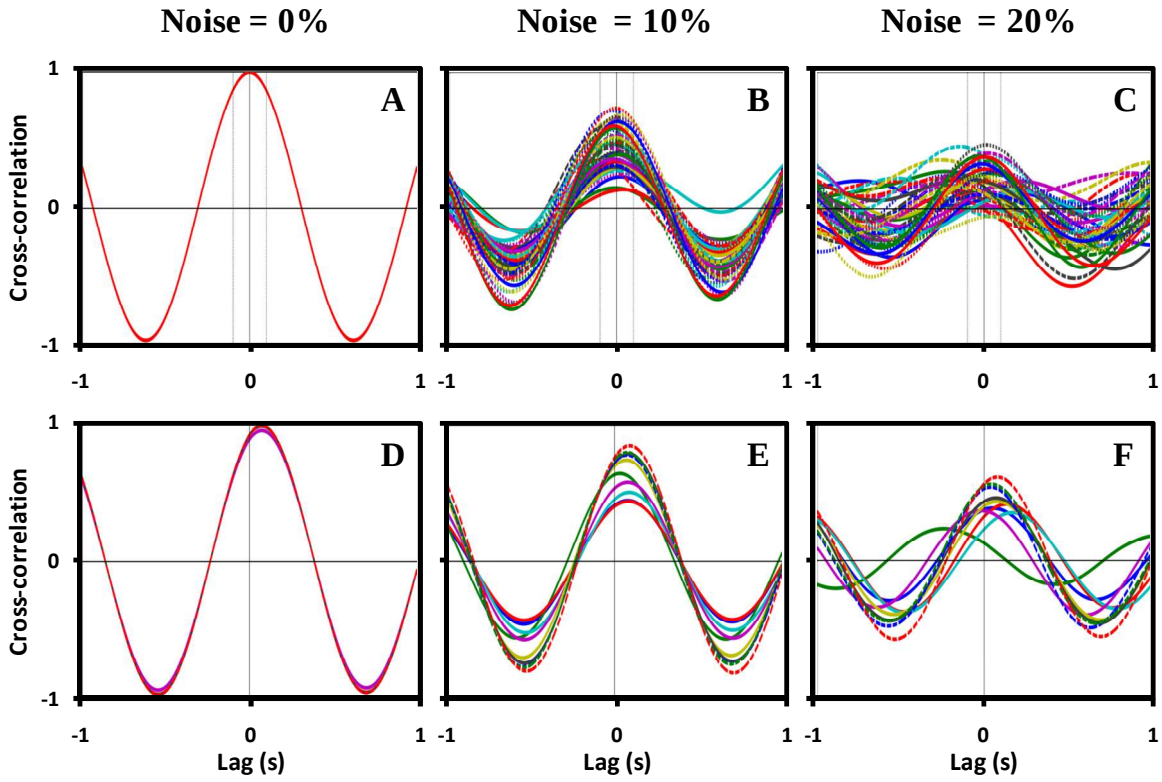

Figure 29: Influence of noise: FDI. A), B), and C) Cross-correlation functions computed for pairs from 10 motor units of the FDI muscle during contraction simulated with increasing CV of the IPIs and a constant level of common drive equal to 20% of the mean IPI. D), E), and F) Cross-correlation functions computed between 10 motor units of the FDI muscle and the force during the same contractions.

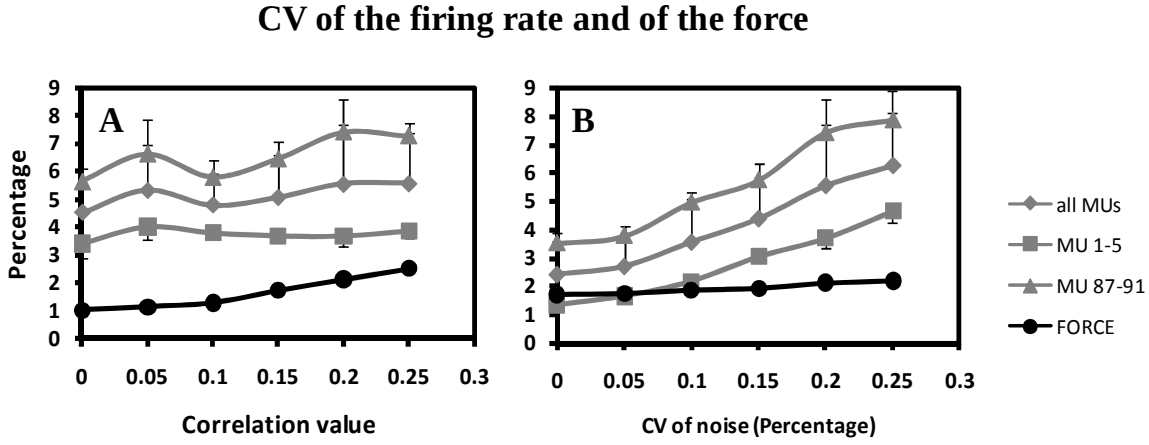

Figure 30: Influence of common drive and noise on the CV of the firing rates and of the force: FDI. The CV of the mean firing rates and the CV of the force as a function of increasing amplitude of the common drive sinusoid (A) and of increasing CV of the noise of the IPIs (B) computed for pairs from 10 motor units of the FDI muscle.

Motor unit firing rates and force during repeated contractions

A prolonged contraction performed at 20% MVC was simulated with and without feedback. In the simulation with no feedback, the excitation was kept constant at a value equal to 20% of the maximal excitation. When feedback was applied, the force output was kept constant at 20% MVC and the simulation was run until the force could no longer be sustained, since the time dependent motor unit twitch forces were decreasing as a result of fatigue.

When no feedback was applied and the contraction was simulated at a constant excitation level, the number of active motor units and their firing rate value remained constant over time. 91 motor units out of 120 were active in the FDI muscle, 410 motor units out of 600 were active in the VL muscle. The force twitches of the active motor units increased in amplitude with excitation, leading to a greater force output during the first minute of the simulated output, and then it began decreasing with fatigue, causing the force output to drop. We could also observe that the force output of the VL muscle was much smoother than the force output of the FDI muscle, since the modeled force twitches had a longer duration. For both muscles, force became smoother as the simulation progressed and the force twitches became smaller in amplitude. (See Figure 31 and 32.)

When feedback was introduced, during the first minute of the contraction some motor units were derecruited and the ones that continued firing decreased their firing rates. These phenomena may be explained with the changes that occurred in the motor unit force twitches. The motor unit force twitches potentiated at the beginning of the contractions and thus, the force produced by the active motor units tended the increase during the first minute. As a result, in order to maintain the force output constant, the excitation to the entire motor unit pool had to decrease, and some motor units stopped firing as the excitation became lower than their recruitment threshold, while the ones which were still above the excitation threshold decreased their firing rates. We observed the derecruitment of 3 motor units in the FDI muscle as the excitation decreased to 96% of the original value after the first minute, whereas 18 motor units were de-recruited in the VL muscle as the excitation decreased to 96% of its initial value in approximately 40 s. As the contraction was sustained over 1 min, the motor unit twitches started decreasing in amplitude and the force produced tended to become lower than the target force. In response to these changes, the excitation

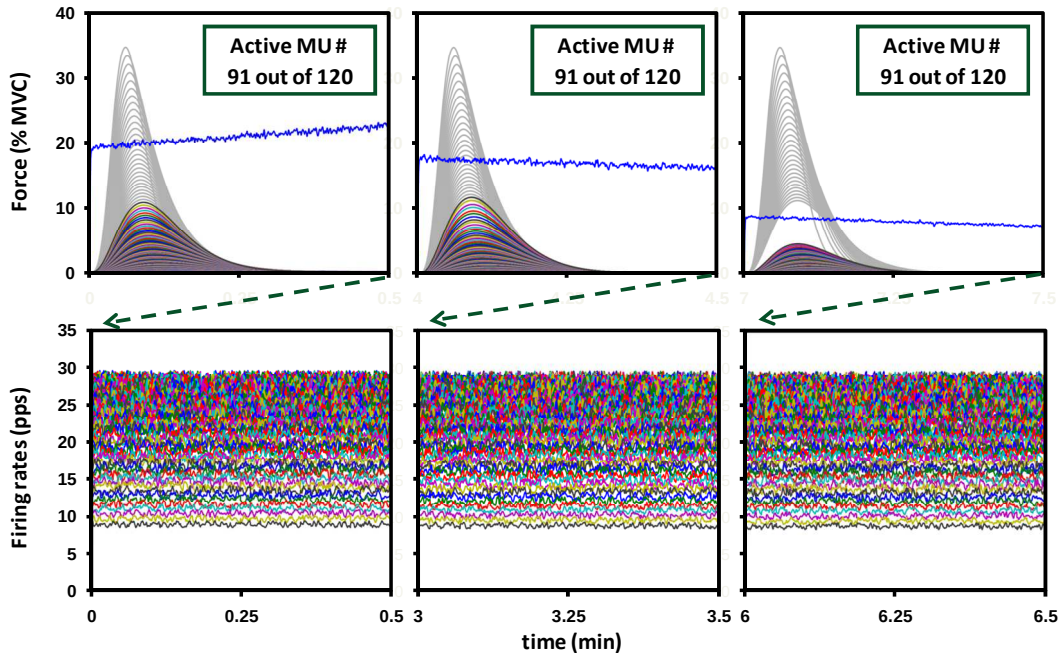

Figure 31: Prolonged contraction, no feedback: FDI. A 30 s interval at the beginning, middle, and at the end of a prolonged contraction sustained at 20% maximal excitation are shown. The top row contains the force twitches at the beginning of the 30 s interval (the twitches of the non-active motor units are shown in gray) and the force output. The bottom row contains the firing rates of all the active motor units. Note that the time axis for the twitches and the force output are different: a 30s interval of the force output is shown, whereas a 300 ms interval is displayed for the force twitches.

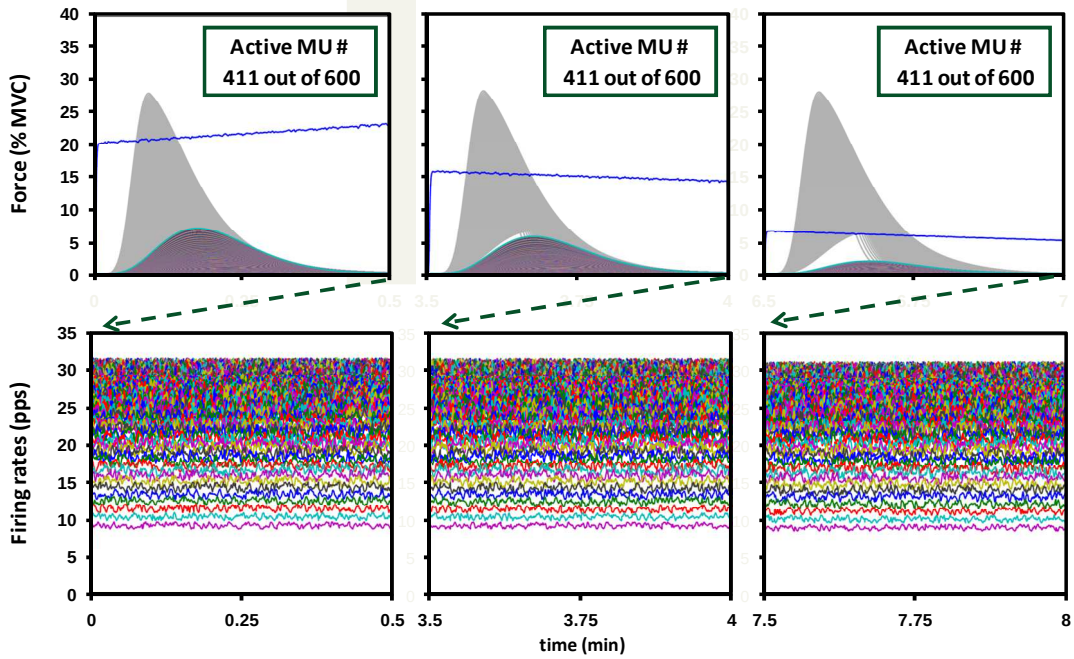

Figure 32: Prolonged contraction, no feedback: VL. A 30 s interval at the beginning, middle, and at the end of a prolonged contraction sustained at 20% maximal excitation are shown. The top row contains the force twitches at the beginning of the 30 s interval (the twitches of the non-active motor units are shown in gray) and the force output. The bottom row contains the firing rates of all the active motor units. Note that the time axis for the twitches and the force output are different: a 30s interval of the force output is shown, whereas a 300 ms interval is displayed for the force twitches.

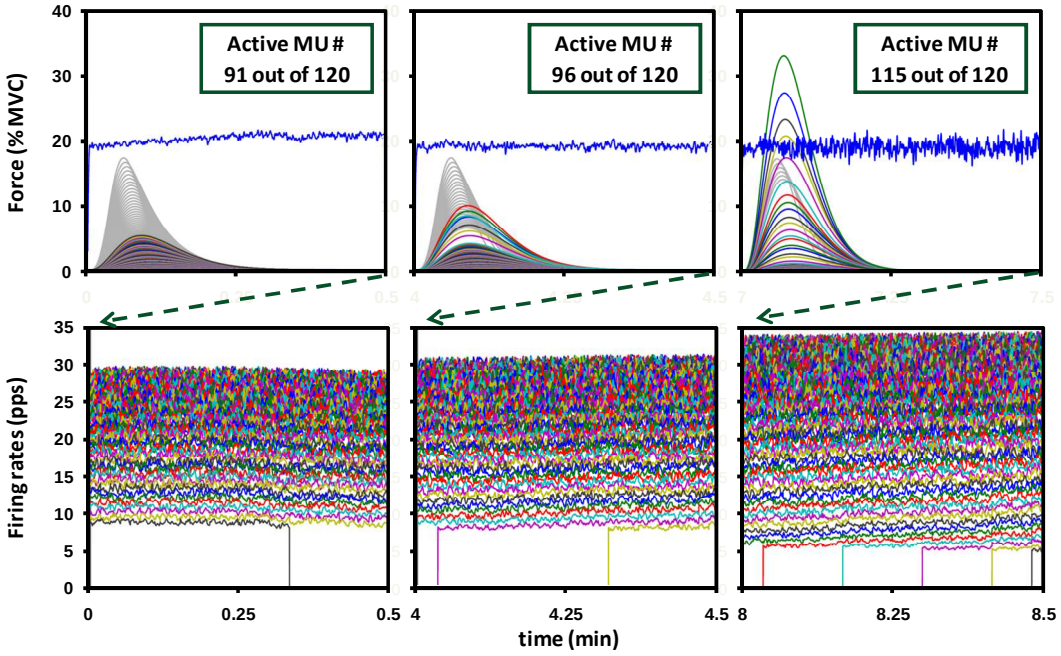

Figure 33: Prolonged contraction, feedback: FDI. A 30 s interval at the beginning, middle, and at the end of a prolonged contraction sustained at 20% MVC are shown. The top row contains the force twitches at the beginning of the 30 s interval (the twitches of the non-active motor units are shown in gray) and the force output. The bottom row contains the firing rates of all the active motor units. Note that the time axis for the twitches and the force output are different: a 30s interval of the force output is shown, whereas a 300 ms interval is displayed for the force twitches.

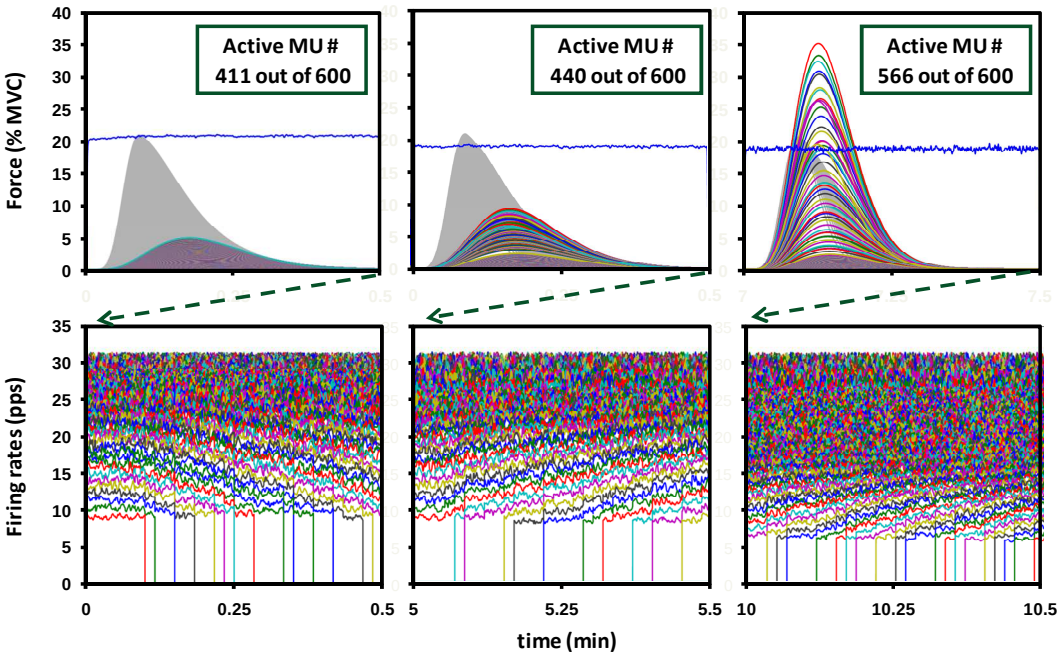

Figure 34: Prolonged contraction, feedback: VL. A 30 s interval at the beginning, middle, and at the end of a prolonged contraction sustained at 20% MVC are shown. The top row contains the force twitches at the beginning of the 30 s interval (the twitches of the non-active motor units are shown in gray) and the force output. The bottom row contains the firing rates of all the active motor units. Note that the time axis for the twitches and the force output are different: a 30s interval of the force output is shown, whereas a 300 ms interval is displayed for the force twitches.

waa increased so that gradually more motor units were recruited and the firing rates of the already active motor units increased. We observed a more evident increase in the firing rates of later recruited motor units, since the earlier recruited motor units already surpassed the steeper part of the excitation plane. (See Chapter 3 and the Methods section). At the endurance limit, the force could no longer be sustained even when all the motor units had been recruited. At this point, the motor unit twitches became too small to sustain the required force level and the force output dropped even if the excitation reached the maximal value. Another observation of the simulation was the increasing fluctuations in the force output as the muscles fatigued, probably due to the gradual recruitment of higher-threshold higher-twitch amplitude motor units. (See Figure 33 and 34.)

Discussion

A model of muscle force production was implemented. It incorporated recent findings on motor unit firing behavior and the concept of common drive. Moreover, the model was provided with a feedback loop in order to simulate tracking tasks, and was capable of adjusting the input excitation in response to changes in the parameters and in the mechanical characteristics of the motor units, thus mimicking the processes of potentiation and fatigue.

Results showed that the model is able to simulate the firing rate patterns that have been experimentally observed during repeated contractions sustained to exhaustion (Adam and De Luca, 2005): in prolonged constant force contractions, the excitation to the motoneuron pool must be adjusted as the contractile properties of the muscle change with potentiation and fatigue. Consequently, motor units decrease or increase their firing rate as the motor unit force twitches potentiate or fatigue. The simulation of prolonged contractions also showed an increase in the fluctuation of the force with time. The increase in force variability, despite the gradual decrease in motor unit force twitches with the progression of muscle fatigue, may be attributed to the gradual recruitment of higher-recruitment threshold larger-amplitude force twitch motor units. This is in agreement with the previous finding that a significant relation exists between the number of newly recruited motor units and the force fluctuation during intermittent contractions sustained at 20%

MVC and performed to exhaustion in the VL muscle We also found a significant relation between force variability and the cross-correlation of firing rates and between force variability and the cross-correlation of firing rates and force. In contrast, the variability of the firing rates had no influence on force fluctuation. (See Chapter 3 and Contessa et al., 2009.) We simulated short contractions (30 s) sustained at 20% MVC with different levels of common drive. The cross-correlation between firing rates and the cross-correlation between firing rates and force increased, as did the coefficient of variation of the force. Interestingly, when the simulation was run with increasing values for the CV of the noise, the variability in the firing rates increased, while the CV of the force did not change.

In conclusion, a physiologically based model of muscle force production was implemented, and proved to be able of simulating various experimentally observed patterns in the firing rate and force behavior. The model may be used to test the influence of various motor unit parameters on muscle force and on the firing rates, and thus to investigate the mechanisms involved in the control of motor units and the generation of muscle force.

CHAPTER 6

SUMMARY AND FINAL DISCUSSION

This study investigated some properties of motor unit firing behavior and included the new findings into a model of muscle force production. The modifications induced by fatigue on various motor unit parameters, such as the firing variability, the synchronization of the motor unit firings, and the common modulation of firing rates, and their influence on force were studied during intermittent contractions sustained at 20% maximum voluntary contraction (MVC) in the vastus lateralis (VL) muscle. The firing rate behavior during linearly increasing force contractions at different rate of force increase was analyzed to model the relation between the excitation received by the motoneuron pool and the motor unit firing rates. Finally, a model of force generation was developed, which faithfully simulated the firing rate and force patterns during prolonged contractions and which could be used to study the influence of various motor unit parameters on the muscle force.

Chapter 2 provides a brief description of the EMG signal, the techniques used to record it and decompose it into its constituent motor unit action potential trains. A summary of the decomposition technique is provided. This is a complex procedure that classifies the individual action potentials by using template matching, resolves superpositions, and allocates with a high accuracy the action potentials to specific motor units. This algorithm has evolved since the late 1970s. It was first applied to intramuscular EMG signals, and later modified for surface EMG signals. The main findings which originated during the past years from the use of the decomposition technique are also presented.

In chapter 3, the behavior of some motor unit parameters during the development of muscle fatigue and their influence and causality on the increasing force fluctuation were studied. Previously acquired data from three healthy subjects performing a series of isometric knee extensions at 20% MVC with their dominant VL muscle were analyzed. The contractions were

repeated until the targeted level could no longer be maintained. We were able to follow the behavior of the same motor units as time progressed. The coefficient of variation of the force increased significantly with endurance time. The behavior of the force was found to be correlated to the common drive of the motor units which increased in progressive contractions (both the cross-correlation between firing rates of concurrently active motor units and the cross-correlation between the firing rates and the force increased with endurance time). The increasing number of newly recruited motor units was also likely to produce the increasing force-fluctuation. The coefficient of variation of the firing rates and the synchronization of the motor unit firings were not found to alter as a function of endurance time, and consequently could not account for the increase in variability of the force during fatigue.

In chapter 4, the excitation-firing rate relationship was derived. We studied the firing rate behavior of motor units in five healthy subjects during linearly increasing force contractions performed up to maximum, or near maximum voluntary contraction force, at different rates of force increase, either 10% MVC/s or 4% MVC/s. We were able to detect a large number of motor units from two different muscles (the first dorsal interosseous (FDI) and the vastus lateralis (VL)) and to observe their firing rate behavior over the entire range of forces. We observed that the firing rate curves of all motor units tended to reach a maximal values, which was linearly related to the recruitment threshold of the motor units. Firing rate behavior appeared to be independent of the rate of force increase, suggesting that once they are recruited motor units increase their firing rates with their own characteristic rate of rise up to the maximal firing rate value. Their behavior could be modeled with a simple exponential function with longer time constants associated with higher recruitment threshold motor units. Based on these results, we defined an excitation plane that describes the relation between the common excitation received by the motoneuron pool and the different electrical responses of each motor unit in the pool.

Chapter 5 describes a model of motor unit firing and force and presents the results of simulation run for the FDI and the VL muscle. The model incorporates the latest findings on motor

unit firing behavior during prolonged contractions and the concept of common drive. Moreover, it is provided with a feedback loop in order to simulate tracking tasks, and is thus capable of adjusting the input excitation in response to changes in the parameters and in the mechanical characteristics of the motor units, mimicking the processes of potentiation and fatigue. Results showed that the model is able to simulate the force and firing rate patterns that has been experimentally observed during repeated contractions sustained to exhaustion. The simulation of prolonged contractions clearly showed that the increase in force variability may be attributed to the gradual recruitment of higher-recruitment threshold larger-amplitude force twitch motor units. A relation was also found between force variability and both the cross-correlation between firing rates and the cross-correlation between firing rates and force.

List of Journal Abbreviations

Abbreviation	Complete Title
Acta Anat	Acta Anatomica
Acta Physiol Scand	Acta Physiologica Scandinavica
Adv Neurol	Advances in Neurology
Am J Phys Med	American Journal of Physical Medicine
Biol Cybern	Biological Cybernetics
Biophys J	Biophysical Journal
Brain Res	Brain Research
Electroencephal Clin Neurophysiol	Electroencephalography and Clinical Neurophysiology
Electromyogr Clin Neurophysiol	Electromyography and Clinical Neurophysiology
Eur J Appl Physiol	European Journal of Applied Physiology
Eur J Appl Physiol Occup Physiol	European Journal of Applied Physiology and Occupational and Occupational Physiology
Exp Brain Res	Experimental Brain Research
Exp Neurol	Experimental Neurology
IEEE Trans Biomed Eng	IEEE Transactions on Biomedical Engineering
J Appl Physiol	Journal of Applied Physiology
J Biomech	Journal of Biomechanics
J Clin Neurophysiol	Journal of Clinical Neurophysiology
J Comput Neurosci	Journal of Computational Neuroscience
J Electromyogr Kinesiol	Journal of Electromyography and Kinesiology
J Exp Biol	Journal of Experimental Biology
J Neurophysiol	Journal of Neurophysiology
J Neurol Neurosurg Psychiatry	Journal of Neurology, Neurosurgery & Psychiatry
J Physiol	Journal of Physiology
Med Hypotheses	Medical Hypotheses
Methods Clin Neurophysiol	Methods in Clinical Neurophysiology
Muscle Nerve	Muscle & Nerve
Neuromusc Disord	Neuromuscular Disorders
Pflügers Arch	Pflügers Archiv
Res Publ Ass Nerv Ment Dis	Research Publications of the Association of

	Nervous and Mental Diseases
Trends Neurosci	Trends in Neurosciences

BIBLIOGRAPHY

1. **Adam A.** Control of Motor Units During Submaximal Fatiguing Contractions. PhD Thesis, Boston University, 2003.

2. **Adam A, and De Luca CJ.** Firing Rates of Motor Units in Human Vastus Lateralis Muscle during Fatiguing Isometric Contractions. *J Appl Physiol*, 99: 268-280, 2005.

3. **Adam A and De Luca CJ.** Recruitment Order of Motor Units in Human Vastus Lateralis Muscle Is Maintained During Fatiguing Contractions. *J Neurophysiol*, 90: 2919-2927, 2003.

4. **Adam A, De Luca CJ, and Erim Z.** Hand Dominance and Motor Unit Firing Behavior. *J Neurophysiol*, 80: 1373-1382, 1998.

5. **Adam A, Morgan A, and De Luca CJ.** Analysis of Synchronized Motor Unit Activity During Fatiguing Muscle Contractions. Society for Neuroscience Annual Meeting, Atlanta, GA, October 14 – 18, 2006.

6. **Andreassen S and Rosenfalck A.** Regulation of the Firing Pattern of Single Motor Units. *J Neurol Neurosurg Psychiatry*, 43: 897-906, 1980.

7. **Avela J, Kyröläinen H, and Komi PV.** Altered Reflex Sensitivity After Repeated and Prolonged Passive Muscle Stretching. *J Appl Physiol*, 86: 1283-1291, 1999.

8. **Avela J, Kyröläinen H, and Komi PV.** Neuromuscular Changes After Long-Lasting Mechanically and Electrically Elicited Fatigue. *Eur J Appl Physiol*, 85: 317-325, 2001.

9. **Bawa P, and Stein RB.** Frequency Response of Human Soleus Muscle. *J Neurophysiol*, 39: 788-793, 1976.

10. **Bellamare F, Woods JJ, Johansson R, and Bigland-Ritchie B.** Motor-Unit Discharge Rates in Maximal Voluntary Contractions of Three Human Muscles. *J Neurophysiol*, 50: 1380-1392, 1983.

11. **Bigland B, and Lippold OCJ.** Motor Unit Activity in the Voluntary Contraction of Human Muscle. *J Physiol*, 125: 322-335, 1954.

12. **Bigland-Ritchie BR, Dawson NJ, Johansson RS, and Lippold OCJ.** Reflex Origin for the Slowing of Motoneurone Firing Rates in Fatigue of Human Voluntary Contractions. *J Physiol*, 379: 451-459, 1986.

13. **Bigland-Ritchie B, Johansson R, Lippold OCJ, Smith S, and Woods JJ.** Changes in Motor Unit Firing Rates during Sustained Maximal Voluntary Contractions. *J Physiol*, 340: 335-346, 1983a.

14. **Bigland-Ritchie B, Johansson R, Lippold OCJ, and Woods JJ.** Contractile Speed and EMG Changes during Fatigue of Sustained Maximal Voluntary Contractions. *J Neurophysiol*, 50: 313-324, 1983b.

15. **Bigland-Ritchie B, Thomas CK, Rice CL, Howarth JV, and Woods JJ.** Muscle Temperature, Contractile Speed, and Motoneuron Firing Rates During Human Voluntary Contractions. *J Appl Physiol*, 73: 2457-2461, 1992.

16. **Binder MD and Stuart DG.** Response of Ia and Spindle Group II Afferent to Single Motor Unit Contractions. *J Neurophysiol*, 43: 621-629, 1980.

17. **Binder-MacLeod SA, and McDermond LR.** Changes in the Force-Frequency Relationship of the Human Quadriceps Femoris Muscle Following Electrically and Voluntarily Induced Fatigue. *Physical Therapy*, 72: 95-104, 1993.

18. **Buchthal F.** The General Concept of the Motor Units. *Neuromusc Dis, Res Publ Ass Nerv Ment Dis*, 38:3-30, 1961.

19. **Buchthal F, and Schmalbruch H.** Contraction Times and Fibre Types in Intact Human Muscle. *Acta Physiol Scand*, 79: 435-452, 1970.

20. **Burke RE.** Motor Units: Anatomy, Physiology, and Functional Organization. In: Handbook of Physiology, The Nervous System, Motor Control, edited by Brooks VB. Bethesda: American Physiological Society, p. 345-422, 1981.

21. **Burke RE.** Motor Unit Types of Cat Triceps Surae Muscle. *J Physiol*, 193: 141-160, 1967.

22. **Burke RE, Levine DN, Tsairis P, and Zajac FE.** Physiological Types and Histochenical Profiles in Motor Units of the Cat Gastrocnemius. *J Physiol*, 234: 723-748, 1973.

23. **Calancie B, and Bawa P.** Voluntary and Reflexive Recruitment of Flexor Carpi Radialis Motor Units in Humans. *J Neurophysiol*, 53: 1194-1200, 1985.

24. **Carpentier A, Duchateau J, and Hainaut K.** Motor Unit Behaviour and Contractile Changes during Fatigue in the Human First Dorsal Interosseous. *J Physiol*, 534: 903-912, 2001.

25. **Chan KM, Doherty TJ, and Brown WF.** Contractile Properties of Human Motor Units in Health, Aging, and Desease. *Muscle Nerve*, 24: 1113-1133, 2001.

26. **Christensen E.** Topography of Terminal Motor Innervation in Striated Muscles from Stillborn Infants. *Am J Phys Med*,38: 65-78, 1959.

27. **Clamann HP.** Activity of Single Motor Units During Isometric Tension. *Neurology*, 20:255-260, 1970.

28. **Clamann HP.** Statistical Analysis of Motor Unit Firing Patterns in a Human Skeletal Muscle. *Biophys J*, 9: 1233-1251, 1969.

29. **Contessa P, Adam A, and De Luca CJ.** Motor Unit Control and Force Fluctuation During Fatigue. *J Appl Physiol*, 107: 235-243, 2009.

30. **Cooper S, and Eccles JC.** The Isometric Responses of Mammalian Muscles. *J Physiol*, 69: 377-385, 1930.

31. **Dartnall TJ, Nordstrom MA, and Semmler JG.** Motor Unit Synchronization is Increased in Biceps Brachii after Exercise-Induced Damage to Elbow Flexor Muscles. *J Neurophysiol* 99: 1008–1019, 2008.

32. **De Luca CJ.** Physiology and Mathematics of Myoelectric Signals. IEEE *Trans Biomed Eng*, 26: 315-325, 1979.

33. **De Luca CJ.** Control Properties of Motor Units. *J Exp Biol*, 115: 125-136, 1985.

34. **De Luca CJ.** Precision Decomposition of EMG Signals. *Methods Clin Neurophysiol*, 4: 1-28, 1993.

35. **De Luca CJ and Adam A.** Decomposition and Analysis of Intramuscular Electromyographic Signals. In: Modern Techniques in Neuroscience Research, edited by Windhorst U and Johansson H. Heidelberg: Springer, 1999, p. 757-776.

36. **De Luca CJ and Erim Z.** Common Drive of Motor Units in Regulation of Muscle Force. *Trends Neurosci*, 17: 299-305, 1994.

37. **De Luca CJ, and Erim Z.** Common Drive in Motor Units of a Synergistic Muscle Pair. *J Neurophysiol*, 87: 2200-2204, 2002.

38. **De Luca, CJ and Forrest WJ.** Some Properties of Motor Unit Action Potential Trains Recorded During Constant Force Isometric Contractions in Man. *Kybernetik*, 12: 160-168, 1973.

39. **De Luca CJ, Adam A, Wotiz R, Gilmore LD, and Nawab SH.** Decomposition of Surface EMG Signals. J *Neurophysiol*, 96: 1646-1657, 2006.

40. **De Luca CJ, Foley PJ, and Erim Z.** Motor Unit Control Properties in Constant-Force Isometric Contractions. *J Neurophysiol*, 76: 1503-1516, 1996.

41. **De Luca CJ, Gonzalez-Cueto JA, and Adam A.** Motor Unit Recruitment and Proprioceptive Feedback Decrease the Common Drive. *J Neurophysiol*, 101: 1620-1628, 2008.

42. **De Luca CJ, LeFever RS, McCue MP, and Xenakis AP.** Behaviour of Human Motor Units in Different Muscles During Linearly Varying Contractions. *J Physiol*, 329: 113-128, 1982a.

43. **De Luca CJ, LeFever RS, McCue MP, and Xenakis AP.** Control Scheme Governing Concurrently Active Human Motor Units During Voluntary Contractions. *J Physiol*, 329: 129-142, 1982b.

44. **De Luca CJ, Roy AM, and Erim Z.** Synchronization of Motor-Unit Firings in Several Human Muscles. *J Neurophysiol*, 70: 2010-2023, 1993.

45. **Doherty TJ, and Brown WF.** A Method for the Longitudinal Study of Human Thenar Motor Units. *Muscle Nerve*, 17: 1029-1036, 1994.

46. **Duchateau J and Hainaut K.** Effects of Immobilization on Contractile Properties, Recruitment and Firing Rates of Human Motor Units. *J Physiol*, 422: 55-65, 1990.

47. **Edin BB and Vallbo AB.** Muscle Afferent Responses to Isometric Contractions and Relaxations in Humans. *J Neurophysiol*, 63: 1307-1313, 1990.

48. **Elek JM, and Dengler R.** Human Motor Units Studied by Intramuscular Microstimulation. In: Fatigue, edited by Simon C. Gandevia et al., Plenum Press, New York, p. 161-171, 1995

49. **Elek JM, Kossev A, Dengler R, Schubert M, Wholfahrt K, and Wolf W.** Parameters of Human Motor Unit Twitches Obtained by Intramuscular Microstimulation. *Neuromusc Disord*, 2: 261-267, 1992.

50. **Enoka RM, Robinson GA, and Kossev AR.** Task and Fatigue Effects on Low-Threshold Motor Units in Human Hand Muscle. *J Neurophysiol*, 62: 1344-1359, 1989.

51. **Erim Z and Aghera A.** 23rd Annual International Conference of the IEEE Engineering in Medicine and Biology Society, 2001.

52. **Erim Z, Beg MF, Burke DT, and De Luca CJ.** Effects of Aging on Motor Unit Firing Behavior. *J Neurophysiol*, 82: 2081-2091, 1999.

53. **Erim Z, De Luca CJ, Mineo K, and Aoki T.** Rank-Ordered Regulation of Motor Units. *Muscle Nerve*, 19: 563-573, 1996.

54. **Feinstein B, Lindegârd B, Nyman E, and Wohlfart G.** Morphologic studies of Motor Units in Normal Human Muscles. *Acta Anat (Basel)*, 23: 127-42, 1955.

55. **Freund HJ, Büdingen HJ, and Dietz V.** Activity of Single Motor Units from Human Forearm Muscles During Voluntary Isometric Contractions. *J Neurophysiol*, 38: 933-946, 1975.

56. **Fuglevand AJ, Macefield VG, and Bigland-Ritchie B.** Force-Frequency and Fatigue Properties of Motor Units in Muscles that Control Digits of the Human Hand. *J Neuroplysiol*, 81: 1718-1729, 1999.

57. **Fuglevand AJ, Winter DA, and Patla AE.** Models of Recruitment and Rate Coding Organization in Motor-Unit Pools. *J Neurophysiol*, 70: 2470-2488, 1993.

58. **Furness P, Jessop J, and Lippold OCJ.** Long-Lasting Increases in the Tremor of Human Hand Muscles Following Brief, Strong Effort. *J Physiol (London)*, 265: 821-831, 1977.

59. **Galganski ME, Fuglevand AJ, and Enoka RM.** Reduced Control of Motor Output in a Human Hand Muscle of Elderly Subjects During Submaximal Contractions. *J Neurophysiol*, 69: 2108-2115, 1993.

60. **Gandevia SC, Allen GM, Butler JE, and Taylor JL.** Supraspinal Factors in Human Muscle Fatigue: Evidence for Suboptimal Output from the Motor Cortex. *J Physiol*, 490: 529-536, 1996.

61. **Garland SJ.** Role of Small Diameter Afferents in Reflex Inhibition during Human Muscle Fatigue. *J Physiol*, 435: 547-558, 1991.

62. **Garland SJ, Enoka RM, Serrano LP, and Robinson GA.** Behavior of Motor Units in Human Biceps Brachii During a Submaximal Fatiguing Contraction. *J Appl Physiol*, 76: 2411-2419, 1994.

63. **Gossen ER, Ivanova TD, and Garland SJ**. The Time Course of the Motoneuron Afterhyperpolarization is Related to Motor Unit Twitch Speed in Human Skeletal Muscle. *J Physiol*, 552: 657-664, 2003.

64. **Gottlieb S, and Lippold OCJ.** The 4-6 Hz Tremor During Sustained Contraction in Normal Human Subjects. *J Physiol (London)*, 336: 499-509, 1983.

65. **Granit R, Kernell D, and Shortess GK.** Quantitative Aspects of Repetitive Firing of Mammalian Motoneurons, caused by Injected Currents. *J Physiol*, 168: 911-931, 1963.

66. **Grimby L, Hannerz J, and Hedman B.** The Fatigue and Voluntary Discharge Properties of Single Motor Units in Man. *J Physiol*, 316: 545-554.

67. **Gydikov A and Kosarov D.** Some Features of Different Motor Units in Human Biceps Brachii. *Pflügers Arch*, 347: 75-88, 1974.

68. **Halliday AM and Redfearn JWT.** An Analysis of the Frequencies of Finger Tremor in Healthy Subjects. *J Physiol*, 134: 600-611, 1956.

69. **Henneman E.** Relation between Size of Neurons and Their Susceptibility to Discharge. *Science*, 126: 1345-1347, 1957.

70. **Henneman E, and Olson CB.** Relation between Structure and Function in the Design of Skeletal Muscles. *J Neurpohysiol*, 28: 581-598, 1965.

71. **Herbert RD, and Gandevia SC.** Twitch Interpolation in Human Muscles: Mechanisms and Implications for Measurement of Voluntary Activation, *J Neurophysiol*, 82: 2271-2283, 1999.

72. **Hill JM.** Increase in the Discharge of Muscle Spindles During Diaphragm Fatigue. *Brain Res*, 918: 166-170, 2001.

73. **Holtermann A, Grönlund C, Karlsson JS, and Roeleveld K.** Motor Unit Synchronization During Fatigue: Described with a Novel sEMG Method Based on Large Motor Unit Samples. *J Electromyogr Kinesiol*, 19: 232-241, 2009.

74. **Kamen G, Sison SV, Duke DU CC, and Patten C.** Motor Unit Discharge Behavior in Older Adults During Maximal-Effort Contractions. *J Appl Physiol*, 79: 1908-1913, 1995.

75. **Kernell D.** The Adaptation and the Relation between Discharge Frequency and Current Strength of Cat Lumbosacral Motoneurons Stimulated by Long-Lasting Injected Currents. *Acta Physiol Scand*, 65: 65-73, 1965a.

76. **Kernell D.** High-Frequency Repetitive Firing of Cat Lumbrosacral Motoneurones Possessing Different Time Course of Afterhypolarization. *Acta Physiol Scand*, 65: 74-86, 1965b.

77. **Kernell D.** The Limits of Firing Frequency in Cat Lumbosacral Motoneurones Possessing Different Time Course of AfterHyperpolarization. *Acta Physiol Scand*, 65: 87-100, 1965c.

78. **Kernell D, Eerbeek O, and Verhey BA.** Relation between Isometric Force and Stimulus Rate in Cat's Hindlimb Motor Units of Different Twitch Contraction Times. *Exp Brain Res*, 50: 220-227, 1983.

79. **Kosarov D, and Gydikov A.** Dependence of the Discharge Frequency of Motor Units in Different Human Muscles Upon the Level of the Isometric Muscle Tension. *Electromyogr Clin Neurophysiol*, 16: 293-306, 1976.

80. **Kossev A, Elek JM, Schubert M, Dengler R, and Wolf W.** Assessment of Human Motor Unit Twitches – a Comparison of Spike-Triggered Averaging and Intramuscular Microstimulation. *Electroencephal Clin Neurophysiol*, 93: 100-105, 1994.

81. **Kukulka CG and Clamann HP.** Comparison of the Recruitment and Discharge Properties of Motor Units in Human Brachial Biceps and Adductor Pollicis During Isometric Contractions. *Brain Res*, 219: 45-55, 1981.

82. **Laidlaw DH, Bilodeau M, and Enoka RM.** Steadiness is Reduced and Motor Unit Discharge is More Variable in Old Adults. *Muscle Nerve*, 23: 600-612, 2000.

83. **LeFever RS and De Luca CJ.** Decomposition of Action Potential Trains. Proceedings of 8th Annual Meeting of the Society for Neuroscience, 229, November, 1978.

84. **LeFever RS and De Luca CJ.** A Procedure for Decomposing the Myoelectric Signal into its Constituent Action Potentials. Part I. Technique, theory and implementation. *IEEE Trans Biomed Eng*, 29: 149-157, 1982a.

85. **LeFever RS, Xenakis AP, De Luca CJ.** A Procedure for Decomposing the Myoelectric Signal into its Constituent Action Potentials. Part II. Execution and test for accuracy. *IEEE Trans Biomed Eng*, 29: 158-164, 1982b.

86. **Lowery MM and Erim Z.** A Simulation Study to Examine the Effect of Common Motoneuron Inputs on Correlated Patterns of Motor Unit Discharge. *J Comput Neurosci*, 19: 107-124, 2005.

87. **Macefield VG, Fuglevand AG, Howell JN, and Bigland-Ritchie B.** Discharge Behavior of Single Motor Units During Maximal Voluntary Contractions of a Human Toe Extensor. J Physiol, 528: 227-234, 2000.

88. **Macefield VG, Hagbarth KE, Gorman R, Gandevia SC, and Burke D.** Decline in Spindle Support to α-Motoneurons During Sustained Voluntary Contractions. *J Physiol*, 440: 497-512, 1991.

89. **Mambrito B and De Luca CJ.** A Technique for the Detection, Decomposition and Analysis of the EMG Signal. *Electroencephalogr Clin Neurophysiol*, 59: 175-188, 1984.

90. **Mannard A, and Stein RB.** Determination of the Frequency Response of Isometric Soleus Muscle in the Cat Using Random Nerve Stimulation. *J Physiol*, 229: 275-296, 1973.

91. **Marsden CD, Meadows JC, and Merton PA.** "Muscular Wisdom" that Minimizes Fatigue during Prolonged Effort in Man: Peak Rates of Motoneuron Discharge and Slowing of Discharge during Fatigue. *Adv Neurol*, 39: 169–211, 1983.

92. **McNulty PA, Falland KJ, and Macefield VG.** Comparison of Contractile Properties of Single Motor Units in Human Intrinsic and Extrinsic Finger Muscles. *J Physiol*, 526: 445-456, 2000.

93. **Miles TS.** The Cortical Control of Motor Neurons: Some Principles of Operation. *Med Hypotheses*, 23: 43-50, 1987.

94. **Milner-Brown HS, Stein RB, and Yemm R.** The Contractile Properties of Human Motor Units during Voluntary Isometric Contractions. *J Physiol*, 228: 285-306, 1973a.

95. **Milner-Brown HS, Stein RB, and Yemm R.** The Orderly Recruitment of Human Motor Units During Voluntary Isometric Contractions. *J Physiol*, 230: 359-370, 1973b.

96. **Milner-Brown HS, Stein RB, and Yemm R.** Changes in Firing Rate of Human Motor Units During Linearly Changing Voluntary Contractions. *J Physiol*, 230: 371-390, 1973c.

97. **Monster AW and Chan H.** Isometric Force Production by Motor Units of Extensor Digitorum Communis Muscle in Man. *J Neurophysiol*, 40: 1432-1443, 1977.

98. **Moritz CT, Barry BK, Pascoe MA, and Enoka RM.** Discharge Rate Variability Influences the Variation in Force Fluctuations Across the Working Range of a Hand Muscle. *J Neurophysiol*, 93: 2449-2459, 2005.

99. **Nawab SH, Chang S, and De Luca CJ.** High-Yield Decomposition of Surface EMG Signals. *J Clin Neurophysiol*, in press.

100. **Nawab SH, Wotiz RP, and De Luca CJ.** Decomposition of Indwelling EMG Signals. *J Appl Physiol*, 105: 700-710, 2008.

101. **Nordstrom MA, Fuglevand AJ, and Enoka ME.** Estimating the Strength of Common Input to Human Motoneurons from the Cross-Correlogram. *J Physiol*, 453: 547-574, 1992.

102. **Nordstrom MA, Miles TS, and Türker KS.** Synchronization of Motor Units in Human Masseter During a Prolonged Isometric Contraction. *J Physiol*, 426: 409-421, 1990.

103. **Person RS and Kudina LP.** Discharge Frequency and Discharge Pattern of Human Motor Units During Voluntary Contraction of Muscle. *Electroencephalogr Clin Neurophysiol*, 32: 471-483, 1972.

104. **Rack PMH, and Westbury DR.** The Effects of Length and Stimulus Rate on Tension in the Isometric Cat Soleus Muscle. *J Physiol*, 204: 443-460, 1969.

105. **Raikova TR, and Aladjov HTs.** Hierarchical Genetic Algorithm versus Static Optimization – Investigation of Elbow Flexion and Extension Movements. *J Biomech*, 35: 1123-1135, 2002.

106. **Seki K, Kizuka T, and Yamada H**. Reduction in Maximal Firing Rate of Motoneurons After 1-Week Immobilization of Finger Muscle in Human Subjects. *J Electromyogr Kinesiol*, 17: 113-120, 2007.

107. **Semmler JG and Nordstrom MA.** Motor Unit Discharge and Force Tremor in Skill- and Strength-Trained Individuals. *Exp Brain Res*, 119: 27-38, 1998.

108. **Semmler JG, Steege JW, Kornatz KW, and Enoka RM.** Motor-Unit Synchronization is Not Responsible for Larger Motor-Unit Forces in Old Adults. *J Neurophysiol*, 84: 358-366, 2000.

109. **Sica REP, and McComas AJ.** Fast and Slow Twitch Units in a Human Muscle. *J Neurol Neurosurg Psychiatry*,34: 113-120, 1971.

110. **Stashuk D and De Bruin H.** Automatic Decomposition of Selective Needle-Detected Myoelectric Signals. *IEEE Trans Biomed Eng*, 35: 1-10, 1988.

111. **Stashuk D and De Luca CJ.** Update on the Decomposition and Analysis of EMG Signals. In: Computer-aided Electromyography and Expert Systems, edited by Desmedt JE. Amsterdam: Elsevier, 1989, p. 39-53.

112. **Stein RB, French AS, Mannard A, and Yemm R.** New Methods for Analysing Motor Function in Man and Animals. *Brain Res*, 40: 187-192, 1972.

113. **Stephens JA, and Usherwood TP.** The Mechanical Properties of Human Motor Units with Special Reference to their Fatigability and Recruitment. *Brain Res*, 125: 91.97, 1977.

114. **Studer LM, Ruegg DG, and Gabriel JP.** A Model for Steady Isometric Muscle Activation. *Biol Cybern*, 80: 339-355, 1999.

115. **Tanaka M, McDonagh MJ, and Davies CT.** A Comparison of the Mechanical properties of the First Dorsal Interosseous in the Dominant and Non-Dominant Hand. *Eur J Appl Physiol Occup Physiol*, 53: 17-20, 1984

116. **Tanji J and Kato M.** Firing Rate of Individual Motor Units in Voluntary Contraction of Abductor Digiti Minimi Muscle in Man. *Exp Neurol*, 40: 771-783, 1973.

117. **Taylor A, and Stephens JA.** Study of Human Motor Unit Contractions by Controlled Intramuscular Microstimulation. *Brain Res*, 117: 331-335, 1976.

118. **Taylor AM, Christou EA, and Enoka RM.** Multiple Features of Motor-Unit Activity Influence Force Fluctuations During Isometric Contractions. *J Neurophysiol*, 90: 1350-1361, 2003.

119. **Thomas CK, Ross BH, and Stein RB.** Motor-Unit Recruitment in Human First Dorsal Interosseous Muscle for Static Contractions in Three Different Directions. *J Neurophysiol*, 55: 1017-1029, 1986.

120. **Thomas CK, Bigland-Ritchie B, Westling G, and Johansson RS.** A comparison of Human Thenar Motor-Unit Properties Studied by Intraneural Motor-Axon Stimulation and Spike-Triggered Averaging. *J Neurophysiol*, 64: 1347-1351, 1990.

121. **Thomas CK, Johansson RS, and Bigland-Ritchie B.** Attempts to Physiologically Classify Human Thenar Motor Units. *J Neurophysiol*, 65: 1501-1508, 1991a.

122. **Thomas CK, Bigland-Ritchie B, and Johansson RS.** Force-Frequency Relation of Human Thenar Motor Units. *J Neurophysiol*, 65: 1509-1516, 1991b.

123. **Tracy BL, Maluf KS, Stephenson JL, Hunter SK, and Enoka RM.** Variability of Motor Unit Discharge and Force Fluctuations Across a Range of Muscle Forces in Older Adults. *Muscle Nerve*, 32: 533-540, 2005.

124. **Vandervoort AA, Quinlan J, and McComas AJ.** Twitch Potentiation after Voluntary Contraction. *Exp Neurol*, 81: 141-152, 1983.

125. **Vollestand NK, Sejersted I, and Saugen E.** Mechanical Behavior of Skeletal Muscle during Intermittent Voluntary Isometric Contractions in Humans. *J Appl Physiol*, 83: 1557-1565, 1997.

126. **Westling G, Johansson RS, Thomas CK, and Bigland-Ritchie B.** Measurement of Contractile and Electrical Properties of Single Human Thenar Motor Units in Response to Intraneural Motor-Axon Stimulation. *J Neurophysiol*, 64: 1331-1338, 1990.

127. **Woods JJ, Furbush F, and Bigland-Ritchie B.** Evidence for a Fatigue-Induced Reflex Inhibition of Motoneuron Firing Rates. *J Neurophysiol*, 58: 125-137, 1987.

128. **Yao W, Fuglevand AJ, and Enoka RM.** Motor-unit Synchronization Increases EMG Amplitude and Decreases Force Steadiness of Simulated Contractions. *J Neurophysiol* 83: 441–452, 2000.

129. **Young JL, and Meyer RF.** Physiological Properties and Classification of Single Motor Units Activated by Intramuscular Microstimulation in the First Dorsal Interosseous Muscle in Man. In: Motor Unit Types Recruitment and Plasticity in Health and Disease, edited by J.E. Desmedt, p. 17-25, 1981.

130. **Zijdewind C, Bosch W, Goessens L, Kandou TW, and Kernell D.** Electromyogram and Force During Stimulated Fatigue Tests of Muscles in Dominant and Non-Dominant Hands. *Eur J Appl Physiol Occup Physiol*, 60: 127-132, 1990.